Advanced Drug Delivery Reviews 132 (2018) 296–332

Contents lists available at ScienceDirect

Advanced Drug Delivery Reviews

journal homepage: www.elsevier.com/locate/addr

3D bioprinting of tissues and organs for regenerative medicine☆

Sanjairaj Vijayavenkataraman [a,*], Wei-Cheng Yan [b], Wen Feng Lu [a], Chi-Hwa Wang [b], Jerry Ying Hsi Fuh [a,*]

[a] Department of Mechanical Engineering, National University of Singapore, 9 Engineering Drive 1, 117576, Singapore
[b] Department of Chemical and Biomolecular Engineering, National University of Singapore, 4 Engineering Drive 4, 117585, Singapore

ARTICLE INFO

Article history:
Received 9 November 2017
Received in revised form 27 May 2018
Accepted 3 July 2018
Available online 7 July 2018

Keywords:
3D bioprinting
Bioprinting
3D printing
Regenerative medicine
Organ printing
Tissue engineering

ABSTRACT

3D bioprinting is a pioneering technology that enables fabrication of biomimetic, multiscale, multi-cellular tissues with highly complex tissue microenvironment, intricate cytoarchitecture, structure-function hierarchy, and tissue-specific compositional and mechanical heterogeneity. Given the huge demand for organ transplantation, coupled with limited organ donors, bioprinting is a potential technology that could solve this crisis of organ shortage by fabrication of fully-functional whole organs. Though organ bioprinting is a far-fetched goal, there has been a considerable and commendable progress in the field of bioprinting that could be used as transplantable tissues in regenerative medicine. This paper presents a first-time review of 3D bioprinting in regenerative medicine, where the current status and contemporary issues of 3D bioprinting pertaining to the eleven organ systems of the human body including skeletal, muscular, nervous, lymphatic, endocrine, reproductive, integumentary, respiratory, digestive, urinary, and circulatory systems were critically reviewed. The implications of 3D bioprinting in drug discovery, development, and delivery systems are also briefly discussed, in terms of in vitro drug testing models, and personalized medicine. While there is a substantial progress in the field of bioprinting in the recent past, there is still a long way to go to fully realize the translational potential of this technology. Computational studies for study of tissue growth or tissue fusion post-printing, improving the scalability of this technology to fabricate human-scale tissues, development of hybrid systems with integration of different bioprinting modalities, formulation of new bioinks with tuneable mechanical and rheological properties, mechanobiological studies on cell-bioink interaction, 4D bioprinting with smart (stimuli-responsive) hydrogels, and addressing the ethical, social, and regulatory issues concerning bioprinting are potential futuristic focus areas that would aid in successful clinical translation of this technology.

Contents

☆ This review is part of the Advanced Drug Delivery Reviews theme issue on "3D-Bioprinting and Micro-/Nano-Technology: Emerging Technologies in Biomedical Sciences".

* Corresponding authors.
E-mail addresses: vijayavenkataraman@u.nus.edu (S. Vijayavenkataraman), jerry.fuh@nus.edu.sg (J.Y.H. Fuh).

https://doi.org/10.1016/j.addr.2018.07.004
0169-409X/

1. Introduction

3D bioprinting is a process of fabricating cell-laden bioinks into functional tissue constructs and organs from 3D digital models [1]. 3D bioprinting possesses several advantages over the classical tissue engineering methods [2, 3]. The inability of classical tissue engineering methods to fabricate complex biomimetic structures results in an over-simplified tissue construct, thus rendering the engineered tissue inaccurate with unrealistic cell microenvironments [4], whereas 3D bioprinting has the potential to fabricate complex, sophisticated, biomimetic tissue constructs. Automation, high precision, geometrical freedom and control (macro-morphology, pore size, porosity, interconnectivity), customizability, printability of wide range of materials, ability to incorporate and precise spatiotemporal placement of proteins, growth factors, drugs, DNA, and other biochemical cues along with the cells [5], wide range of cell density and possibility of cell density gradient, reproducibility, and repeatability are some of the many advantages of this technology. Given its potential to fabricate three-dimensional biomimetic functional tissue constructs, 3D bioprinting has multi-fold application in the healthcare sector, including disease modelling, drug discovery and testing, high-throughput screening, and regenerative medicine.

The difference between “3D printing” and “3D Bioprinting” has to be understood clearly as both these terms are used interchangeably in the scientific community [6]. Both the processes build a 3D object layer by layer from a 3D model. However, 3D bioprinting involves the use of cell-laden bioinks and other biologics to construct a living tissue while 3D printing technologies do not use cells or biologics. 3D printing of porous polymeric scaffolds for cell seeding should not be confused with bioprinting of cell-laden bioinks. 3D printing also has numerous biomedical applications including medical devices, surgical instruments, prostheses, customized implants (inert materials such as metals, ceramics, or polymers without cells), and anatomical models for surgical planning and training [7, 8]. This review exclusively focusses on the bioprinting of tissues and organs for regenerative medicine applications, which involves the printing of cell-laden bioinks and hence, general 3D printing technologies and applications do not fall within the scope of this work.

The need for bioprinting technology justifies the rapid progress made in the field in the past decade. Organ shortage continues to be one of the major problems in healthcare. In the USA, there were 122,071 patients waiting for organ transplantation in 2016, with 48% of them waiting for >2 years [9] (Fig. 1A). While the demand for organ transplants has increased considerably, the supply is almost stagnant for a decade (Fig. 1B). Bioprinting has a great potential to solve this ever-increasing organ shortage crisis. Though bioprinting of fully functional organs has a long way to go [10], considerable progress has been made to realize the greater goal of organ printing. Bioprinted tissues could be used as in vitro testing beds in place of animal testing [1]. Given the ethical concerns surrounding animal testing and the high cost involved, bioprinting is a viable alternate. In pharmaceutical research, bioprinting could be used as in vitro models for testing of drug efficacy, toxicity, chemotherapy or chemo-resistance to reduce the high cost and shorten the time of drug discovery [11, 12].

Bioprinting related research has grown substantially over the last decade. The number of publications related to 3D bioprinting has

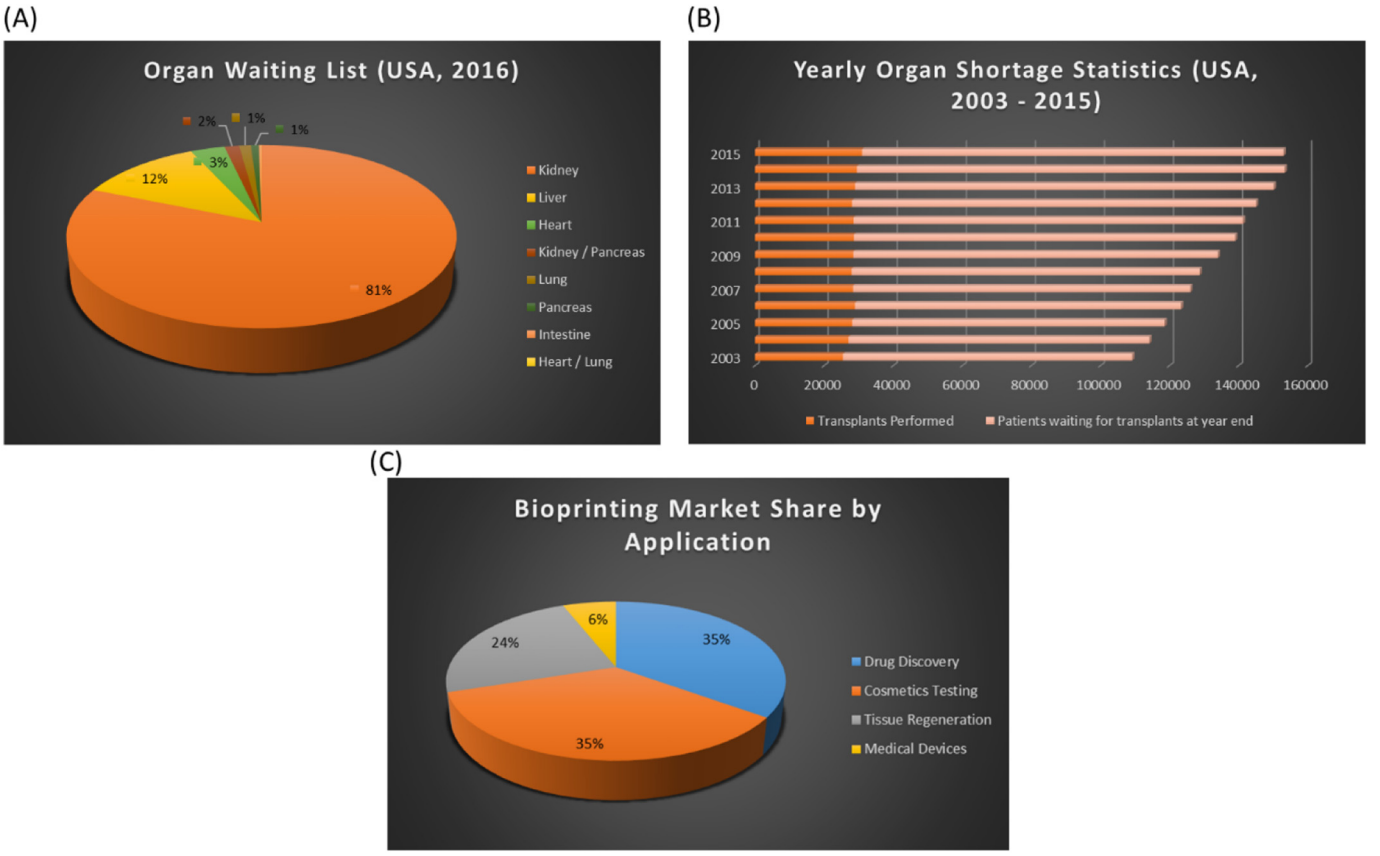

Fig. 1. (A) Number of patients waiting for Organ transplantation (by Organ Type) in the USA in 2016 (Source: United Network for Organ Sharing – www.unos.org), (B) Yearly Organ Shortage Statistics in the USA from 2003 to 2015 (Source: Organ Procurement and Transplantation Network – www.optn.transplant.hrsa.gov), and (C) Forecasted market share for each of the primary bioprinting applications in 2027 (Source: SmarTech Publishing Reports - www.smartechpublishing.com).

increased 3300% from 2000 to 2015 (24 in 2000 to 792 in 2015), indicating the rapid pace at which the field is growing [13]. The total market for Additive Manufacturing was valued at $5.1 billion in 2015, having grown at a Compound Annual Growth Rate (CAGR) of 26.2% over the last 27 years, with the medical and healthcare sector accounting for nearly 16% of the total revenue [7]. Increasing demand for customized, patient-specific medical products accounted for this surge in the market value. The market potential of 3D bioprinting is expected to grow at a CAGR of 26.5%, from USD 411.4 million in 2016 to USD 1332.6 million by 2021 [14]. The major driving factors outlined in the report are the rising demand for organ transplantation, growing R&D, increasing public and private investments in research, and rising use of 3D bioprinting in drug discovery. Drug discovery, cosmetics testing, tissue regeneration and medical devices are the four primary bioprinting applications and their share in the bioprinting market is shown in Fig. 1C.

In this review, we discuss in detail the applications of 3D bioprinting in regenerative medicine. First, the steps involved in bioprinting are briefly explained. The pre-processing steps in bioprinting, which includes imaging and 3D modelling are touched upon briefly. Other numerical simulation and mathematical modelling possibilities for better design and optimization of the bioprinting process is also included in the same section. The different types of bioprinting processes, namely laser-based, droplet-based (inkjet, EHD-jet, acoustic, microvalve-based bioprinting), extrusion-based and stereolithography bioprinting are discussed in detail, along with the pros and cons of each method. There has been a commendable progress in the bioprinting field, with various types of tissues being printed and tested. The applications of bioprinting in regenerative medicine are then discussed in great detail pertaining to different organ systems present in the human body. Bioprinting of tissues and organs in eleven important organ systems including skeletal, muscular, nervous, lymphatic, endocrine, reproductive, integumentary, respiratory, digestive, urinary, and circulatory systems are critically reviewed, with the challenges and future perspectives of bioprinting under each organ system. To the best of our knowledge, our work is the first to review the applications of bioprinting pertaining to different organ systems in great detail. Finally, the implications of 3D bioprinting in drug discovery, development, and delivery systems are briefly discussed.

2. Steps in 3D bioprinting

A typical bioprinting process consists of three major steps namely pre-processing, processing and post-processing (Fig. 2). Pre-processing involves imaging of the tissue or organ using computed tomography (CT), magnetic resonance imaging (MRI), and ultrasound imaging techniques and reconstruction of 3D models from the imaging. The generated 3D models are then converted into STL file format, which is a commonly accepted file format by most of the commercially available bioprinters. The processing step starts with harvesting primary cells from patients, culturing and expanding it ex vivo for the bioprinting process. Though cancer cell lines and other non-human cells are being used, the ideal condition for fabricating transplantable living tissues would be to use the patient's own cells. Suitable bioinks with properties mimicking the intended tissue to be printed are selected and the cells are suspended in these bioinks. The cell-laden bioinks are then fabricated into required 3D living tissue/organ according to the 3D model using a bioprinter. Post-processing involves maintaining the bioprinted tissue/organ in a bioprinter for tissue maturation before being transplanted into patients or used as in vitro models for disease modelling, or drug testing.

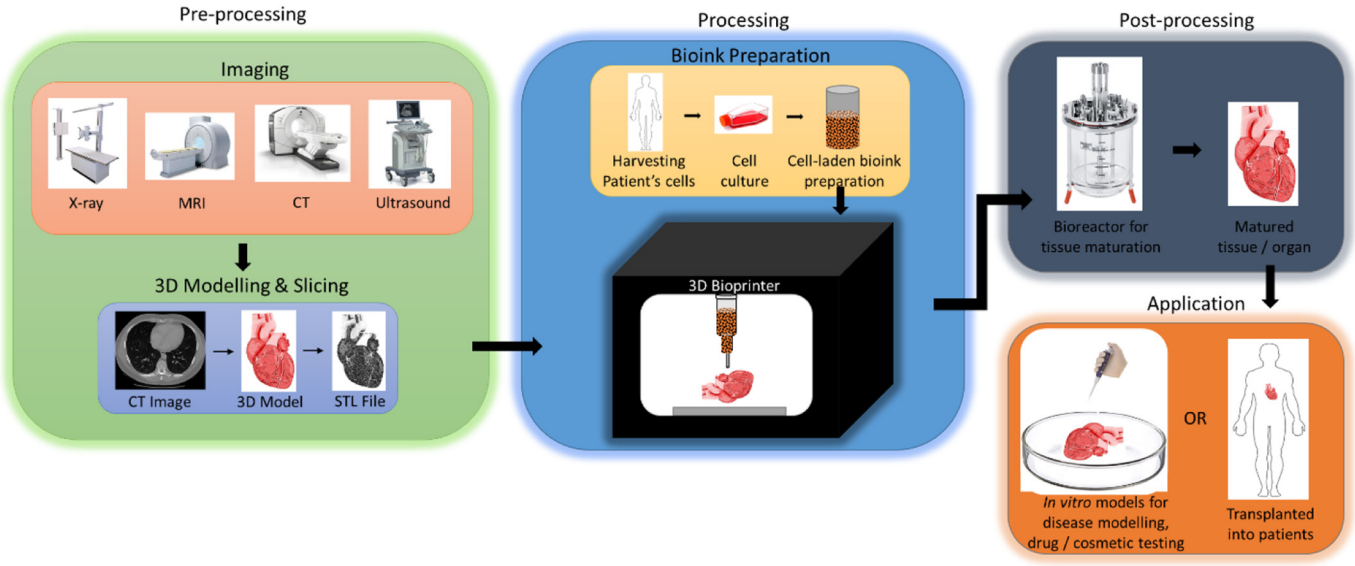

Fig. 2. A typical bioprinting process flow consisting of three steps namely pre-processing (Medical imaging using X-ray, MRI, CT or Ultrasound, 3D modelling, and slicing; preparation of cell-laden bioink) (Image courtesy: www.southernstatesimaging.com, www.istockphoto.com, www3.gehealthcare.com), processing (actual bioprinting process), and post-processing (tissue maturation in a bioreactor) (Image courtesy: www.broadleyjames.com).

3. Pre-processing

The pre-processing steps in bioprinting a tissue or organ predominantly consists of two steps, namely (i) acquisition of imaging data, and (ii) reconstruction of 3D tissue models. Medical imaging tools with proper software are utilized to acquire anatomic data first. Subsequently, these data are processed by various modelling approaches to creating the 3D models which are used to guide the printing process based on the designed printing path plan.

3.1. Imaging

Prior to actual bioprinting, it is crucial to understand the internal and external structure of the targeted tissue/organ for the printing to be biomimetic [6]. Computed tomography (CT), magnetic resonance imaging (MRI), ultrasound imaging techniques and optical microscopy are the most common imaging modalities used for obtaining patient-specific information.

3.1.1. Computed tomography

CT utilizes ionizing radiation (X-ray) to scan the samples and create consecutive 2D images by detecting the absorption of radiation. A 3D view is then generated by stacking the obtained 2D images via tomographic reconstruction algorithms [15]. CT displays better performance in imaging hard tissues such as bone and tumor, and the boundaries between bone tissue and soft tissue can be well differentiated via CT [6, 16]. Reasonably high-resolution images (0.24–0.3 mm) can be obtained with relatively short scan time. However, the utilization of ionizing radiation possesses a potential risk to patients [17] and only a limited dose at controlled frequencies can be applied to patients. In addition to CT, Micro-CT (with high resolution from 1 to 200 μm) being able to characterize the mechanical properties of scaffolds and the microstructures [18–20] has been used in imaging the bone density changes and tissue regeneration in small animals [21]. For the imaging of the soft tissue components using CT, contrast agent may be used to enhance the image quality.

3.1.2. Magnetic resonance imaging

MRI utilizes pulsed radio frequency electromagnetic waves to scan the samples, instead of using ionizing radiation as with CT. By detecting the excited radio-frequency signal from hydrogen atoms in the samples via a magnetic resonance coil, images can be generated after being processed through computer software. A number of 3D images are stacked and segmented to create MRI images. Although both hard and soft tissues can be imaged by MRI, it is highly preferred for imaging of soft tissues [16]. MRI has been extensively used in the imaging of soft tissue components in the human body as there is no ionizing radiation involved. However, the resolution is relatively low, which is only 250 mm × 250 mm × 0.5 mm at a scan time of 5–40 min [17].

Micro-MRI can achieve higher resolution with an extremely high magnetic field strength (7–9 T) [22], however, such high magnetic field levels are intolerable to patients [23]. Instead, contrast agents such as magnetic nanoparticles may be used to improve the imaging quality [24].

3.1.3. Ultrasound imaging

Ultrasound technology utilizes sound energy to scan the sample by emitting sound waves. The reflected waves are detected by a receiver and are further processed to generate computer images. It has a limited resolution (1 mm × 1.5 mm × 0.2 mm) [25], compared to MRI or CT. However, since there is no exposure to radiation, ultrasound imaging is a safe and easy way to differentiate the structure of targeted tissue/organs. With the application of ultrasound elastography, the mechanical properties of tissues can also be measured quantitatively [26].

3.1.4. Optical microscopy

By stacking a large number of 2D images taken from optical microscope, images of 3D tissue models can be obtained. This requires the modelling software to reassemble the dissected histology slices and precisely align them in correct position [16]. By the optical microscopic methods, an individual cell is able to differentiate via staining. Thus, each tissue type in an organ can be differentiated.

3.1.5. Other tools and software

Other imaging tools that are used to visualize the targeted tissue/organ includes positron emission tomography (PET) and single photon emission computed tomography (SPECT) [27]. To fulfil the criteria of design for bioprinting, hybrid imaging modalities have also been used. For instance, 3D models obtained from CT and MRI were combined to represent a heterogeneous soft tissue [28], and CT/PET was used to precisely locate cancer [29].

Many image processing software is used to process the acquired images from the imaging techniques discussed above. ITK-Snap (Open source) [30], Amira, Materialize Mimics, and Avizo 3D [6] are the common software/programs used for image segmentation. By determining the threshold value of the region of interest, the tissue anatomy can be captured. Subsequently, region growing techniques are used to merge all pixel values within the region to form a color mask. This approach is the most commonly used segmentation method in processing the images, which is suitable for capturing information from a tissue with large volume and heterogeneity. Sun et al. [31] proposed a homogenization approach to solving the problem by using different threshold values for a number of sub-regions.

3.2. 3D modelling

After the acquisition of images of the targeted tissues/organs by imaging techniques, the internal architectures have to be designed to complete the 3D model creation, such as internal channels and pores which enable cell attachment, proliferation, nutrient flow and tissue maturation [32]. The regenerated 3D model from image segmentation is usually presented in stereolithography (STL) format, which is an acceptable format with the majority of recent 3D bioprinters. This 3D image with a continuum of image and surface intensity data [33] is reconstructed via a volumetric representation of segmentation, involving volume rendering [34]. The appearance of 3D surfaces generated via volumetric techniques consists of tiny picture elements (basic units of volumetric representation: voxels) [35]. Upon generation of targeted tissues/organs models in a digital form, the 3D surface model is then processed to design the internal architecture to mimic the anatomy of tissues/organs.

CAD-based design, image-based design, freeform design, implicit surfaces, and space-filling curves are the main approaches used in designing the internal structures of the tissue constructs (Fig. 3). In the CAD-based system, constructive solid geometry (CSG), boundary representation (B-Rep) and spatial occupancy enumeration (SOE) are employed as modelling approaches to design the tissue architectures [36]. CSG modelling generates design models based on solid primitives and Boolean operations. B-Rep, however, uses boundary elements to define the geometry. SOE represents solid objects using cubic unit elements. CSG and SOE can be used in constructing complex objects while they are computationally costly and require huge data storage as compared to B-Rep approach. Commercial CAD software such as SOLIDWORKS, NX, MIMICS, PTC Creo, and CATIA are often employed to design the tissue structures.

To design a construct with controlled porosity, Cheah et al. [37] proposed algorithms enabling subtraction of the negative geometry from a CAD model to generate 3D bone structures. In an image-based system proposed by Hollister et al. [38], the defected regions in medical images were filled with binary unit cells. With this method, the tissue models were reconstructed with irregular pores. Smith et al. [39] first applied this approach in reconstructing the mandibular bone tissue model (Fig. 3B) and subsequently printed the 3D model by a laser sintering process. Freeform design approach enables the construction of tissues/organs with controlled architecture as well as material composition. Ozbolat et al. [32] used this approach to generate several wound devices (Fig. 3C). Implicit surfaces design is another approach that can design complex tissue scaffolds with periodic minimal surfaces [40]. Space-filling curves design can serve as an alternative approach to fulfil the requirement of extrusion-based bioprinting where the above-mentioned approaches (CAD- or image-based systems) cannot be applied. Due to the difference of compatibility between difference bioprinters, bioprinter-specific software should be used for successful completion of bioprinting. Currently, the majority of software which enables the design of internal architecture still have limited design flexibilities, such as poor distance control between the material footprint dimensions and printed material [6].

3.3. Other numerical methods/mathematical modelling in bioprinting

In addition to the imaging and 3D modelling steps, there are other numerical methods, mathematical modelling and simulation that could facilitate better design and optimization of the bioprinting process. For example, finite element analysis (FEA) could be used to determine the mechanical, fluid flow properties, and diffusivity [43] and computational fluid dynamics (CFD) can be employed to study the permeability of the designed 3D tissue model. FEA could be combined with empirical studies to investigate the impact of matrix degradation [44, 45]. CFD could be used to design and optimize the scaffold/tissue microstructures in terms of shear stress [46–48], mass transfer [49], and influence of micro-architectural parameters [50, 51].

3.3.1. Macroscopic models of tissue growth

The understanding of macroscopic models of tissue growth [52–54] which describe the tissue growth process in terms of macroscopic parameters would help in the biomimetic design of the 3D model, selection of suitable bioinks and determination of the bioprinting process. Biological and biochemical mechanisms, being crucial for explaining the reason for tissue growth, have not been thoroughly understood yet. Continuous efforts on developing more comprehensive models are still required.

Modelling of living tissues can be categorized into two types: (i) Discrete cell model where tissue is considered as a set of discrete cells; (ii) continuum cell model where tissue is considered as continuum cells. In addition, tissue fusion after bioprinting is another key issue that requires computational simulations [55].

3.3.1.1. Discrete cell model. Steinberg [Steinberg 1963] proposed differential adhesion hypothesis (DAH) which states that (i) cell adhesion in multi-cellular systems relies on energy differences between the cell types, and (ii) cell aggregates are active enough to reach lowest energy status. The majority of discrete cell models are proposed based on DAH. Monte Carlo simulations of the large-N Poots model are the typical example where a lattice is used to represent the tissue [56]. DAH based models could be used to predict the formation of bioprinted tissue, with co-culture and multi-culture systems. Glazier et al. [57] used Metropolis algorithm to model cell migration and changes of shape in systems with several thousand cells, suggesting that temperature may be one of the parameters affecting cell motility. In addition to DAH, several other models were also developed to simulate the tissue growth, such as cell differentiation, chemical signalling and ECM production [58, 59]. Palsson et al. [58] have combined Glazier-Graner model with partial differential equations to describe cAMP signalling, by which morphogenetic influence of genes can be potentially characterized.

3.3.1.2. Continuum cell model. Murray et al. [60] proposed the continuum approach where continuum mechanics methods were applied, considering the modelling of tissues with realistic cell numbers. In this study, the cell distributions of various cell types are described by cell density in the whole tissue. Fluxes are used to describe the morphogenetic rearrangements. Semple et al. [61] had investigated morphogenesis, scar formation, and dermal wound healing, vasculogenesis and contraction based on continuum cell modelling. It is known that understanding the vasculogenesis mechanisms is important for generating tissue constructs that can be perfused, especially in large organ replacements.

3.3.1.3. Tissue fusion. The success of bioprinting 3D tissue or organ requires the stacking of cell-laden bioinks layer by layer and in a manner mimicking the native tissue architecture. Hence, a fusion of droplets of bioink or subsequent layers of bioink to form the tissue or organ needs attention. Cell-laden bioinks, cell aggregates or multicellular spheroids are similar to liquids in terms of flow behaviour, tending to minimise their surfaces and fuse when they are in contact with each other [62, 63], and also have similar viscous, elastic and plastic

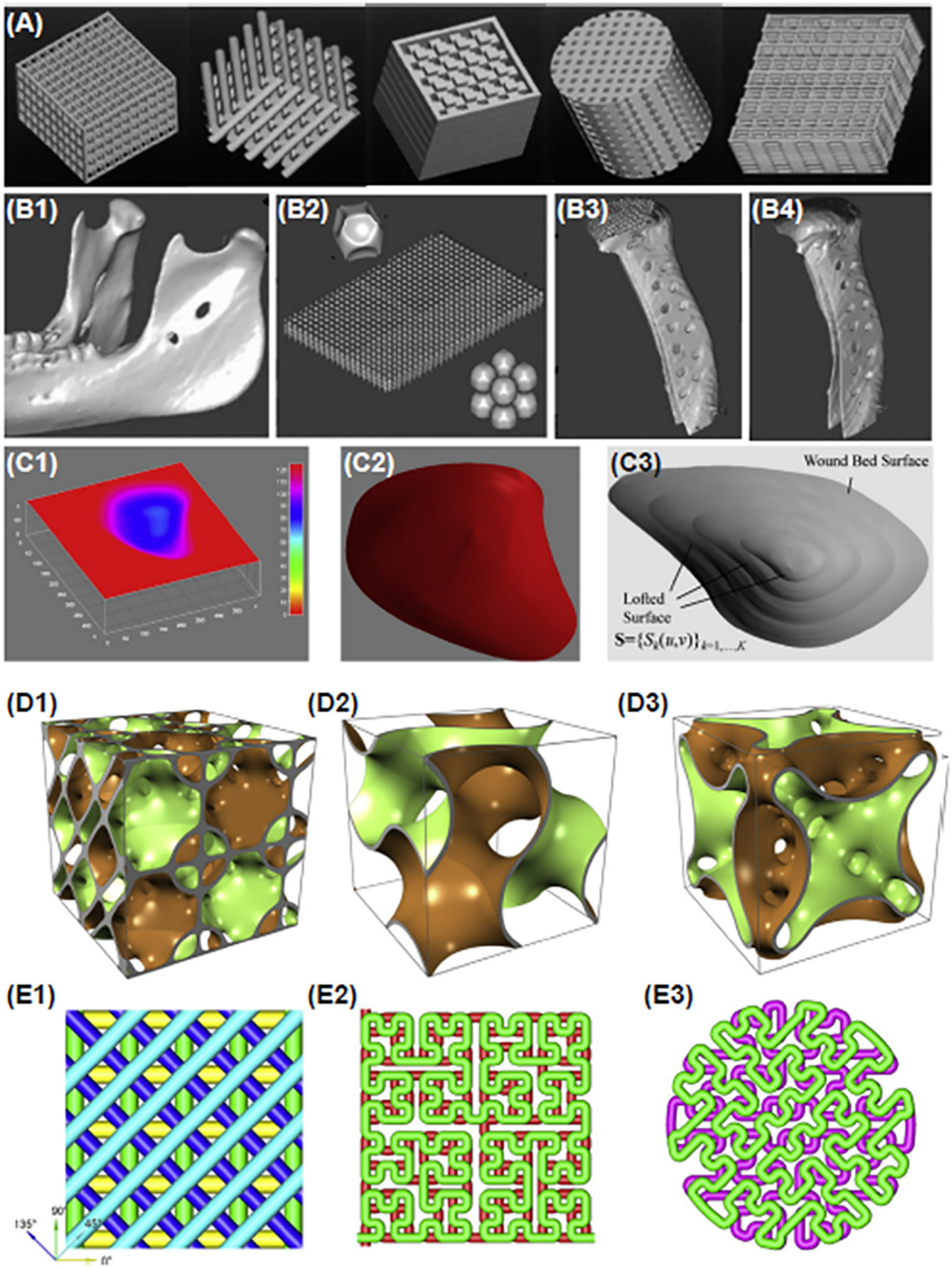

Fig. 3. (A) Computer-aided design based systems constructed from different primitives. Reprinted with permission from [31]. (B1–B4) Image-based design of mandibular condyle scaffolds. Reprinted with permission from [39]. (C1–C3) Freeform design of a wound device. Reprinted with permission from [32]. (D1–D3) Triply periodic minimal implicit surfaces. Reprinted with permission from [41]. (E1–E3) Space-filling curves. Reprinted with permission from [42].

properties [64]. Several modelling approaches have been developed to describe the fusion of cell aggregates, which is important to adequately optimize and control the bioprinting process.

A basic model to mimic a system with living cells in bioink, ECM or cell culture medium is 2D lattice model, which can simulate the evolution of cell aggregates by Monte Carlo algorithm. The Monte Carlo

simulation can be classed into two categories: (i) Metropolis Monte Carlo and (ii) Kinetic Monte Carlo. Metropolis Monte Carlo creates and constructs the initial state based on the shape and the compositions of the targeted system. The conformational changes are made via the interfacial cells. Kinetic Monte Carlo method is an alternate method [65], in which the transition rate is calculated for the changes in each step and then the new configuration with a probability is selected. The corresponding time evolution of the system could then be expressed via the transition rates. Use of Kinetic Monte Carlo method to simulate the evolution of a multicellular system had higher precision [66] compared to the Metropolis Monte Carlo method. To further understand this concept, Sun et al. [67] used Kinetic Monte Carlo simulation to describe the fusion of six vascular cell aggregates. Each cell aggregate has a radius of about 7 cell diameters, containing 982 cells (680 muscle cells at outer layer (in red) and 302 endothelial cells inside (in green) shown in Fig. 4). As shown in Fig. 4, partial fusion occurs for the muscle cells once the aggregates contact with each other. After 2.5 × 106 time steps, the inner layer fused to form a tube.

Another simulation method which is based on phase field approach was proposed to study the fusion of cell aggregates and morphological development after bioprinting [68–70]. Multiphase fluids were used to simulate the multicellular aggregates. The interphase force interactions were employed to describe the phase mixing/separation. In addition to the above-mentioned simulation techniques, cellular particle dynamics are another extensively used simulation method, which treats cells as a set of particles. Using cellular particle dynamics, the morphological evolution of the 3D multicellular system can be predicted instantaneously during passive relaxation of biomaterials [66].

Application of such mathematical models and numerical simulation to understand the cell biomechanics and predict the tissue formation post-printing is an interesting area of future research. Such studies would help in the selection of suitable bioinks, optimal cell

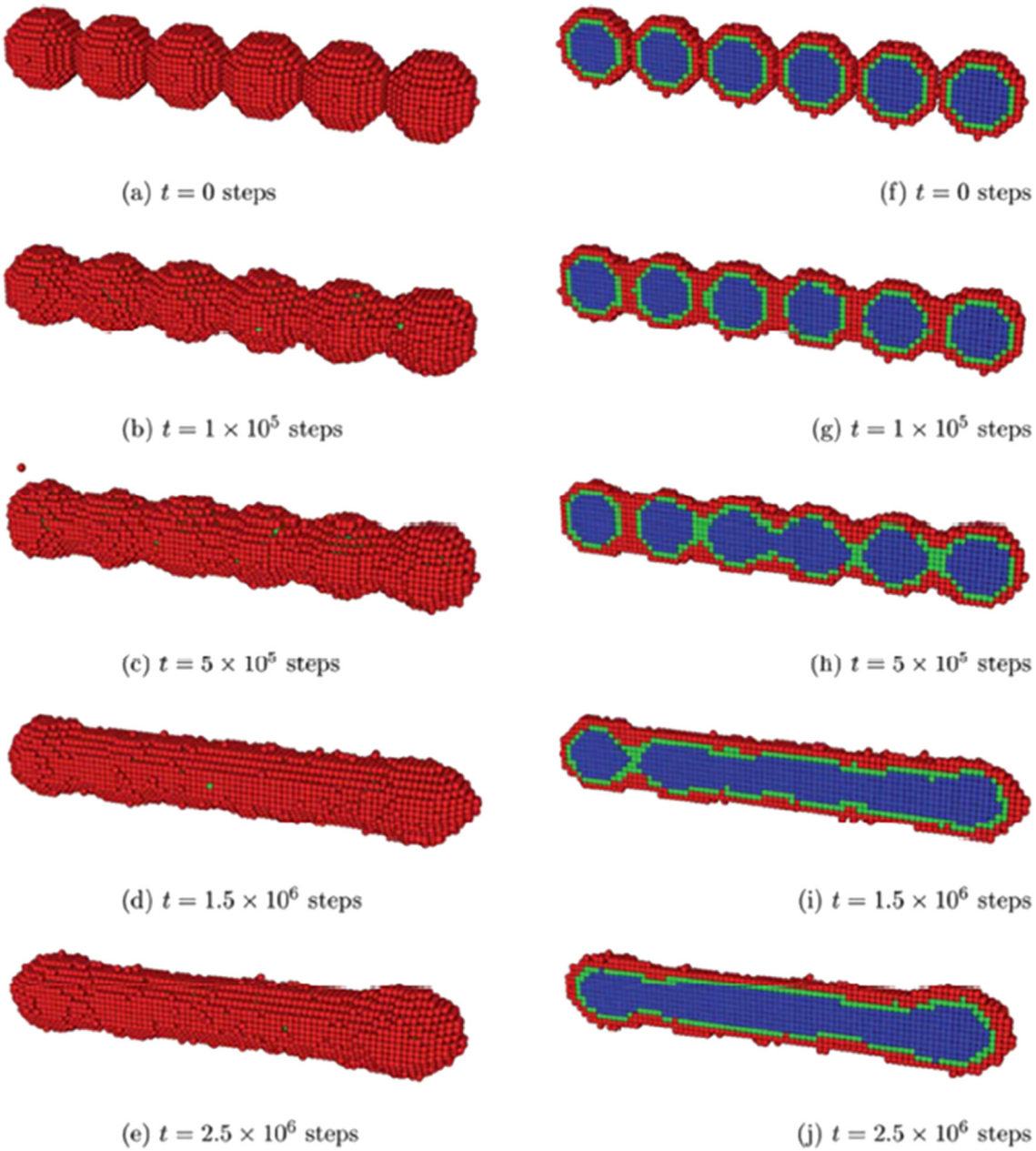

Fig. 4. Fusion of six uniluminal vascular spheroids predicted via a Kinetic Monte Carlo simulation.
Reprinted with permission from [67].

concentration, type of bioprinting process, and optimization and control of the bioprinting process.

4. Bioprinting processes

Bioprinting is an umbrella term that encompasses several different processes. Bioprinting processes can be broadly classified under four main categories (Table 1) namely, (i) Laser-based bioprinting, (ii) Droplet-based bioprinting, (iii) Extrusion-based bioprinting, and (iv) Stereolithography-based bioprinting. Laser-based bioprinting encompasses Laser-induced Forward Transfer (LIFT), Absorbing Film-assisted Laser-induced Forward Transfer (AFA-LIFT), Biological Laser Processing (BioLP), Matrix-assisted Pulsed Laser Evaporation Direct Writing (MAPLE DW), Laser-guided Direct Write (LG DW), and LG DW with an optical fibre guidance. Droplet-based bioprinting processes can further be divided into Inkjet bioprinting, electro-hydrodynamic jetting (EHD-jetting), acoustic bioprinting and microvalve-based bioprinting. Inkjet bioprinting is classified into continuous inkjet bioprinting (CIJ), and drop-on-demand inkjet bioprinting (Thermal, Piezoelectric and electrostatic DOD). Extrusion-based bioprinting could be pneumatic, piston or screw-based. Stereolithography bioprinting could be divided into two based on the use or non-use of patterns. The schematics of all the bioprinting processes are shown in Fig. 5.

4.1. Laser-based bioprinting

Laser-based bioprinting processes utilise laser energy to pattern cell-laden bioinks in a three-dimensional spatial arrangement with the aid of Computer-aided Design and Manufacturing (CAD/CAM). Laser radiation, being highly monochromatic, coherent, and highly focussed, was used for precise patterning of metals like Ag, $BaTiO_3$, and NiCr into active and passive mesoscopic circuit elements including conductors, capacitors and resistors, with a high spatial resolution of 1–3 μm [71]. High resolution and reproducibility of this process made it a viable option for use in biomedical applications such as cell printing [72]. The main components of a laser-bioprinting setup are a laser source (pulsed or continuous), laser transparent print ribbon (with or without a laser energy absorbing layer) coated with a layer of cell-laden bioink and a substrate or collector slide placed on a motorized stage. Based on the type of laser source and laser transparent print ribbon, the processes have slight variations and they include LIFT, AFA-LIFT, BioLP, MAPLE DW, and LG DW (with or without optical fibre guidance).

Laser-induced Forward Transfer (LIFT) (Fig. 5A) is a common laser-bioprinting method used for cell patterning and bioprinting of tissue constructs [73–75]. When the laser is irradiated on the laser transparent print ribbon, the laser energy is absorbed by the laser energy absorbing layer (which is a thin layer of metal such as gold), thereby creating a high gas pressure and thus, propelling a droplet of cell-laden bioink towards the substrate. When a thick (~100 nm) sacrificial metal layer (absorbing film) is coated on the laser transparent print ribbon to facilitate laser interaction, the process is called Absorbing Film-assisted Laser-induced Forward Transfer (AFA-LIFT) (Fig. 5B) [76, 77]. BioLP is a slightly modified version of AFA-LIFT, with use of a CCD camera to focus the laser radiation [78, 79]. AFA-LIFT and BioLP reduce the exposure of laser on the cell-laden bioink due to the presence of thick sacrificial layer thus reducing the risk of cell damage [78]. MAPLE DW (Fig. 5C) is similar to AFA-LIFT. While high power laser pulses are used in LIFT, AFA-LIFT, and BioLP, low power laser pulses operating in the UV or near-UV wavelength are used in MAPLE DW that prevents the penetration of laser into the bioink layer [72, 80]. In addition to the low powered laser pulses, the sacrificial energy absorbing layer is made of a biopolymer instead of metals that also facilitates initial cell attachment [81]. LG DW (Fig. 5D) is another technique that uses a weakly focused ~800 nm laser beam to move the cells in a liquid suspension (usually in cell media) using the laser force on to a moving substrate [82, 83]. LG DW with optical fibre guidance (Fig. 5E) is a modification of LG DW process, where the laser beam is coupled with hollow optical fibers to increase the working distance of LG DW from 300 μm to several millimetres or centimetres [72].

Laser-based bioprinting possesses many unique advantages. It is a non-contact process and hence, result in high post-printing cell viabilities (>95%) [77]. Being a nozzle-free approach, the problem of clogging is eliminated. High resolution, with the ability to print single cell per droplet, the capability of printing high cell densities (up to 10^8 cells

Table 1
Classification of 3D bioprinting processes.

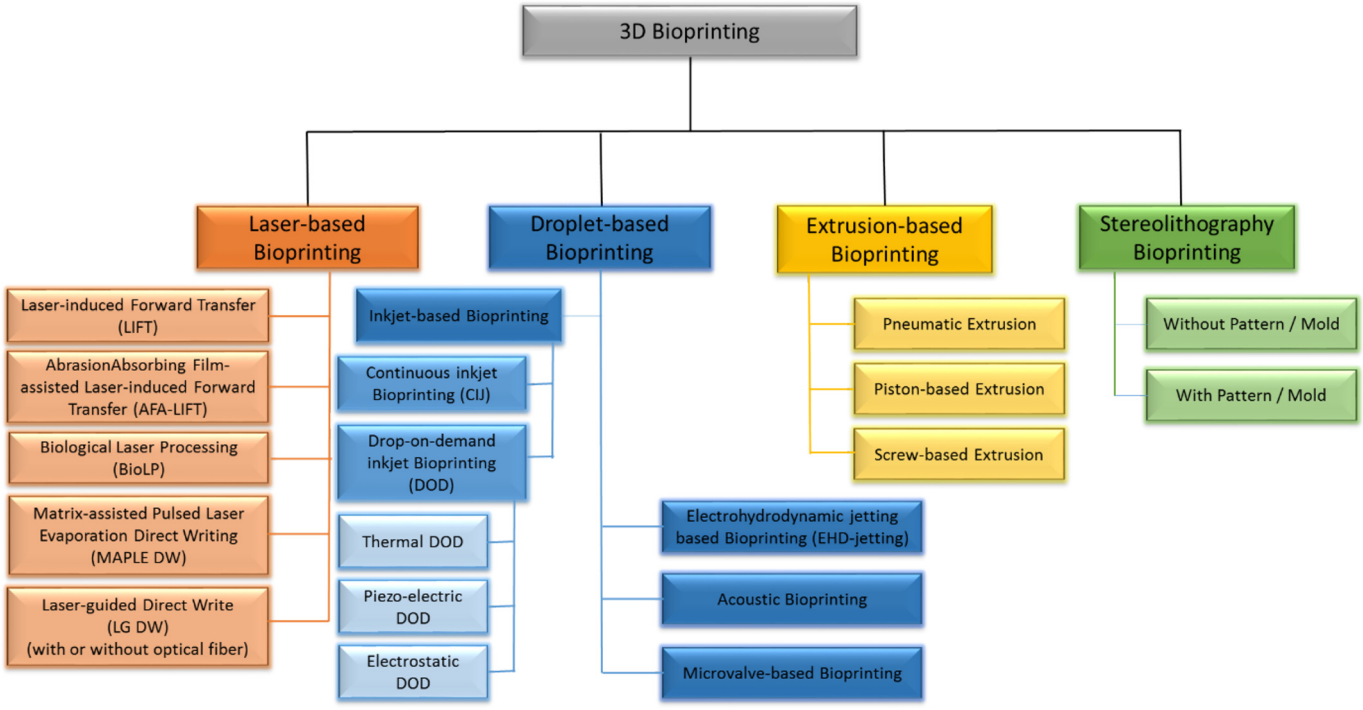

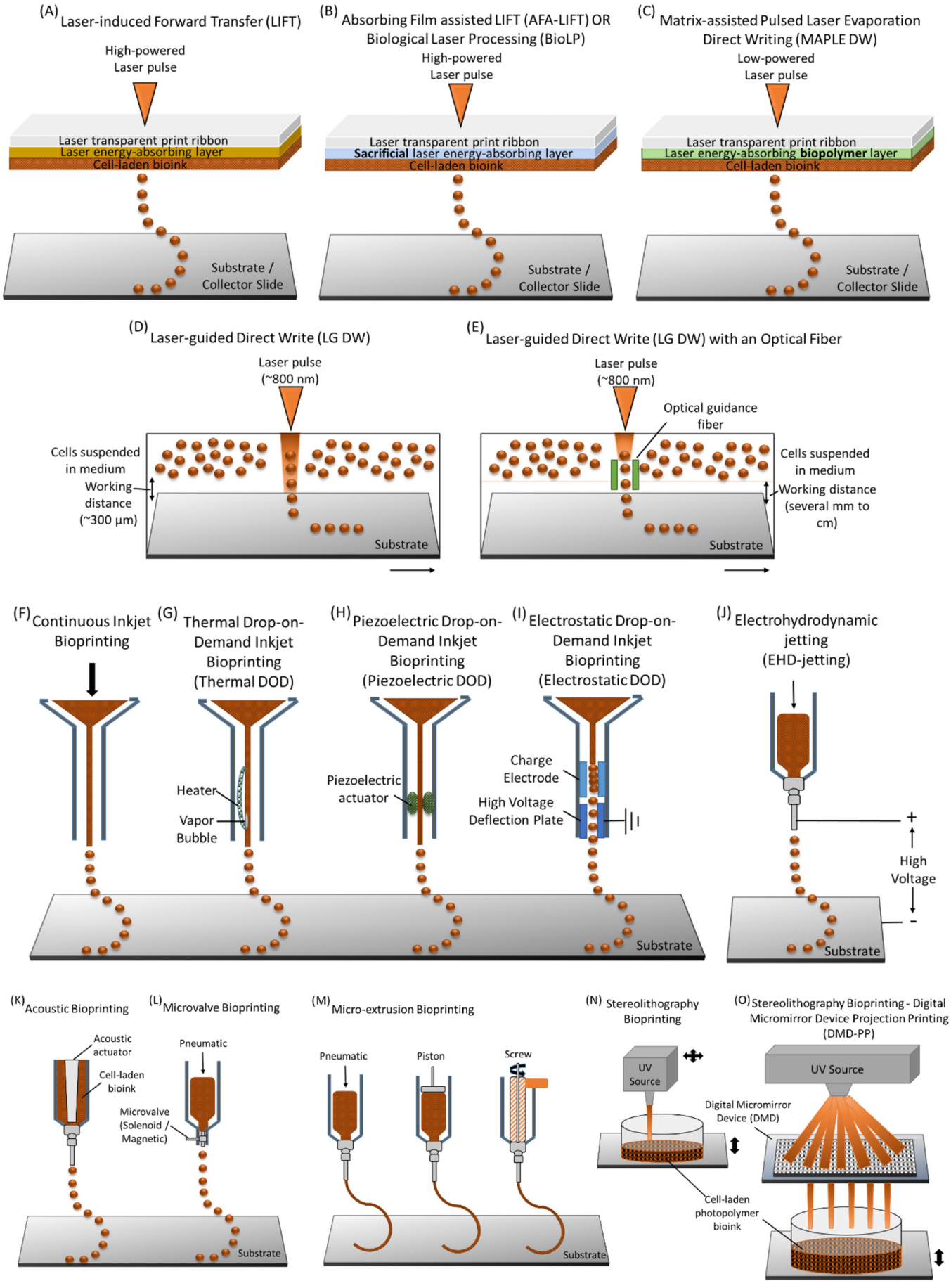
(A) Laser-induced Forward Transfer (LIFT)
High-powered Laser pulse
Laser transparent print ribbon
Laser energy-absorbing layer
Cell-laden bioink
Substrate / Collector Slide
(B) Absorbing Film assisted LIFT (AFA-LIFT) OR Biological Laser Processing (BioLP)
High-powered Laser pulse
Laser transparent print ribbon
Sacrificial laser energy-absorbing layer
Cell-laden bioink
Substrate / Collector Slide
(C) Matrix-assisted Pulsed Laser Evaporation Direct Writing (MAPLE DW)
Low-powered Laser pulse
Laser transparent print ribbon
Laser energy-absorbing biopolymer layer
Cell-laden bioink
Substrate / Collector Slide
(D) Laser-guided Direct Write (LG DW)
Laser pulse (~800 nm)
Cells suspended in medium
Working distance (~300 µm)
Substrate
(E) Laser-guided Direct Write (LG DW) with an Optical Fiber
Laser pulse (~800 nm)
Optical guidance fiber
Cells suspended in medium
Working distance (several mm to cm)
Substrate
(F) Continuous Inkjet Bioprinting
(G) Thermal Drop-on-Demand Inkjet Bioprinting (Thermal DOD)
Heater
Vapor Bubble
(H) Piezoelectric Drop-on-Demand Inkjet Bioprinting (Piezoelectric DOD)
Piezoelectric actuator
(I) Electrostatic Drop-on-Demand Inkjet Bioprinting (Electrostatic DOD)
Charge Electrode
High Voltage Deflection Plate
Substrate
(J) Electrohydrodynamic jetting (EHD-jetting)
+
High Voltage
-
Substrate
(K) Acoustic Bioprinting
Acoustic actuator
Cell-laden bioink
Substrate
(L) Microvalve Bioprinting
Pneumatic
Microvalve (Solenoid / Magnetic)
(M) Micro-extrusion Bioprinting
Pneumatic
Piston
Screw
Substrate
(N) Stereolithography Bioprinting
UV Source
Cell-laden photopolymer bioink
(O) Stereolithography Bioprinting - Digital Micromirror Device Projection Printing (DMD-PP)
UV Source
Digital Micromirror Device (DMD)

per ml) and low viscosity cell suspensions (1–300 mPa s) [77, 84] are some of the other advantages.

There were several successful attempts of using laser-based bioprinting to print cells in a 3D spatial arrangement reported in the literature including NIH3T3 fibroblasts and HaCaT keratinocytes [85], human dermal fibroblasts [86], human mesenchymal stem cells (hMSCs) [85], rat Schwann cells and astroglial cells [77], Human umbilical-vein endothelial cells (HUVEC) and Human umbilical-vein smooth muscle cells (HUVSMC) [87], and Multipotent adult progenitor cells (MAPC) [88]. Not only living cells but also peptides [89] and DNA [90] are patterned using Laser-based bioprinting processes. In addition to the cell patterning, fabrication of multi-layered tissue constructs such as skin tissue [75, 91], were also attempted using Laser-based bioprinting processes.

In spite of the several advantages that Laser-based bioprinting holds over the other bioprinting methods, there are also many challenges. Despite the attempts to mitigate the effect of laser radiation on the cells by using a low-powered laser and/or coating a thick sacrificial layer, the risk of laser exposure still could not be completely eliminated. Hence, there is always a risk of photonic cell damage [72]. The use of metals as a laser-energy absorbing layer in processes such as LIFT and AFA-LIFT poses the problem of metallic nanoparticles induced cytotoxicity [92]. Scalability of the process is another limitation [1]. Fabrication of the laser print ribbon, the high cost of laser systems and complexity of controlling the laser pulses adds to the list of disadvantages of this method.

The disadvantages of laser-based bioprinting outweigh its advantages. The nature of the method makes it unsuitable for fabrication of full-scale tissue constructs that are suitable for regenerative medicine. But, the process can be used for high-resolution cell level patterning of multi-cellular microenvironments such as tumor microenvironment (TME) for disease modelling or drug testing [93]. Since laser-based bioprinting is based on optical principles and forces, optically selective cell targeting and transfer could be possible in the future [72]. However, a detailed study on process-induced photonic cell damage has to be done before translational use. Complete elimination of laser exposure of the cells during the process, simplification of the print ribbon fabrication, and eliminating the use of metals or other non-biological materials as the laser energy absorbing layer are some of the areas of process improvement that could be worked on. Despite all the improvements, the scalability of the process and complexity of handling the whole system hinders laser-based bioprinting from becoming translational.

4.2. Droplet-based bioprinting

Droplet-based bioprinting processes eject cell-laden bioinks out of the nozzle onto a substrate in the form of droplets. They can be classified further into Inkjet bioprinting (CIJ and DOD - Thermal, Piezoelectric and electrostatic), electro-hydrodynamic jetting (EHD-jetting), acoustic bioprinting and microvalve-based bioprinting.

4.2.1. Inkjet bioprinting

Inkjet bioprinting is adapted from the inkjet printing technology, with the printing ink cartridges replaced by cell-laden bioink cartridges. Inkjet bioprinting can be broadly classified under two headings, namely continuous inkjet (CIJ) and drop-on-demand (DOD) inkjet printing. CIJ (Fig. 5F) bioprinting ejects a stream of cell-laden bioink droplets by the formation of Rayleigh-Plateau instability when pressurized through a nozzle [94]. Due to the nature of the process, the droplet could not be precisely controlled in CIJ and hence, DOD is the preferred method for bioprinting [95]. DOD inkjet bioprinting techniques eject droplets on demand or only when a trigger is given, aiding in precise control and positioning of droplets. Based on the type of trigger, the DOD inkjet bioprinting could be thermal, piezo-electric, or electrostatic DOD systems. In thermal DOD inkjet bioprinting (Fig. 5G), a voltage pulse is applied to a thermal actuator to locally heat the bioink. The localized heating creates a vapour bubble, which rapidly expands and explodes, thereby overcoming the surface tension force of the bioink at the nozzle tip and forcing the bioink droplet out of the nozzle. Piezoelectric DOD inkjet bioprinting (Fig. 5H) employs a piezoelectric actuator which expands or contracts when a voltage pulse is applied. This expansion or contraction upon application of a voltage pulse is used to deform the bioink chamber, causing a pressure wave inside the chamber and a droplet of bioink is ejected out from the nozzle. Electrostatic DOD inkjet bioprinting (Fig. 5I) utilizes a high voltage deflection plate, which changes the volume of the bioink chamber when a high voltage is applied between the plate and charge electrode, thus ejecting droplets of bioink out of the nozzle. Cell-laden bioinks were bioprinted using thermal DOD [96, 97], piezoelectric DOD [98, 99], and electrostatic DOD [100] inkjet bioprinting methods with a post-printing cell viability of >80% [5, 101]. Inkjet bioprinting had been used for printing cells and tissue constructs of bone [102, 103], cartilage [104, 105], skin [106], cardiac [107], and nervous tissue [108].

The advantages of inkjet bioprinting are high resolution (~50 μm), high printing speed (up to 10,000 droplets per second), affordability, and the ability to introduce cell concentration gradients [84, 101]. However, there are several limitations. Only low-viscosity bioinks (~3–12 mPa s) can be printed, which requires an additional cross-linking step to render the construct structural stability. Nozzle clogging is another challenge with the inkjet bioprinting systems, which limits the cell concentration in the bioink to be $<10^6$ cells per millilitre [84].

4.2.2. Electro-hydrodynamic jetting (EHD-jetting)-based bioprinting

In EHD-jetting-based bioprinting (Fig. 5J), a high voltage (0.5–20 kV) is applied between the nozzle and the substrate as a back-pressure supply delivers the bioink to the nozzle tip [109, 110]. When the applied electric field force overcomes the viscoelastic force of the bioink and surface tension force at the nozzle tip, droplets of bioink are ejected out of the nozzle by the formation of a Taylor cone [110–112]. EHD-jetting, based on the applied voltage and the nozzle-to-substrate distance, can be operated in different modes, namely dripping, spindle, oscillating jet and cone-jet mode [113]. Living cells such as Jurkat cells [114], mouse neuronal cells (CAD) [115], human embryonic kidney cells (HEK 293 T) [116], and 3 T3 mouse fibroblasts [117] were patterned using EHD-based bioprinting, demonstrating that the cells can survive the high electric fields and forces associated with the jetting process [109]. The process had been successfully used for printing patterned protein arrays [118] and DNA Oligonucleotides [119].

The greatest advantage of EHD-jetting-based bioprinting is the high resolution it offers compared to the other bioprinting methods. A nanoscale resolution of ~100 nm had been achieved using this method [119]. Bioprinting of very high viscosity bioinks (up to 20% w/v) [114] is possible with this technique, which is another unique advantage of EHD-jetting-based bioprinting. There are two main limitations of this technology. Although the cell viability immediately after printing or a few hours or days after printing might be high, application of high voltage and subjecting the cells through high electric fields might affect the long-term post-printing cell viability [120]. Secondly, the process creates a continuous stream of droplets or jet rather than droplets on demand and hence, precise spatial placement of cells is onerous, if not impossible [95].

4.2.3. Acoustic bioprinting

Acoustic bioprinting (Fig. 5K) is relatively a new method of bioprinting that can eject droplets of cell-laden bioinks on demand.

Fig. 5. Types of 3D bioprinting Processes (A–E) Laser-based bioprinting methods, (F–I) Inkjet-based bioprinting methods, (J) Electrohydrodynamic jetting bioprinting, (K) Acoustic bioprinting, (L) Microvalve-based bioprinting, (M) Micro-extrusion bioprinting, (N) Stereolithography bioprinting, and (O) Stereolithography bioprinting – Digital Micromirror Device-Projection Printing (DMD-PP).

Cell-laden bioink is held in an open pool, with an acoustic actuator at the centre, as shown in Fig. 3k. Surface tension force keeps the bioink static at the small nozzle tip. When the acoustic actuator, containing a piezoelectric substrate and interdigitated gold rings, is actuated, circular acoustic waves are generated with its focal point at the air-bioink interface at the nozzle tip, overcoming the surface tension force and thereby ejecting droplets of bioink onto the substrate [121]. Several cell types including mouse embryonic stem cells, fibroblasts, AML-12 hepatocytes, human Raji cells, and HL-1 cardiomyocytes were printed using this technique [121], with post-printing cell viabilities of >90%.

The advantage of this method over other DOD techniques is that the bioink is an open pool rather than in a nozzle, thus eliminating the exposure of cells to detrimental stressors such as heat, high pressure, and high voltage [95]. High resolution (~37 μm) and high printing speed (up to 10,000 droplets per second) are other advantages. With high viscosity bioinks or bioinks with high cell concentration, the acoustic force required to eject a droplet will also considerably increase, causing a detrimental effect on cells. There are only a few studies published on acoustic bioprinting and further detailed studies are required for objective evaluation of this technology.

4.2.4. Microvalve bioprinting

Electromechanical or solenoid valves are used to control the ejection of droplets of cell-laden bioink in a microvalve bioprinting system (Fig. 5L). The bioink is delivered to the nozzle tip by pneumatic pressure. Application of voltage pulse to the valve causes the valve to open due to solenoid action and when the pneumatic pressure overcomes the viscoelastic force of the bioink and surface tension force at the nozzle tip, a droplet of bioink is ejected out of the nozzle [122]. This is also a drop-on-demand system and the droplets are ejected only when a voltage pulse is applied to the valve. Microvalve bioprinting had been used to print several types of cells including HFF-1 fibroblasts and HaCaT keratinocytes [91], primary bladder smooth muscle cells (SMCs) [123, 124], and human alveolar epithelial type II cell line A54956 and the EA.hy926 hybrid human cell line [125], with a post-printing cell viability of >80% [125]. The method was also used to print 3D tissue constructs like multi-layered skin tissue [91], and lung tissue analogue [125].

Microvalve bioprinting, if used with multiple print heads, has the greatest advantage of synchronized ejection from different print heads [122], aiding in the printing of co-culture, and multi-culture tissue constructs. The range of pneumatic pressure used in microvalve bioprinting is lesser than that used in inkjet bioprinting and hence, the cells are less prone to damage or injury [95]. It has moderate printing speeds of up to 1000 droplets per second [91], which is far lesser than inkjet bioprinting and a low resolution compared to other droplet-based bioprinting systems. Clogging of the nozzle is a challenge with microvalve bioprinting, limiting the bioink viscosity to 1–200 mPa s and a cell concentration of fewer than 10^6 cells per millilitre. A candid evaluation of this bioprinting technique is not possible now, with only a very few published studies available [95].

4.3. Extrusion-based bioprinting

Extrusion-based bioprinting is the most widely used of all bioprinting modalities. The bioink is extruded out of the nozzle using pneumatic pressure or mechanical force by means of a piston or screw (Fig. 5M). Extrusion-based bioprinting had been used to bioprint cells, tissues, organ modules, and organ-on-a-chip devices, for tissue engineering, cancer research, drug testing, and transplantation [6]. Several tissue types including but not limited to bone [126, 127], cartilage [128], skeletal muscle [129], skin [1, 130], cardiac tissue [131], nervous tissue [132], and liver [133].

Extrusion-based bioprinting has many advantages. The first and foremost advantage of this method is the scalability i.e. the ability to print human-scale tissue, which is impossible with any of the other bioprinting methods. The continuous flow of bioink and large deposition rate makes this method scalable. Printability of high viscosity bioinks (~600 kPa s) and high cell concentration commensurate with natural tissues [134] is another advantage. Though scalability is the greatest asset that this technology possesses, it comes at the cost of resolution. Extrusion-based bioprinting has the lowest resolution (~100 μm) of all the bioprinting systems [135]. The resolution of the system could be improved by reducing the nozzle diameter but the increased shearing force might result in cell damage and injury [136]. Post-printing cell viability could be 40% to 95% [84], depending on the bioink viscosity, cell concentration and nozzle size. Nozzle-clogging is an inherent problem with extrusion-based bioprinting. Another limitation posed by this process is the requirement of bioinks with shear-thinning property for successful printing, which limits the versatility of the bioinks that could be used.

4.4. Stereolithography bioprinting

Stereolithography, though developed in 1996 by 3D Systems, is still a fledgling technology in the bioprinting space. The working principle of stereolithography is discussed elsewhere [137]. Briefly, a layer of photopolymer resin is cured (or polymerized) by light (usually UV) irradiation, the light movement controlled by a computer code/images/CAD files, forming a 3D structure as the build stage is translated vertically building the object layer by layer. There are two modalities of stereolithography. In the first one (Fig. 5N), the light source is computer controlled and moves per the structure required in each layer of the 3D object. The second modality (Fig. 5O) employs an array of several thousand micro-mirrors called a Digital Micromirror Device (DMD), each of the micromirror could be controlled to reflect light in a spatial pattern (coding/image/CAD/STL file), thus polymerizing a whole layer at once [138]. Stereolithography using DMD is referred to as Digital Micromirror Device-Projection Printing (DMD-PP). DMD-PP thus significantly reduces the print time as the whole layer is polymerized at once rather than the light source travelling according to the pattern in each layer. Stereolithography bioprinting is still not explored in detail and hence, only a very few studies were reported till date. These include bioprinting of NIH-3T3 murine embryonic fibroblasts and C3H/10T1/2 murine mesenchymal progenitor cells [138], human dermal fibroblasts (HDFs) [139], and embryonic dorsal root ganglia (DRG) [140].

Stereolithography bioprinting offers the highest resolution (~6 μm) of all the bioprinting methods [138]. With the advent of two-photon polymerization based stereolithography [141], very high resolution in nanometre scale (~200 nm) could be obtained. With DMD-PP, reduced printing time is an advantage. Since it is a nozzle-free process, the problem of nozzle clogging is eliminated and bioinks with high cell concentrations (>10^6 cells per millilitre) can be used. Despite the highest resolution offered by this process, it suffers from serious limitations that hinder its use in bioprinting of cells and tissues. Firstly, only photopolymerizable bioinks or bioinks containing a UV-activated photo initiator (Irgacure 2959 (2-hydroxy-1-[4-(2-hydroxyethoxy)phenyl]-2-methyl-1-propanone is commonly used) can be used. Though there are a few works on development of biodegradable photopolymerizable bioinks including Poly(ethylene glycol) dimethacrylate (PEGDMA), poly(propylene fumarate) (PPF), trimethylene carbonate (TMC), and ε-caprolactone (CL) [139, 142, 143], the photoinitiator (Irgacure 2959, which is least cytotoxic among the photoinitiators) is cytotoxic and the post-printing cell viability after 24 h is as low as 25% [139]. Secondly, the cells are exposed to UV radiation and are prone to cell lysis and DNA damage [84]. The UV radiation could also damage the DMD system [144]. To overcome this problem, a visible-light DMD-PP is reported, which uses visible-light activated eosin-Y-based photoinitiator [144]. Post-printing cell viability (NIH-3 T3 fibroblasts) was over 85% after five days. Further studies are required to evaluate the long-term effects of the photoinitiator and photo-initiated cell damage. Only low viscosity (~5 Pa s) bioinks could be used with stereolithography bioprinting.

Each of the bioprinting methods has its own pros and cons as detailed in this section (refer Table 2 for comparison of different bioprinting methods). No one method could be used singly to realize the goal of fully functional tissue or organ printing. Laser-based bioprinting and stereolithography bioprinting has the highest resolution but lacks scalability and cannot be used to print human scale tissues and organs. Though there were several studies reporting high post-printing cell viabilities, further detailed studies on photo-initiated cell damage and the long-term effects of laser/UV radiation on the cells are required. Droplet-based bioprinting, particularly DOD, can be used to precisely pattern the cells in a co-culture or multi-culture platforms but bioprinting human scale tissues is still an onerous task with DOD bioprinting. Extrusion-based bioprinting has the least resolution of all the bioprinting systems but has the highest potential to bioprint human scale tissues and organs. Hence, it is important to develop hybrid bioprinting systems, combining the advantages of several bioprinting methods to bioprint physiologically relevant functional tissues. There are a few works reporting this trend. Kim et al. [145] reported a hybrid bioprinting system that could simultaneously print using extrusion-based and inkjet-based dispensing methods. They demonstrated a single-step bioprinting of 3D human skin model using this hybrid system, consisting of three printing methods – melt extrusion was used to print PCL mesh, which serves as the scaffold or support structure, extrusion-based bioprinting for the dermal layer of the skin, and inkjet DOD bioprinting for patterning of the keratinocytes over the dermal layer which forms the epidermal layer. The future of bioprinting lies in building such hybrid bioprinting systems, with the ability to simultaneously use different bioprinting modalities, taking advantage of different methods and thus trading off with the limitations, to bioprint fully functional, physiologically relevant tissues and organs with complex multi-layer, multi-cellular architecture.

5. 3D bioprinted tissues and organs

There has been a considerable progress in the bioprinting domain, with various types of tissues being printed and tested. The human body consists of several organ systems that work together to maintain homeostasis and normal body functioning. An organ system, in turn, consists of several organs, tissues and anatomical structures that work together to perform a defined function. There are eleven organ systems in the body namely skeletal, muscular, nervous, lymphatic, endocrine, reproductive, integumentary, respiratory, digestive, urinary, and circulatory systems. This section reviews in detail the status of application of bioprinting in all these organ systems (Fig. 6).

5.1. Skeletal system

The skeletal system consists primarily of bones and cartilages, along with bands of fibrous connective tissues namely tendons and ligaments. This system serves as the structural framework of the human body, giving support and shape to the body. The loss or damage to the skeletal tissue is caused by a variety of factors which include trauma, disease, injury and ageing, and leads to significant morbidity and socio-economic burden [146]. There is an exceedingly high demand for functional bone grafts worldwide, with more than half a million patients receiving bone defect repairs annually in the US alone [147]. Hence, bioprinting of skeletal tissues such as bone and cartilage is one of the major focus areas in the field of tissue engineering and regenerative medicine.

5.1.1. Bone

Bone, being a dynamic vascularized tissue, is capable of self-healing and remodeling without scarring [148]. However, bone replacement or surgical intervention is often required for critical-size bone defects [149]. These critical-size bone defects might be congenital or acquired, most often resulting from trauma or tumors [148, 149]. Due to the inherent limitations of the autografts, and allografts, including donor site morbidity, immune rejection, and availability [3, 10], metal or ceramic implants are being used as alternative intervention method. But, these inert implants fail over time due to repetitive loading [150]. Hence, tissue-engineered bone constructs are looked upon as a potential treatment method. With traditional tissue engineering methods, porous ceramic or polymeric scaffolds are used to fabricate an engineered bone [151], With the advent of bioprinting, more complex bone structures could be printed, with multiple types of cells suspended in a hydrogel be spatially arranged to form a biomimetic bone construct for testing and clinical transplantation.

In one of the earlier studies [152], bone marrow stromal cells (BMSCs) (obtained from iliac bone marrow aspirates of two-year-old Dutch milk goats) suspended in alginate hydrogel (2% w/v) at a concentration of 1×10^6 cells per millilitre were bioprinted using pneumatic extrusion bioprinting method. Post-printing cell viability after 2 weeks indicated that there is no difference between the printed and unprinted constructs. The printed cells also retained the differentiation ability to the osteogenic lineage, as evaluated by the osteogenic marker alkaline phosphatase (ALP). In another study [153], human osteogenic sarcoma cells, SaOS-2, was suspended in an alginate/gelatin hydrogel (5% w/v of sodium alginate and 5% w/v of gelatin) at a concentration of 5×10^5 cells per millilitre and bioprinted using pneumatic extrusion bioprinting method. While the cells were in a non-proliferating state in the hydrogel, there was a marked increase in cell proliferation when an overlay of agarose and the calcium salt of polyphosphate [polyP·Ca^{2+}-complex] was added, evaluated using MTT assay, 6 days post-printing. Alizarin Red S staining done on day 7 post-printing showed better mineralization in the samples treated with polyP·Ca^{2+}-complex, compared with those samples without polyP·Ca^{2+}-complex overlay. This study is weak with limited data on the quantification of cell differentiation and being a short-term study.

Gao et al. [154] used inkjet bioprinting to print human MSCs (harvested from a 22-year-old male) suspended in PEG-GelMA hydrogel (10% w/v of PEG and 1.5% w/v of GelMA, supplemented with 0.05% w/v

Table 2
Comparison of various bioprinting methods.

Properties	Laser-based bioprinting	Inkjet bioprinting	EHD-jetting based bioprinting	Acoustic bioprinting	Microvalve bioprinting	Extrusion-based bioprinting	Stereolithography bioprinting
Bioink viscosity	1–300 mPa·s	3–12 mPa·s	1–1000 mPa·s	–	1–200 mPa·s	~600 kPa·s	~5 Pa·s
Cell density	10^8 cells/ml	10^6 cells/ml	10^6 cells/ml	10^6 cells/ml	10^6 cells/ml	10^8 cells/ml	>10^6 cells/ml
Speed	200–1600 mm/s	10,000 droplets per second	10–500 mm/s	10,000 droplets per second	1000 droplets per second	10–50 μm/s	High
Resolution	50 μm	50 μm	100 nm	37 μm	–	100 μm	200 nm–6 μm
Accuracy	High	Medium	Low	Medium	Medium	Low	High
Cell viability	>95%	>80%	>80%	>90%	>80%	40–95%	25–85%
Structural integrity	Low	Low	High	Low	Low–Medium	High	Medium–High
Scalability	Low	High	High	Medium	High	High	Medium-High
Cost	High	Low	High	Medium–High	Medium	Low–Medium	Medium

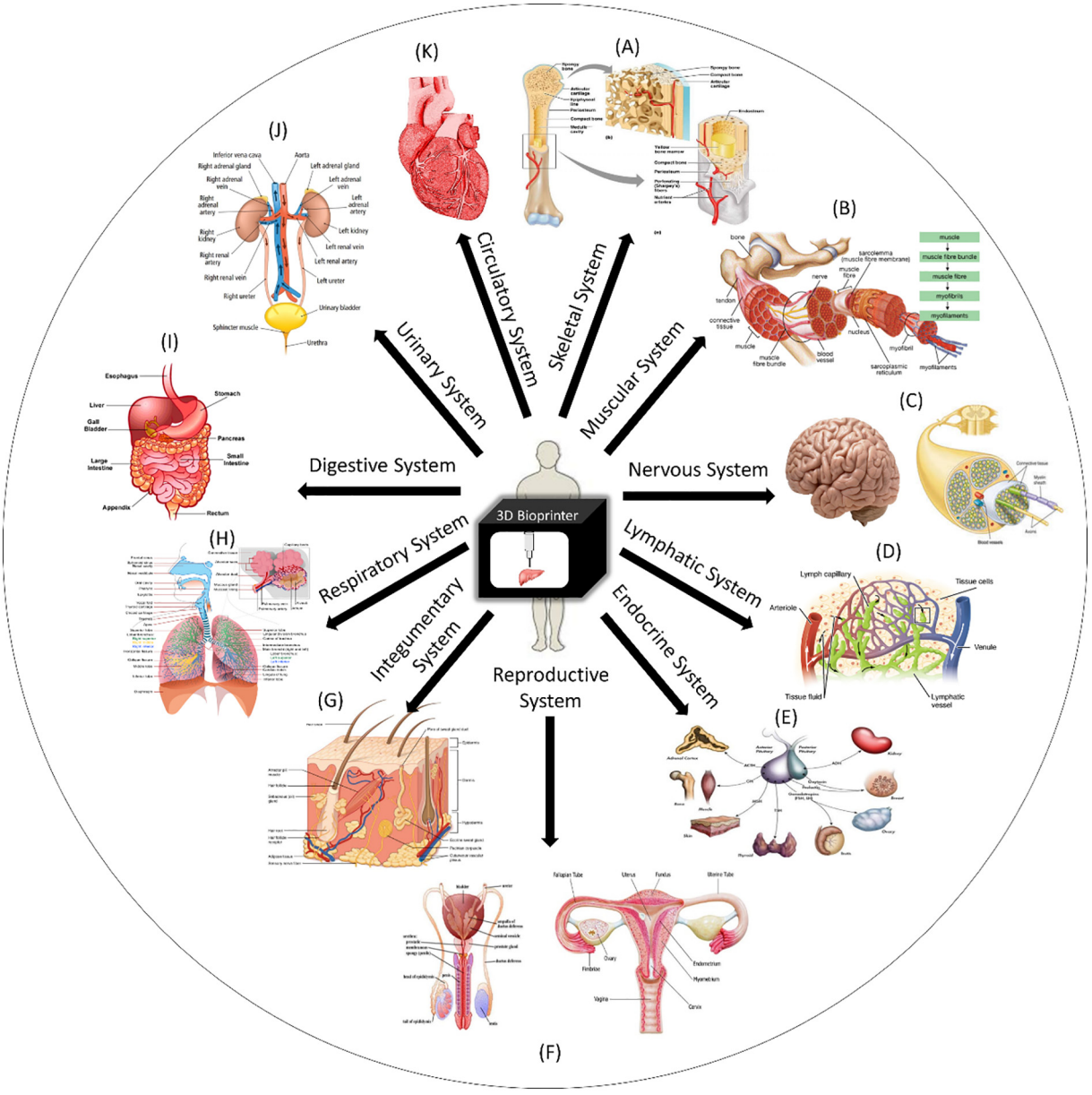

Fig. 6. Applications of bioprinting in different organ systems of the human body (A) Skeletal (www.jouefct.com), (B) Muscular (www.notinmycolour.com), (C) Nervous (www.medical-dictionary.thefreedictionary.com), (D) Lymphatic (www.medical-dictionary.thefreedictionary.com), (E) Endocrine (www.conceiveeasy.com), (F) Reproductive (http://www.med.umich.edu), (G) Integumentary (www.humananatomy-libs.com), (H) Respiratory (www.medicinembbs.blogspot.sg), (I) Digestive (www.kidshealth.org), (J) Urinary (www.tes.com), and (K) Circulatory systems. Individual image sources are given in parentheses.

of Irgacure 2959) at a concentration of 6×10^6 cells per millilitre, with PEG hydrogel (10% w/v of PEG, supplemented with 0.05% w/v of Irgacure 2959) as control. Addition of GelMA promoted early differentiation of hMSCs to osteogenic lineage as determined by specific gene and protein expression analysis (RUNX2, SP7, DLX5, ALPL, Col1A1, IBSP, BGLAP, SPP1, Col10A1, MMP13, SOX9, Col2A1, ACAN) compared to the control, 21 days post-printing. In another study by Campos et al. [155], human bone marrow-derived MSCs (isolated from femoral heads of patients receiving hip-joint arthroplasty) at a concentration of 1.6×10^6 cells per millilitre were suspended in agarose/collagen (AG/COL) hydrogel, with agarose and collagen concentrations varying from 0.5 to 2.0 g/ml, and 0.21 to 0.05 g/ml, respectively, for less stiff AG0.5-COL0.21, intermediate stiff AG1-COL0.10, and stiffer AG2-COL0.05. The higher the concentration of collagen, the less stiff the hydrogel is. Cell viability of over 98% was achieved 21 days after the MSCs are bioprinted in AG/COL hydrogels with varying concentrations using inkjet bioprinting method. The cells also maintained the mesenchymal phenotype, as proved by positive staining of vimentin (VIM) and negative staining of CD34. Similar mineralization results were obtained with all three hydrogel variations and hence, the stiffness of the hydrogel didn't play a role in mineralization. While ALP activity was similar in all three hydrogels irrespective of the stiffness, the less stiff hydrogel (AG0.5-COL0.21) showed significantly higher gene expression of COL1 and RUNX2, in comparison to hydrogels with intermediate stiff and stiffer matrices (AG1-COL0.10, and AG2-COL0.05 respectively). From the literature [156], stiffer matrices promote osteogenic differentiation than softer substrates. However, this study is not conclusive enough to pronounce the hypothesis as the qPCR results and ALP activity signals don't match. Further research is needed to arrive at a conclusion as to the effect of hydrogel stiffness on the differentiation of MSCs.

Cui et al. [157] used a hybrid bioprinting system consisting of a Fused Deposition Modelling (FDM) printer and stereolithography bioprinting to fabricate vascularized bone biphasic constructs. FDM was used to print PLA fibers and stereolithography bioprinting to print cell-laden

GelMA hydrogel. PLA scaffolds were coated with polydopamine (pDA) on which BMP2 peptides were immobilized, which represents the bone region in the biphasic construct while VEGF-peptides conjugated GelMA represented the vascular region. A co-encapsulation of hMSCs (2×10^5 cells/ml) and HUVECs (1×10^6 cells/ml) in the GelMA hydrogel (10% w/v) was bioprinted using stereolithography bioprinting on the PLA scaffold which was pre-seeded with hMSCs (2×10^5 cells/ml). The osteogenic and angiogenic differentiation of the printed biphasic construct was evaluated four weeks post-printing by ALP activity, collagen type I expression, assaying VEGF secretion, quantifying calcium deposition, and differentiation markers osteopontin (OPN) for osteogenic differentiation, von Willebrand factor (vWf) as angiogenic specific marker, and CD31 for endothelial cells representing the capillary network formation. This study serves as a proof of concept for fabrication of vascularized, hierarchically biomimetic construct, with multiphasic characteristics.

Levato et al. [158] used microcarriers (MCs) in hydrogels to bioprint an osteochondral graft model. MCs are micron-sized particles with a high specific surface area designed to promote cell attachment and proliferation. In this study [158], PLA MCs functionalized with human recombinant collagen type I with a mean diameter of 120 μm, and a surface area of 2 cm^2 mg^{-1} were used. MSCs (isolated from the long bones of 2–4 weeks old Lewis rats) at a concentration of 8×10^6 cells per millilitre and MCs (30 mg/ml) were mixed together with GelMA-gellan gum (GelMA-GG) hydrogel (10% w/v GelMA supplemented with 5.4% w/v D-mannose and 0.1% w/v of Irgacure 2959, and 1% w/v gellan gum) and subsequently bioprinted using extrusion bioprinting system. Bioprinted constructs evaluated by ALP activity, osteocalcin (OCN) secretion, and alizarin red staining, 21 days post-printing, revealed that the cells differentiated and the mineralized matrix was deposited.

Keriquel et al. [159] used LIFT method for in situ printing of mesenchymal stromal cells (multipotent mouse bone marrow stromal precursor D1 cell line (ATCC) at a cell density of 120×10^6 cells/ml) suspended in a nano-hydroxyapatite (nHA) – collagen hydrogel (1.2% (w/v) nHA in 2 mg/ml type I rat collagen) on a calvaria defect model in mice (sixty-four 12-week-old Balb/c female mice). Two different patterns were printed, namely a ring (external and internal diameter of 3 and 2.1 mm respectively) and a disk (2 mm diameter). Two experimental groups tested were D1 cells suspended in the nHA-collagen hydrogel in a ring pattern (with nHA-collagen hydrogel without D1 cells in a ring pattern as control) and nHA-collagen hydrogel in disc pattern (with nHA-collagen hydrogel without D1 cells in a disc pattern as control). In situ printed constructs were monitored for 42 days post-printing using luminescence imaging of luciferase-positive D1 cells. X-ray micro tomography (μCT) images were taken and hematoxylin-eosin saffron (HES) staining was performed to evaluate the bone regeneration rate 2 months post-printing. Results revealed that the bone regeneration was only marginal in a ring geometry (both experimental and control) witnessed at the periphery of the defect while a substantial new bone formation, well distributed throughout the defect was seen with the disc geometry (shown in Fig. 7A). This study not only proved the potential of laser-based bioprinting in bone tissue regeneration but also the effect of different cellular patterns (ring and disc in this study) on the regeneration potential.

Daly et al. [160] reported an interesting approach of bioprinting a developmental precursor that would act as a template for organogenesis in vivo. Bone marrow-derived MSCs (isolated from the femoral shaft of 4-month-old pigs) suspended in a hydrogel containing gamma-irradiated alginate incorporating Arg-Gly-Asp (RGD) specific adhesion peptides (RGD-γ alginate hydrogel) (2.45% w/v) was bioprinted alongside PCL fibers to form a hypertrophic cartilage rudiment structure. The bioprinted construct, after being chondrogenically primed, was implanted subcutaneously into the back of nude mice (Balb/c; Harlan, UK) for 12 weeks to evaluate the potential of organogenesis. H&E staining, μCT, and Goldner's trichrome staining after 12 weeks showed an extensively vascularized and mineralized bone organ containing trabecular-like endochondral bone with a supporting marrow structure (shown in Fig. 7B&C). It was reported that the bone formation happened via an endochondral pathway through remodeling of the hypertrophic cartilage template, substantiated by the intense staining for collagen type X, thus proving the hypothesis that a bioprinted developmental precursor would act as a template for organogenesis in vivo, forming a matured organ over time. Since bioprinting a developmental precursor is undemanding compared to bioprinting a biomimetic matured solid organ with its intricate complexities, this is a promising approach that could be used to engineer more complex solid organs.

5.1.2. Cartilage

Osteoarthritis is a degenerative joint disease, characterized by progressive loss of hyaline cartilage in the synovial joints [161], affecting millions of people worldwide. About 37% of the adults over 65 years of age are affected by osteoarthritis in the USA, with an associated economic burden of $3.4 to $13.2 billion per year [162]. Joint arthroplasty, where the diseased cartilage and the underlying bone are replaced with a metal or polymer prosthesis, is the current gold standard, which suffers serious limitations and post-surgical complications [161]. Hence, tissue-engineered cartilages are seen as a potential alternative therapy. Cartilage is an avascular tissue with a low number of cells (10–15%), which accounts for its limited regenerative capacity [128, 163]. The disadvantage of cartilaginous tissue serves as the advantage for bioprinting as an avascular low cell density tissue is comparatively easier to be bioprinted than vascularized highly-complex tissues.

The most commonly used hydrogels for cartilage bioprinting are alginate and collagen [164]. Maintaining the shape fidelity with these hydrogels is difficult and it poses a major limitation. Synthetic polymers such as PCL, polyglycolic acid (PGA), hydroxyapatite, and methacrylate were coupled with the hydrogels to increase the shape fidelity [165]. To improve the shape fidelity, Rhee et al. [164] used a highly concentrated collagen hydrogel (10–20 mg/ml) to bioprint meniscal fibrochondrocytes (isolated from 1 to 3-day old bovine joints) at a concentration of 10×10^6 cells per millilitre. Higher the collagen concentration higher was the shape fidelity. Post-printing cell viability was above 90% until 10 days. Recently, use of nanofibrillated cellulose (NFC) to improve the shape fidelity of the hydrogels, and to provide structural and mechanical support are reported. In one such study [163], NFC was mixed with sodium alginate to improve the shape fidelity of the alginate hydrogel. NFC (2.5%) mixed with alginate hydrogel (2.5%), with human nasoseptal chondrocytes (hNC) suspended in it at a concentration of 15×10^6 cells per millilitre, was used to bioprint (microvalve bioprinting) human ear-shaped and sheep meniscal tissue shaped constructs (shown in Fig. 7D–F). Post-printing cell viability after 7 days was over 85%. While NFC can provide structural stability, it might affect the cell viability at higher concentrations. In another study [166], higher cell viability is observed with a lower concentration of NFC (60 wt%) although a higher concentration of NFC (80 wt%) resulted in a more structural stability when coupled with alginate hydrogel. In the same study, human-derived induced pluripotent stem cells (iPSCs) suspended in two hydrogels, namely NFC with alginate (60/40, dry wt% ratio), and NFC with hyaluronic acid (5% w/v) exhibited different pluripotency post-printing. While the cells underwent phenotypic changes away from pluripotency in NFC with hyaluronic acid, pluripotency was maintained in NFC with alginate hydrogel, forming a hyaline-like cartilaginous tissue after five weeks (shown in Fig. 7K). The choice of bioink plays a major role in bioprinting of stem cells, as it would affect the post-printing differentiation. Daly et al. [167] compared four different bioinks namely alginate (3.5% w/v), agarose (2% w/v), PEGMA (BioINK™, a commercial product), and GelMA (10% w/v with 0.05% Irgacure) for bioprinting of fibrocartilage and hyaline cartilage. Results revealed that alginate and agarose hydrogels favored the development of hyaline-like cartilage while PEGMA and GelMA favored the development of fibrocartilage-like tissue. BMSCs (obtained from the femur of a 4-month-old porcine

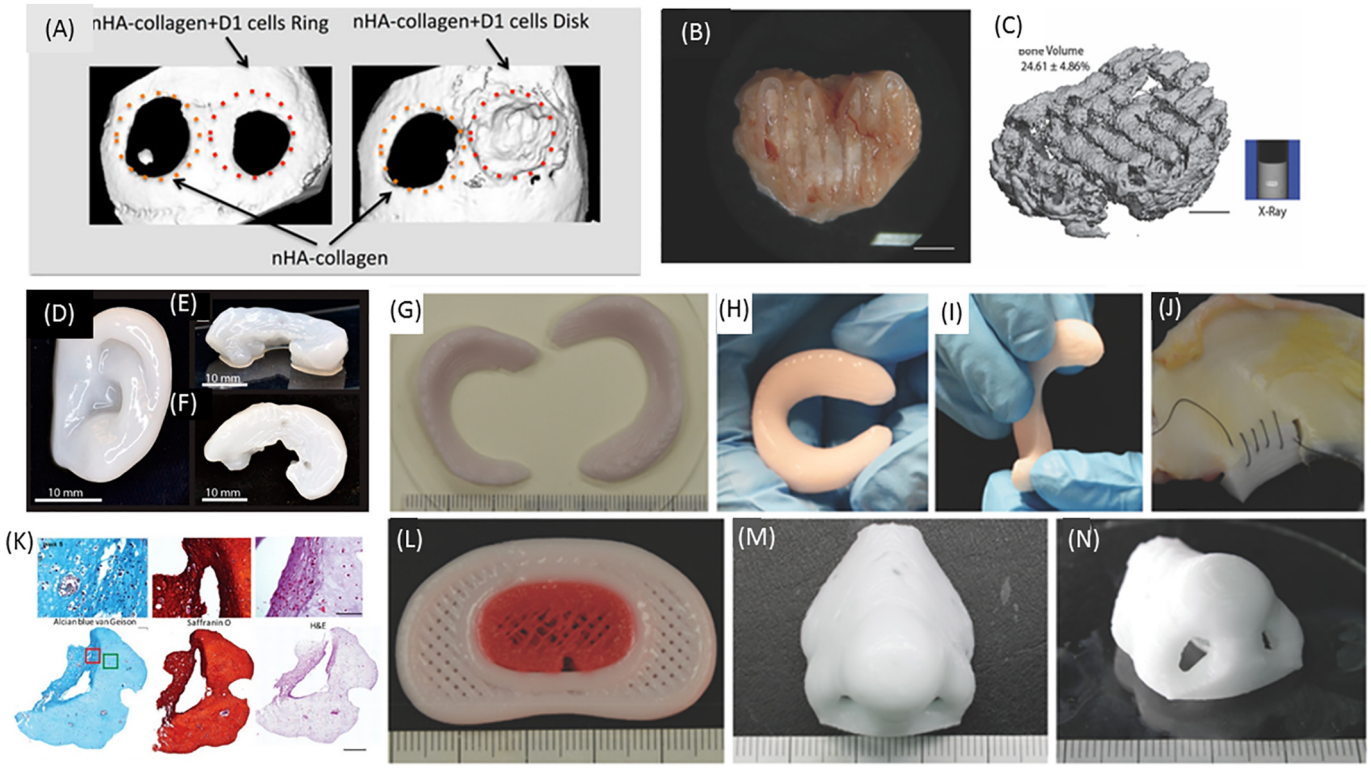

Fig. 7. Bioprinting in Skeletal System (A) Representative X-ray micro tomography (μCT) reconstruction images of nHA collagen and D1 cells printed in a ring or disk geometry (calvaria defect in the right side), or nHA collagen alone (calvaria defect in the left side), at 2 months post printing in a mice calvaria model. Reprinted with permission from [159]. (B & C) Development of vascularized bone organ in vivo following implantation of cartilage rudiment. b) Macroscopic image of anatomically shaped vertebrae constructs 12 weeks post-implantation scale bar 2 mm. (C) μCT reconstruction and X-ray of the whole construct, scale bar 2 mm. Reprinted with permission from [160]. (D) 3D printed human ear and (E & F) sheep meniscus with. Side view (E) and top view (F) of the meniscus. Reprinted with permission from [163]. (G–J) Cartilaginous meniscus grafts (G) were flexible in manipulation and (H,I) were stable upon suturing to (J) a bovine meniscus. Reprinted with permission from [168]. (K) The 3D-bioprinted chondrocyte-derived iPSCs (printed together with iChons, which had been diminished) at week 5 of differentiation, zoomed in (upper row) and whole section (lower row) images of sections stained for GAGs, Safranin O for cartilage (with nuclear counterstain), and hematoxylin and eosin (H&E) for extracellular matrix (with nuclear counterstain) (the scale bar represents 100 μm or 500 μm). Reprinted with permission from [166]. (L–M) Cartilaginous grafts such as (L) intervertebral disks and (M, N) noses were printed. Reprinted with permission from [168].

donor) were suspended at a concentration of 20×10^6 cells per millilitre in this study.

Kesti et al. [168] developed a novel bioink with gellan (3% w/v), alginate (2% w/v) and the clinical product BioCartilage (cartilage extracellular matrix particles) (40% w/w). Bovine chondrocytes (harvested from full-thickness articular cartilage of the lateral and medial femoral condyles of four 6-month-old calves) were suspended in the hydrogel at a concentration of 6×10^6 cells per millilitre. Post-printing cell viability after 7 days was over 95%. Auricular, nasal, meniscal, and vertebral cartilage were printed as a proof of concept (shown in Fig. 7G–J, L–N) and the in vitro study proved that the bioink supported the proliferation of chondrocytes after 8 weeks, with deposition of cartilage matrix proteins.

Duchi et al. [169] reported a handheld co-axial extrusion-based bioprinting for in situ cartilage bioprinting. A core-shell structure, with an acellular, photo-crosslinkable shell and a cellular core was printed. The core consisted of Adipose-Derived Stromal/Stem cells (ADSCs) (isolated from sheep infrapatellar fat pad) suspended in Gelatin-methacryloyl/hyaluronic acid methacryloyl (GelMa/HAMa) hydrogel (10% GelMA, and 2% HAMa) at a concentration of 5×10^6 cells per millilitre while the shell consisted of GelMa/HAMa hydrogel (10% GelMA, and 2% HAMa) with Lithium-acylphosphinate (LAP) (0.1% w/v) as the photo-initiator. The shell structure was cross-linked later using high-intensity UV light (700 mW/cm^2) for 10 s. Post-printing cell viability after 7 days, assessed by Cell Titer-Blue® Cell viability assay, was >90%. Though the study lacks detailed biological characterization to assess the long-term effect of printing and UV exposure, this work serves as a proof of concept study that showcases the potential of bioprinting for in situ cartilage repair. Though extrusion-based bioprinting is the most common method used for bioprinting of cartilaginous tissue [128], there are other methods like inkjet bioprinting used for cartilage bioprinting. Cui et al. [170] used thermal inkjet bioprinting to fabricate a 3D neocartilage construction by suspending human chondrocytes (5×10^6 cells/ml) in PEGDA hydrogel (10% w/v, supplemented with 0.05% of Irgacure). Cells were viable and maintained chondrogenic phenotype up to 6 weeks post-printing.

5.1.3. Challenges and future outlook

The first and foremost challenge with bioprinting of bone is in vitro culture of bioprinted bone in clinically relevant sizes [171]. Maintaining cell viability throughout the entire thickness and ensuring homogenous perfusion of nutrients and growth factors throughout the three-dimensional structure is a challenge yet to be addressed. Exploration of alternate methods like bioprinting with microcarriers [158], and bioprinting a developmental precursor that would act as a template for organogenesis in vivo [160] could help in overcoming this limitation. Secondly, in order to fabricate biomimetic bone tissue, the presence of porous scaffold structure is necessary. A hybrid bioprinting system (such as [157]), with a 3D printing module for printing porous acellular/cellular scaffold, followed by bioprinting of cell-laden hydrogels. Thirdly, different regions of bone and cartilage might have different properties and hence, could be divided into different zones. Bone, for instance, has an outer solid part is called cortical bone while the inside of the bone is a spongy structure called trabecular bone. Similarly, the articular cartilage has a complex zonal architecture, with three distinct layers – the superficial layer which is shear and tension resistant, the intermediate middle zone and the deeper zone with high stiffness, with different cell densities, architecture, and mechanical properties in each

region. Though 3D printing of zonal architecture scaffolds is reported earlier [172, 173], bioprinting of such a biomimetic structure is not attempted yet. Tuning of scaffold architecture and properties, optimizing cell densities, tuning the hydrogel properties according to each zone is necessary to fabricate zone-specific compositional and mechanical heterogeneity found in the native articular cartilage. Fourthly, the challenge of seamlessly integrating the bioprinted cartilage with the subchondral bone has to be addressed. Finally, the limited availability of chondrocytes [174] poses a challenge to bioprint cartilaginous tissue. Several kinds of stem cells (BMSCs, iPSCs, ADSCs) are used currently for bioprinting cartilaginous tissues. However, the challenges associated with the use of stem cells need to be addressed. Tuning the hydrogel properties so as to achieve directed differentiation to the desired lineage [156], growth factor or gene delivery for localized and controlled release of differentiation-inducing agents [174] are some of the strategies that could be used to tackle the challenges of using stem cells.

5.2. Muscular system

The muscular system consists of three types of muscles, namely skeletal, cardiac and smooth muscles. Skeletal muscles are those that are attached to the bones and are responsible for voluntary skeletal movements. Muscles that make up the walls of the heart are cardiac muscles and those that are found in the walls of hollow internal organs like the gastrointestinal tract, blood vessels, bladder, and uterus are called smooth muscles. Both cardiac and smooth muscles are involuntary muscles as they cannot be consciously controlled. This section mainly focusses on the skeletal muscles, cardiac muscles are covered in the circulatory/cardiovascular system and the smooth muscles along with their respective organs.

The current gold standard for skeletal muscle defects caused by trauma or a tumor is autografts involving muscle pedicle flap from adjacent regions [175]. Due to the inherent limitations of the autografts, including donor site morbidity, and availability [3, 10], alternate treatment methods such as engineered muscle tissue becomes a necessity. The mechanical and biological heterogeneity of the musculoskeletal system poses a challenge for engineering biomimetic muscle tissues [176]. One of the earliest attempts to engineer 3D muscle tissue was reported by Levenberg et al. [177] in 2005. In this study, mouse skeletal myoblast cells (C2C12) and endothelial cells (either HUVECs or HES cell-derived CD31+ endothelial cells) were co-cultured on a 3D porous, sponge-like, polymeric scaffolds composed of 50% poly-(L-lactic acid) (PLLA) and 50% polylactic-glycolic acid (PLGA). Though this study is done by traditional tissue engineering methods and not by bioprinting, it serves as a proof of concept study for engineering a vascularized muscle tissue where the endothelial cells organized into tubular structures in between the myoblasts and throughout the construct, forming vessel networks within the engineered muscle tissue in vitro. Another study [175] seeded human skeletal muscle cells (hSkMCs) (taken from biopsies of the rectus abdominalis of male patients aged 50–65 undergoing routine surgery) on electrospun PCL/collagen (5% w/v each) nanofibrous scaffold to fabricate an implantable muscle tissue. Electrospun scaffolds with aligned fibers induced cell alignment and myotube formation compared to electrospun scaffolds with random fibers.

Phillippi et al. [178] printed primary muscle-derived stem cells (MDSCs) (isolated from adult mice) in culture media using inkjet bioprinting method. Though the objective of this study is not bioprinting a muscle tissue but to create spatially defined patterns of immobilized growth factors for directed stem cell differentiation, this was the first reported work on bioprinting of muscle cells. Cui et al. [179] also used inkjet bioprinting to pattern mouse C2C12 myoblasts on micro-sized cantilevers for Bio-MEMS/biosensor applications. The printed cells formed matured myotubes 4 days post-printing. Both these studies were not directly aimed at bioprinting a muscle tissue. Recently, Kang et al. [180] reported bioprinting of a human scale muscle tissue (15 mm × 5 mm × 1 mm) using a self-developed integrated tissue–organ printer (ITOP). Mouse C2C12 myoblasts (3×10^6 cells/ml) suspended in gelatin/fibrinogen/hyaluronic acid/glycerol composite hydrogel (35, 20, 3 mg/ml, and 10% v/v respectively) were bioprinted using extrusion bioprinting, with a PCL framework on the outer layers and corners of each layer for structural support. Muscle-like structure with aligned myotubes was formed after 7 days. In vivo implantation of this structure in 14- to 16-week-old nude rats showed well-organized muscle fibre structures 2 weeks post-implantation (shown in Fig. 8). In order to effect the movement, the skeletal muscle transfers the force to the bone through tendon [176]. Hence, bioprinting a multi-phasic structure such as muscle-tendon-bone structure, with distinct tissue interfaces and tissue-specific mechanical and biological properties would be much helpful. To this end, Merceron et al. [176] fabricated a single integrated muscle-tendon unit (MTU) construct, demonstrating the potential of bioprinting to fabricate such multi-phasic skeletal muscle tissue. Mouse C2C12 myoblasts (40×10^6 cells/ml) and NIH/3 T3 fibroblasts (40×10^6 cells/ml), suspended in a gelatin/fibrinogen/hyaluronic acid composite hydrogel (35, 25, and 3 mg/ml respectively) were printed for muscle and tendon phases respectively. Thermoplastic polyurethane (PU) was co-printed with the former for the elasticity of the muscle construct while PCL was co-printed with the later for stiffness of the tendon construct. Post-printing cell viability was >80% after 7 days with signs of initial tissue development and differentiation.

5.2.1. Challenges and future outlook

There are not many studies reported on bioprinting of muscle tissue. The challenge lies with the mechanical and biological heterogeneity of the musculoskeletal system as discussed before. There are >600 muscles in the body and the muscles can be grouped according to their size (vastus (huge); maximus (large); longus (long); minimus (small); brevis (short)), shape (deltoid, rhomboid, latissimus, teres (round), trapezius), and direction of muscle fibers (rectus (straight); transverse (across); oblique (diagonally); orbicularis (circular)) [181]. Bioprinting a biomimetic muscle with these different structures and fibre orientations is an interesting work to be pursued in future. In addition, bioprinting of integrated multi-phasic structures such as MTU or muscle-bone or muscle-tendon-bone structure could be looked at. Vascularization and innervation play a major role in muscle tissue as they are important components for regulating the skeletal movements. Hence, bioprinting of vascularized and innervated skeletal muscle tissue is a potential future step in the bioprinting domain.

5.3. Nervous system

The nervous system consists of the brain, spinal cord, and nerve networks and is responsible for controlling, regulating and communicating between the brain and the other organs. The most prevalent clinical problem associated with the nervous system is neuron degeneration due to neurodegenerative diseases such as Alzheimer's, Parkinson's, and Huntington's diseases. Since there are no established treatment methods to address these neurodegenerative diseases, neural stem cell-laden hydrogel constructs transplanted into the injured site is looked upon as a potential treatment method [182]. Hence, most of the bioprinting studies relating to nervous system focus on this objective.

Hsieh et al. [182] developed a polyurethane (PU) nanoparticles based bioink (25–30% w/v) for bioprinting of murine neural stem cells (NSCs) (isolated from adult mouse brain) (4×10^6 cells/ml) using an extrusion-based bioprinting system. A soft segment comprised >65% of the PU chemical structure. The soft segment was either PCL diol/poly(L-lactide) (PLLA) diol (4:1 M ratio) or PCL diol/poly(D,L-lactide) diol (PDLLA) diol (4:1 M ratio). PU bioink with the latter soft segment favored excellent cell proliferation and differentiation than the former. In vivo study in a zebrafish embryo, neural injury model also demonstrated nervous regeneration. In another study [183], Schwann cells

(isolated in primary culture from the sciatic nerve of Sprague-Dawley rats) suspended in a fibrin-factor XIII-hyaluronic acid hydrogel (50 mg/ml, 1 U/ml, and 4 mg/ml respectively) was printed into a thrombin/PVA solution (50 U/ml, and 1.4% w/v respectively) with post-printing cell viability of >95% after 7 days. Graphene-based scaffolds and bioinks are explored for use in neural tissue engineering [184, 185] as the conductivity and large surface to volume ratio (being a 2D material) would help in better neural cell growth and differentiation. In one such study [186], mouse neural stem cells (2×10^6 cells/ml) were suspended in a GelMA/graphene nanoplatelets (10–20% w/v, and 1 mg/ml respectively, supplemented with 0.5% w/v Irgacure) and bioprinted using a stereolithography bioprinting method. Though the cells showed high viability and differentiated, there was no significant effect of the addition of graphene nanoplatelets. Though the use of graphene and its derivatives looks attractive, the non-availability of long-term effects of graphene on the cells and its biodegradability [187], limits its use as bioinks for clinical use.

Biological cues and growth factors play an important role in regulating and controlling the stem cell differentiation and hence nerve regeneration. An effective strategy to deliver the growth factors to the differentiating stem cells during nerve regeneration process is worth focusing on. Lee et al. [188] embarked on such a study. Murine NSCs (C17.2) suspended in collagen hydrogel (0.87–1.74 mg/ml) were printed using an extrusion-based bioprinting system. Vascular endothelial growth factor (VEGF)-releasing fibrin hydrogel (62.8 mg/ml) was also developed. MNSCs-containing collagen and VEGF-releasing fibrin were printed side by side. VEGF printed directly on collagen and fibrin hydrogel without VEGF acted as a control. While excellent cell proliferation, differentiation, and migration towards VEGF-releasing fibrin construct were witnessed in the experimental group, the cells neither proliferated nor migrated in the control groups. Though the study has several limitations such as non-quantification of VEGF release/delivery rate, and lack of differentiated cell phenotypic information, it underscores the importance of growth factors in neural regeneration and the method adopted to deliver them.

Bioprinting a functional brain structure is an onerous task to achieve if not impossible. Lozano et al. [189] bioprinted 3D brain-like structures consisting of discrete layers of primary cortical neurons (harvested from E18 embryos of BALB/cArcAusb mice) (1×10^6 cells/ml) encapsulated in RGD peptide-modified gellan gum hydrogel (0.5% w/v). Multi-layered structure (three layers with the first and third layer containing cells and the middle layer without cells) were printed (shown in Fig. 9). The structure maintained its stability up to 7 days and showed penetration of axons from cell-containing layers to the middle no-cell layer. This study, though lacking long-term biological characterization and detailed cell phenotypic studies, demonstrates the ability of bioprinting to fabricate a multi-layered cortical brain tissue construct.

5.3.1. Challenges and future outlook

Relatively few studies were reported on bioprinting of neural tissue [182], given the complexity of the tissue. Although bioprinting of neural stem cells with high post-printing viabilities was reported as discussed above, there are not many studies like [189] focussing on bioprinting a biomimetic neural tissue with its intricate layered microarchitecture. Furthermore, since mostly stem cells are involved in bioprinting of neural tissue, cell differentiation studies using different hydrogel types and incorporation of growth factors that induce differentiation in vivo by localized growth factor delivery should be explored.

5.4. Lymphatic system

The lymphatic system consists of the lymph, lymphatic vessels, and lymphatic organs such as lymph nodes, tonsils, spleen, and thymus. This system has many functions including maintenance of interstitial fluid homeostasis, and fat absorption, of which its role in immunological defense to external agents is notable [190]. Lymphedema is a disease that results from dysfunction of lymphatic fluid uptake or damage to lymph nodes. There are many causes associated with lymphedema, of which surgical procedures for cancer treatment combined with radiation therapy is the main cause. About 140 to 250 million people suffer from lymphedema worldwide [190]. Though there are no established treatment procedures for lymphedema, engineered lymphatic vessels and lymph nodes could be a potential treatment method.

Engineering artificial lymph nodes and lymphatic vessels is a relatively new field, compared to the other engineered tissues such as bone, blood vessel, and skin. Very few works were reported on engineering a 3D lymphatic vessel or tissue. These include PGA tubes seeded with lymphatic endothelial cells (LECs) and implanted into mice [191] which failed to forma tube-like lymphatic vessel, co-culturing LECs onto a feeder sheet of fibroblasts resulting in a 3D lymphatic capillary network induced by fibroblast-derived VEGF and hepatocyte growth factor (HGF) [192], co-culturing LECs and blood vascular endothelial cells (BECs) in a 3D VEGF-fibrin-collagen matrix leading to formation of densely branched lymphatic vessel structure [193], and transplantation of cell-laden (thymus-derived stromal cell line, TEL-2 and dendritic cells (DCs)) sponge-like collagenous scaffold into naive normal or severe combined immunodeficiency (SCID) mice [194]. Though these works followed traditional tissue engineering methods, they established some success in engineering lymphatic vessels. It is worth noting that some of these very few studies achieved their results (formation of lymphatic vessels or tissues or lymphoid tissue–like organoid) in in vivo conditions [194, 195] and not in in vitro conditions. Bioprinting of lymphatic vessels and lymphatic organs is an unexplored field. Recently, Nakamura et al. [196] attempted to engineer an artificial lymph node using an extrusion-based printing method using microfabricated spinneret nozzles. This study demonstrated that lymph node-like structure could be fabricated using their method, however, no cell-laden hydrogels was printed nor characterized.

5.4.1. Challenges and future outlook

Bioprinting of lymphatic vessels and lymph nodes is an unexplored area with huge research and clinical potential. Bioprinted lymphatic vessels and lymph nodes might aid in the development of artificial immune systems based therapeutic devices to treat intractable infectious diseases, immunological disorders and diseases, and even cancer [196], and implantable tissue constructs for wound healing and enhancement of lymphatic ingrowth after plastic surgery [190]. In addition to the regenerative medicine applications, bioprinted lymphatic systems or organ-on-a-chip devices might help the researchers to study the complex immunological phenomena and mechanisms [196]. All vascularized tissues have the presence of lymphatic system, including the central nervous system [197]. So, the first potential step in this field would be to incorporate the cells and growth factors related to the lymphatic system in the bioprinting of other vascularized tissues that are now being extensively focussed on. Bioprinting a biomimetic lymph node is an extremely formidable task worth focussing on. Strategies to bioprint a biomimetic lymph node has to be developed as the lymph node is a highly complex structure with highly organized stromal and lymphoid structure and large variety of cells, including highly organized lymphatics, marginal reticular zone stroma, T cell zone stroma, multiple B cell follicles, vascular networks and medullary regions containing plasma cells and macrophages [195, 198].

5.5. Endocrine system

The endocrine system consists of hormone-secreting glands, the hormones being carried directly through the bloodstream to the target organs, thus regulating vital functions of the body. Hyper or hypofunctioning of these glands lead to several kinds of disorders and diseases. Current treatment method for hormonal or gland dysfunction is the hormone replacement therapy. However, this is not a perfect

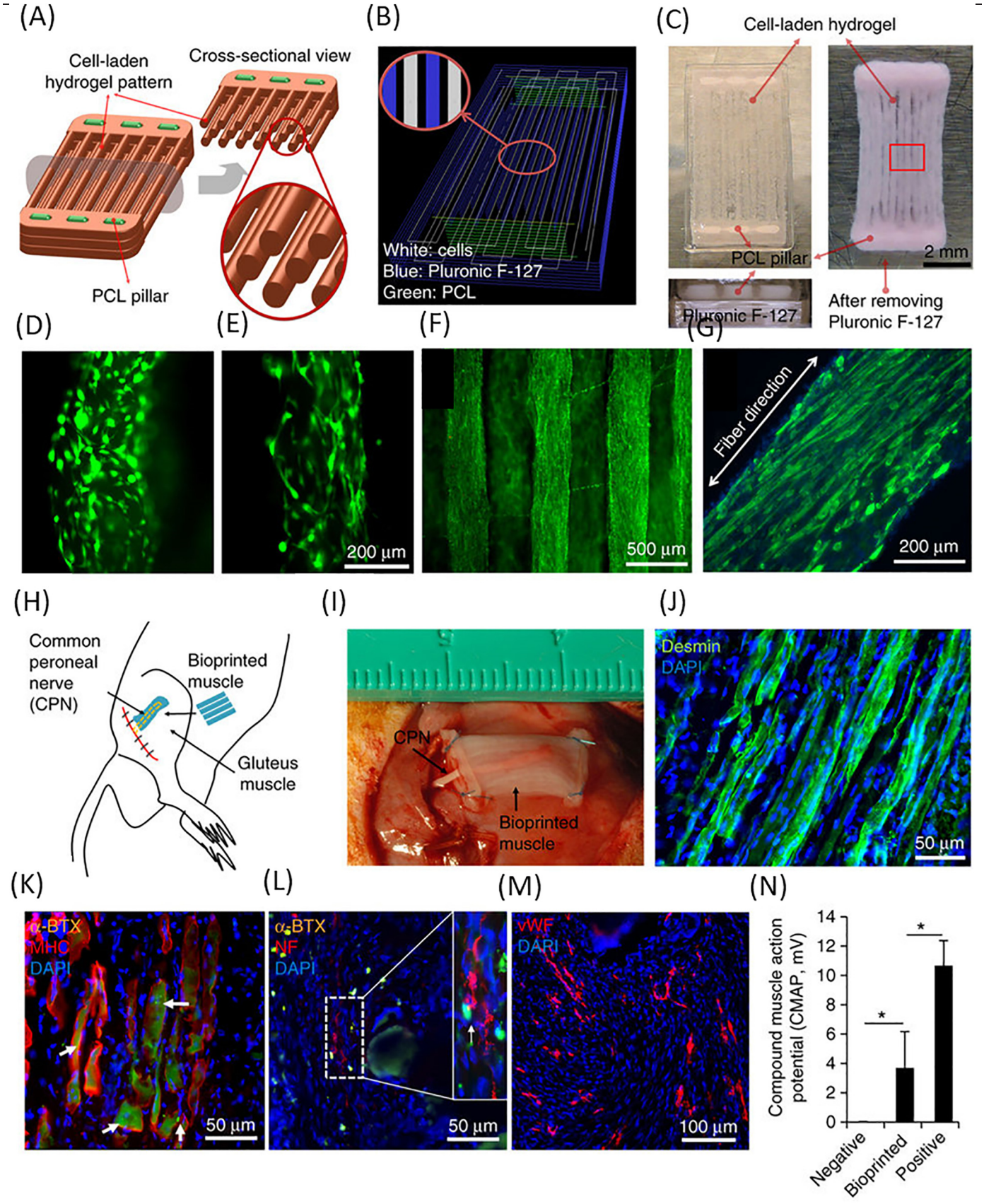

Fig. 8. Bioprinting in Muscular System (a) Designed fibre bundle structure for muscle organization. (b) Visualized motion program for 3D printing muscle construct. (c) 3D patterning outcome of designed muscle organization (left) before and (after) removing the sacrificial material (Pluronic F127). (d,e) The PCL pillar structure causes cell alignment in a longitudinal direction of the printed constructs; without PCL pillar (d) and with PCL pillar (e). (f) The live/dead staining of the encapsulated cells. (g) Immunofluorescent staining for myosin heavy chain of the 3D printed muscle organization after 7-d differentiation. (h–n) Structural maintenance and host nerve integration of the bioprinted muscle construct in in vivo study.
Reprinted with permission from [180].

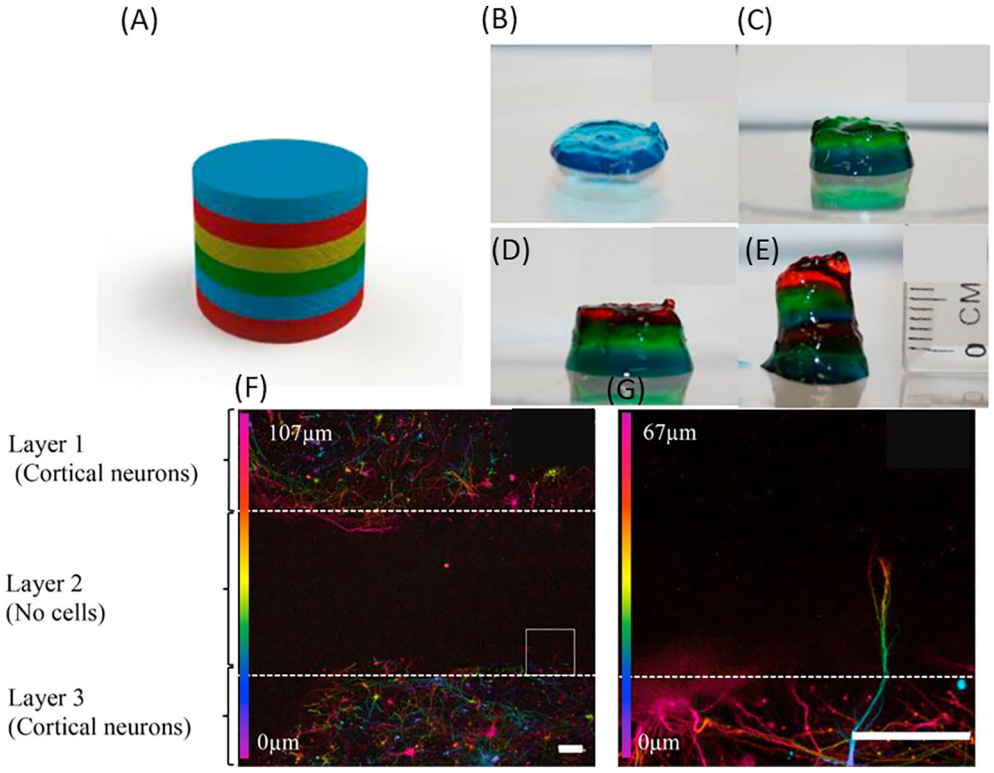

Fig. 9. Bioprinting in Nervous System (A–G) Printed brain-like layered structure. A) Solidworks representation of proposed brain-like layer structure. (B–E) Printing process to create a brain-like structure, each color represents a layer. (F) Confocal microscope images of neurons in different layers after 5 days of culture. The image is colored for the distribution of the cells through the z-axis in the bio-ink RGD-GG gel as indicated. (G) An expanded view of the area from the square of panel F, showing an axon penetrating into the adjacent layer. Scale bars represent 100 μm.
Reprinted with permission from [189].

treatment method as it will not allow for the fine regulation of hormones according to the changing physiological conditions [199] and the patient is dependent on these synthetic hormones for the rest of their lives. Ex situ bioengineering of transplantable endocrine glands could be a possible solution to address this challenge. However, fabrication of such glands ex-situ with traditional tissue engineering methods is near impossible due to the complex structure of some of these glands such as the pancreas. For example, the islets of Langerhans present in the pancreas and which is responsible for the hormone production has at least five types of cells namely alpha cells (secreting glucagon), beta cells (secreting insulin and amylin), delta cells (secreting somatostatin), gamma cells (secreting pancreatic polypeptide), and epsilon cells (secreting ghrelin) in varying percentages, arranged in a particular cytoarchitecture. Engineering such a complex environment, with the precise patterning of multiple cells, is now possible with the advent of bioprinting.

Despite the advantages and the potential of bioprinting to fabricate various endocrine glands, it has not been in the focus of bioprinting community thus far. Only a limited number of works have been reported on the subject area. Recently, Bulanova et al. [199] reported on bioprinting of a functional vascularized mouse thyroid gland construct. They used an extrusion bioprinting system with a turnstile function to pattern thyroid spheroids (TS) (explanted from e14.5 mouse embryos) and allantoic spheroids (AS) (explanted from e8.5 mouse embryos) as a source of thyrocytes and endothelial cells (EC), which 'self-assembled' to form a thyroid tissue. Vascularized tissue construct formed after 4 days, with EC (from AS) invading and vascularizing the TS while epithelial cells from the TS progressively formed follicles. The functionality of the construct was evaluated by transplanting it into a hypothyroidism mouse model under the kidney capsule. Blood sampling for plasma T4 measurements and histological examination of the kidneys 5 weeks after transplantation demonstrated successful host tissue integration and maturation, thereby aiding in the functional recovery of the experimentally induced hypothyroidism. This is the first study reported to have bioprinted a functional endocrine gland. However, thyroid gland has a relatively simpler structure and the same strategy might not work for printing of other complex glands like the pancreas. Of the five different types of cells present in the pancreas (as stated in the previous paragraph), beta cells are of particular interest as they are responsible for the production of insulin. Dysfunction in insulin production would lead to diabetes and millions of people all over the world suffer from diabetes. Hence, research on bioprinting of beta cells is of a particular interest to the bioprinting community. Marchioli et al. [200] bioprinted INS1E β-cell line (derived from rat insulinoma) (10×10^6 cells/ml) suspended in alginate/gelatin hydrogel (4% and 5% w/v respectively). Although post-printing cell viability after 21 days was over 95% and the cells retained their morphology, the functionality of the printed islet construct could not be proved and is attributed to the high viscosity of the bioink which hinders the glucose diffusion.

One major limitation that hinders engineered endocrinal glands is the scarce availability or non-scalable generation of primary cells from the endocrinal glands [199]. Stem cells could be a viable alternate. Song et al. [201] differentiated human pluripotent stem cells (hPSCs) (Harvard University Embryonic Stem cell 8 line (HUES8)) into insulin-producing β cells (SC-β) and suspended them in fibrinogen hydrogel (10 mg/ml) at a concentration of 5×10^6 cells/ml to be extruded into a 3D PLA scaffold. To test the functionality of the printed construct, it was subcutaneously transplanted into SCID Beige mice aged 10–12 weeks. The transplanted constructs secreted insulin in vivo in response to glucose up to 12 weeks. Further studies on these lines could overcome the shortage of primary cells associated with endocrine glands.

5.5.1. Challenges and future outlook

Availability of primary cells from endocrinal glands is a challenge, as stated earlier. More studies are required to obtain these cells by differentiation of stem cells. Secondly, the functionality of the printed construct depends on how comfortable the cells are inside the bioink. These endocrinal cells are very sensitive to the environment as shown by Marchioli et al. [200], where the printed and transplanted construct didn't produce insulin as the high viscous bioink hinders glucose permeation. Development of suitable bioinks that doesn't affect the functionality is another area to be focussed. With the growing diabetic population, bioprinted insulin-producing β cell constructs hold a very promising future. Bioprinting a fully functional endocrine gland with all the different types of cells and cytoarchitecture could be a later target.

5.6. Reproductive system

Survival of the species rests with the reproductive system. About 14% of couples at reproductive age suffer from infertility [202]. Infertility is caused by myriad different conditions in male and female. In the male, the causes could be pathologic penile conditions (penile carcinoma, trauma, etc.) or congenital conditions (hypospadias, epispadias, ambiguous genitalia, etc.) [203]. Female infertility could result from congenital uterine malformations or endocrine, structural, and iatrogenic causes, such as chemotherapy, occlusion of fallopian tube, uterine injuries, massive intrauterine adhesions, and hysterectomy [204]. The scarcity of autologous tissue for reconstructive surgery is a major limitation with the treatment of reproductive organ anomalies. Tissue engineering and bioprinting offers alternate treatment methods to overcome this limitation.

While a fully engineered organ associated with the reproductive system is not reported yet, engineered tissue constructs using cell-laden decellularized ECMs, and porous scaffolds have been reported previously [204]. Bioengineering of uterus, ovary, and cervicovaginal tissues were explored. The uterus is a three-layered, pear-shaped muscular female reproductive organ, consisting of outer perimetrium (connective tissue), middle myometrium (smooth muscle), and inner endometrium (epithelial tissue) [202]. Traditional tissue engineering methods have been used to engineer parts of the uterus. The first in vitro construction of endometrium was reported by Bentin-Ley et al. [205], where a 3D endometrium structure was fabricated from stromal and epithelial cells isolated from human endometrial biopsies suspended in collagen enriched Matrigel hydrogel. Several similar studies were reported on engineered uterus tissue by seeding autologous cells on collagen-Matrigel matrix [206], fibrin-agarose matrix [207], silk-protein sponge scaffold [208], electrospun PGA scaffold [209], and decellularized ECM such as porcine small intestinal submucosa (SIS) [210]. Matrices containing various growth factors such as basic fibroblast growth factor (bFGF) [211], and collagen-binding vascular endothelial growth factor (CB-VEGF) [212] as a potential growth factor for uterine repair were also explored.

Since primary ovary deficiency is the leading cause of female infertility [204], fabrication of engineered ovarian tissues is an interesting topic in tissue engineering. Ovarian cells, oocytes and ovarian follicles harvested from animals or humans were seeded on decellularized ECM [213] or encapsulated in hydrogels such as alginate [214, 215], and agarose [216] to fabricate ovarian tissue. Similar strategies were adopted to fabricate cervicovaginal tissue constructs. Cervical tissue constructs were fabricated by seeding cervical cells on decellularized ECM such as porcine SIS [217, 218], or scaffolds [208]. An engineered vaginal organ constructed with autologous muscle and epithelial cells by seeding these cells on a poly(DL-lactide-*co*-glycolide) scaffold was implanted into humans and the 8-yearlong study proved normal functioning of the implanted construct [219].

Though most of the tissue engineering studies pertaining to the reproductive system were predominantly done on female reproductive organs, there are a few studies published on engineered male reproductive organs and tissues. Atala et al. [220, 221] seeded autologous cavernosal smooth muscle and endothelial cells on a collagen matrix and implanted the cell-laden matrix in a rabbit model. Results proved the formation of penile tissue phenotypes and structural and functional biomimicry was demonstrated by cavernosography, cavernosometry, and mating studies. Recently, Vermeulen et al. [222] explored the possibility of developing a bioartificial testis as a viable option for fertility restoration of prepubertal boys who underwent chemo/radiotherapy. Cryopreserved immature testicular tissue (ITT) of such patients can be used to engineer an artificial testis to restore their fertility when they reach the appropriate age.

Although there were many studies on tissue engineering of tissues associated with male and female reproductive systems, research related to bioprinting of reproductive system-related cells or tissue is scarce and has to be explored.

5.6.1. Challenges and future outlook

Bioprinting has not yet been explored for addressing the problems of male and female infertility. Bioprinted reproductive system tissues such as phallic tissue, uterus, ovary, and cervicovaginal tissue would serve as potential treatment options for addressing the infertility problems. Availability of primary cells from reproductive tissues [202, 204] is a challenge and use of stem cells could be a viable solution. However, more studies are required to optimize the biological conditions to effect the differentiation of stem cells to the appropriate cell lineage. Testing protocols to test the functionality of the printed tissues and organs are to be developed as there are not many studies pertaining to this domain [202]. With the rise in a number of patients requiring hysterectomy year by year, bioprinting a whole functional uterus is a potential research direction in the near future.

5.7. Integumentary system

The integumentary system consists of skin, along with its derivative structure and accounts for about 15% of the body weight in adults [1]. Skin is a three-layered structure (outer epidermis, middle dermis, and inner hypodermis), constituting several kinds of cells including keratinocytes, fibroblasts, and melanocytes, and serves several vital functions such as protective (barrier, UV light absorption, immune surveillance, mechanical), perceptive (touch, temperature, pain), and regulatory (thermal, hydration, excretory) functions. The demand for engineered skin substitutes stems from two major needs, namely wound management and drug/cosmetic testing. The global wound management market is forecasted to be worth over $22 billion by 2024 and the global market for tissue-engineered skin substitutes was projected to reach 3873.5 million by 2023 [223]. With the ban on animal testing in several countries, the demand for artificial skin substitutes is on the rise.

Bioprinted skin is a major area of focus in the bioprinting domain. Many bioprinting methods had been explored for printing of skin tissue construct, including laser-based bioprinting, droplet-based bioprinting, and extrusion bioprinting. Koch et al. [85] reported bioprinting of skin cells (NIH3T3 fibroblasts and HaCaT keratinocytes) ($1–2 \times 10^6$ cells/ml) suspended in a 1:1 mixture of ethylenediaminetetraacetic acid (EDTA) human blood plasma and alginate hydrogel (4 wt%), using laser-based bioprinting (LIFT) for the first time, with post-printing cell viability of 98%. The study also proved that there was no increase of apoptosis or DNA fragmentation as a result of LIFT. This was a preliminary study evaluating the feasibility of laser printing of skin cells and no 3D constructs were fabricated. In a follow-up study [224], using the same bioprinting system, skin cells (NIH3T3 Swiss albino fibroblasts and HaCaT human immortalized keratinocytes) (1.5×10^6 cells/ml) suspended in collagen hydrogel (3 mg/ml) was printed to form a 3D skin tissue construct consisting of 20 layers of fibroblasts and 20 layers of keratinocytes. Post-printing cell viability assessed after 10 days

showed that the cells are viable and formation of adherens junctions and gap junctions were witnessed, demonstrating tissue morphogenesis. On further testing of the bioprinted skin construct in vivo [225], transplanting into the full-thickness wounds in the dorsal skin fold chamber in nude mice, showed that the transplanted construct was fully connected to the surrounding tissue after 11 days, with formation of stratum corneum, epidermal differentiation, and blood vessels growing into the construct from the wound edges.

Using microvalve bioprinting method, Lee et al. [226] fabricated a multi-layered skin tissue, consisting of 10 layers of collagen (2.05 mg/ml), with the fibroblasts (primary adult human dermal) and keratinocytes (primary adult human epidermal) (1×10^6 cells/ml) present in the second and eighth layer respectively, with a post-printing cell viability of >80% after 1 day. Detailed biological characterization was lacking in this study. However, they demonstrated printing of skin tissue on a polydimethylsiloxane (PDMS) mold with a non-planar, which could aid in direct in situ printing of skin on wounds. In another study [227], fibroblasts (HFF-1 from ATCC) (2×10^6 cells/ml), and HaCaT keratinocytes (5×10^6 cells/ml), suspended in collagen hydrogel (3 mg/ml) were printed using microvalve bioprinting into a multi-layered skin construct, consisting of dermal and epidermal layers. The histological examination and immunofluorescence characterization after 14 days revealed morphological similarities of the printed construct to that of the native in vivo human skin tissue. However, this study also lacks certain important biological characterizations such as collagen production, and epidermal differentiation. Rimann et al. [228] bioprinted a multi-layered skin construct using microvalve bioprinting. Human primary dermal fibroblasts (9×10^6 cells/ml) and epidermal keratinocytes (1×10^7 cells/ml) were suspended in a PEG-based photo-polymerizable bioink for bioprinting. The printed constructs were characterized up to 42 days, one of the longest time period tested among the other bioprinted skin studies. Epidermal layer printing was undertaken after culturing the printed dermal construct for varying time periods up to 6 weeks. Formation of stratum corneum was observed only on those constructs that were cultured for 6 weeks prior to epidermal layer printing and not seen on those constructs that were cultured for <6 weeks. This observation emphasized the importance of the quality of dermal layer for fabricating a biomimetic skin tissue. Fibroblasts in the dermal layer proliferated up to 42 days and produced their own ECM (collagen I). This is one of the first studies to prove that bioprinting could be used in a production scale, with only 7 min to construct the whole dermal construct.

Extrusion-based bioprinting systems were also used to bioprint skin tissue constructs. Cubo et al. [229] used a multi-nozzle extrusion bioprinting system to fabricate a human bi-layered skin. Three syringes were used, with cell-containing media extruded through the first nozzle, human plasma containing fibrinogen (30 mg) and tranexamic acid (200 μl) in the second, and $CaCl_2$ solution (to crosslink fibrinogen into fibrin) in the third. The dermal layer was formed with human dermal fibroblasts (1.75×10^4 cells/ml) suspended in cell media. Human epidermal keratinocytes (0.6×10^6 cells/ml) suspended in cell media were printed on top of the dermal layer after 30 min of incubation. In vitro and in vivo studies (in immunodeficient athymic mice (skin-humanized mice)) showed that the printed skin exhibited structural and biological similarities to that of the native human skin. Pourchet et al. [230] fabricated a human skin construct with primary normal human fibroblasts and keratinocytes (1×10^6 cells/ml) suspended in a gelatin/alginate/fibrinogen hydrogel (10%, 0.5%, and 2% w/v respectively) using a extrusion-based bioprinting system. Histological and morphological characterization of the bioprinted skin 26 days post-printing exhibited the characteristics of human skin, both at the molecular and macromolecular level, substantiated by biomarkers of dermal layer and epidermal differentiation.

Although the majority of the bioprinted skin constructs consisted of only fibroblasts and keratinocytes, there were attempts to incorporate other types of cells present in the native skin such as melanocytes and other skin appendages such as sweat gland. Recently, Min et al. [231] reported bioprinting of a full-thickness skin model containing pigmentation using microvalve bioprinting. The dermal layer was constructed from human dermal fibroblasts (1×10^6 cells/ml) suspended in collagen hydrogel (6 mg/ml). Human epidermal melanocytes (2×10^7 cells/ml), and keratinocytes (7×10^6 cells/ml) suspended in collagen hydrogel (6 mg/ml) were sequentially printed on the dermal layer upon subsequent air-liquid interface culture (for one day) of the dermal layer, for fabricating a pigmented skin construct. The histological examination and immunofluorescence characterization after 10 days showed the evidence of pigmentation and melanin granules inside the epidermal layer. Freckle-like pigmentations were seen at the dermal-epidermal junction. Sweat gland regeneration by directed differentiation of epithelial progenitors by extrusion based bioprinting was reported by Huang et al. [130]. Epithelial progenitors and dermal homogenates (isolated from wild-type C57/B16 mice aged 3–4 weeks), suspended in a gelatin/alginate hydrogel (20%, and 4% w/v respectively) were bioprinted using an extrusion-based bioprinting system. In vitro studies including immunofluorescence staining for relevant biomarkers confirmed the differentiation of epithelial progenitors into sweat glands. The printed constructs were transplanted to the burned paws of mice (wild-type C57/B16 mice) to evaluate the in vivo regeneration of sweat glands. An iodine/starch-based sweat test performed 14 days after transplantation proved the sweat gland regeneration from epithelial progenitors and the regenerated sweat glad was functional.

5.7.1. Challenges and future outlook

Due to the huge market demand, bioprinting of skin has gained much attention recently. It is expected to be one of the first bioprinted tissue to be put to use clinically or for drug/cosmetics testing applications [232]. There is substantial progress in the field, with several studies reporting bioprinted skin constructs the structurally and biologically mimic the native human skin. However, bioprinting of a fully-functional skin with all the cell types and skin appendages is still challenging. While printing of skin appendages such as sweat glands and hair follicles is difficult, alternate approaches such as sweat gland regeneration from stem cells [130] have to be investigated. In situ skin bioprinting systems could be a very potential project that would help in wound management of burn wounds.

5.8. Respiratory system

The respiratory system consists of lungs, pharynx, larynx, trachea, bronchi, and diaphragm and is responsible for the exchange of oxygen and carbon dioxide between the atmosphere and the body. Human lungs lack regeneration ability and hence, lung transplantation is the only way to treat severe lung diseases [233]. However, high cost, shortage of donors and low survival rate [234] are major concerns associated with this procedure. Hence, there is a need for tissue engineered lung and lung tissues. Similarly, the gold standard for treatment of most airway diseases resulting from stenosis, tracheomalacia, or cancer is tracheal resection and end-to-end anastomosis [235]. Tissue-engineered airways are a potential treatment method.

Bioprinting of lungs and the airways for respiratory tissue regeneration is a relatively new field, notwithstanding the fact that tissue-engineered lungs [233], and airway/trachea [236, 237] by seeding cells on decellularized structures or on 3D porous scaffolds by traditional tissue engineering techniques had already been reported. For example, Shan et al. [235] fabricated a biomimetic tracheal graft using 3D printing (Fused Deposition Modelling) and subsequently seeded BMSCs (isolated from the tibial plateau of rabbit) to evaluate the biocompatibility of the printed graft. Detailed reviews of such works were reported elsewhere [238, 239]. To the best of our knowledge, there is only one study reported so far on bioprinting of a lung tissue analogue. Horváth et al. [240] used microvalve bioprinting method to fabricate a lung tissue analogue closely recapitulating the in vivo human air-blood barrier

architecture. A two-cell layer model with A549 (alveolar epithelial type II cells; AT-II) (4.5×10^6 cells/ml) representing the epithelial layer, and EA.hy926 (endothelial hybrid human cell line derived by fusing human umbilical vein endothelial cells (HUV-EC) with A549 cells) cells representing the endothelial layer, with a thin Matrigel™ layer separating them that represents the basement membrane. Though this study successfully fabricated a lung tissue analogue with air-blood barrier architecture, the functionality of the printed construct is not evaluated.

5.8.1. Challenges and future outlook

Bioprinted lungs and airway are still a future reality. There are many challenges associated with lung tissue engineering. The first major challenge is the availability of cells specific to lung tissue. While differentiation of PSCs or iPSCs to the lineage of lung-derived cells is an option, the protocols are only being recently looked into and incompletely developed so far [241]. Hence, the first mission of the researchers should be to focus on these procedures and protocols to achieve differentiation of stem cells into lung-specific cell lineages. Bioprinting of cell-laden hydrogels on the decellularized ECM to fabricate the lungs could be the next step before embarking on bioprinting of a whole lung, given the complex structural arrangement and cytoarchitecture. Wilson et al. [241] provided an outlook of how bioprinting could be applied to respiratory tissue reconstruction. Two functional compartments of the respiratory system, namely the trachea/airway and the alveolar space could be the first target for bioprinting. This could be achieved by fabricating a tube-like structure lined by a pseudostratified epithelium for tracheal bioprinting and a single alveolar sac, a grape-like structure composed of clusters of alveoli, and hollow cavity-like structures lined by type I and II alveolar epithelial cells (AECs) for bioprinting of the alveolar space. A combination of bioprinting and microfluidics might advance the research of bioprinting lungs to the next level.

5.9. Digestive system

The digestive system has two main parts namely, the gastrointestinal/alimentary tract consisting of the mouth, oesophagus, stomach, small and large intestines, rectum and anus, and solid organs such as liver, pancreas, and gall bladder. The main function of the digestive system is digestion and absorption, where food is broken down into smaller molecules such as glucose, fatty acids, and amino acids and absorbed by the body. Of the different tissues and organs consisting of the digestive system, oesophagus, intestines, liver and pancreas were of interest to the tissue engineering community.

5.9.1. Liver

The liver performs many important body functions such as bile secretion that helps in digestion and absorption of fats, detoxification, metabolizing drugs, production of serum proteins, and in maintaining homeostasis. Though liver has the capacity to regenerate, severe or chronic liver diseases such as hepatocellular carcinoma, and liver cirrhosis, the regenerative capacity of the liver is lost [242]. In such cases, liver transplantation is the ultimate treatment method. In the United States alone, about 30 million people suffer from various liver disorders, which leads to 30,000 deaths annually and 1 million deaths in developing countries [243]. The demand for liver transplants is projected to increase by 23% in the next 20 years [243]. Given the limited availability of donors, engineered liver tissues have a huge need.

Tissue engineering of the liver is not new and there are several studies published on engineered liver tissue and bioartificial liver as early as 1996 [244, 245]. However, engineering a functional liver ex vivo was not successful due to the large size, and complex structure with interwoven biliary, lymph and vascular networks [244]. With the advent of bioprinting, fabrication of a functional liver has become an impending reality. Several successful studies of bioprinted liver tissues were reported in the recent past. Chang et al. [246] used microvalve bioprinting to fabricate a liver tissue construct with HepG2 cells ($1–4 \times 10^6$ cells/ml) suspended in alginate hydrogel (3% w/v). The printed construct was housed in a chamber with microfluidic channels mimicking the in vivo microenvironment and evaluated a drug metabolism model, which is a liver-specific function. In another study [247], a liver tissue was bioprinted from coculture of primary human hepatocytes, hepatic stellate, HUVEC cells, and non-parenchymal cells suspended in NovoGel^R 2.0 hydrogel at a concentration of 150×10^6 cells/ml. Histological analysis demonstrated the presence of distinct intercellular hepatocyte junctions, CD31+ endothelial networks, and desmin positive, smooth muscle actin negative quiescent stellates, mimicking the in vivo human tissue. Both these studies [246, 247] focus on the drug metabolism function of the printed liver tissue and hence, the other vital functions of the bioprinter liver tissue such as bile secretion is not evaluated.

Arai et al. [248] suspended primary hepatocytes (isolated from the liver tissue of male 6- to 8-week-old ICR 12 mice) in a galactosylated alginate hydrogel (12 mg/ml) and used inkjet bioprinting method to fabricate a two-layered liver tissue. The asialoglycoprotein receptor (ASGPR) present in hepatocytes interacted with the galactose chain of galactosylated alginate hydrogel, thus promoting better cell adhesion. The printed construct was morphologically similar to the native liver tissue and expressed liver-specific proteins and receptors such as albumin, MPR2, and ASGPR, thus proving the functionality of the printed liver tissue. Using an extrusion-based bioprinting system, Kim et al. [249] printed mouse primary hepatocytes (isolated from the livers of 6–8 weeks old mice) (4×10^7 cells/ml) suspended in alginate hydrogel (3% w/v) into 3D liver tissue constructs. Cells were viable for 14 days, with liver-specific gene expressions namely albumin, hepatocyte nuclear factor 4 alpha (HNF-4α), forkhead box protein A3 (Foxa3), and asialoglycoprotein receptor 1 (ASGR1), increased gradually up to day 14. Recently, Kizawa et al. [250] bioprinted a liver tissue by the spheroid assembly of primary hepatocytes (1×10^4 cells/ml) that maintained functionality up to 60 days, one of the longest period observed for a bioprinted liver tissue. In addition to drug, glucose, and lipid metabolism, bile secretion was also observed up to 60 days. Though only a small portion of liver tissue is printed, this study demonstrates the long-term functionality of the bioprinted liver tissue and hence, lead to whole organ (liver) bioprinting in the future.

One of the challenges in engineering liver tissue is the isolation, proliferation, long-term culture and maintenance of hepatocyte function ex vivo of primary hepatocytes [247, 249]. An alternate approach is the use of stem cells. Differentiation of iPSCs to liver-specific cell lines is gaining attention. Faulkner-Jones et al. [251] for the first time, bioprinted pluripotent stem cells (human induced pluripotent stem cell lines (hiPSCs) RCi-22 and RCi-50; and human Embryonic stem cell lines (hESCs) RC-6 and RC-10) (1×10^7 cells/ml) suspended in alginate hydrogel (1.5% w/v), using a microvalve bioprinting system. These cells differentiated into hepatocyte-like cells (HLCs) post-printing, exhibited a morphology similar to that of hepatocytes and showed the presence of hepatocyte-related genes HNF-4α, and albumin. This is the first successful work reported on bioprinting of pluripotent stem cells that differentiated into HLCs post-printing. Ma et al. [252] used stereolithography bioprinting to print hiPSC-derived hepatic progenitor cells (hiPSC-HPCs) suspended in GelMA hydrogel (5% w/v, supplemented with 0.3% w/v LAP as photoinitiator), along with supporting cells HUVECs and ADSCs (to form the vasculature) suspended in GelMA/Glycidal methacrylate-hyaluronic acid (GMHA) hydrogel (2.5% and 1% w/v respectively, supplemented with 0.45% w/v LAP as photoinitiator) in to 3D liver tissue construct. Post-printing differentiation evaluated by expression levels of hepatic markers demonstrated higher levels of markers associated with mature hepatocytes (HNF-4α, albumin, and TTR). In addition, the expression levels of key enzymes related to liver drug metabolism (CYP1A2, CYP2B6, CYP2C9, CYP2C19, and CYP3A4) were also witnessed, which is responsible for 60% of human drug oxidation.

Apart from the liver, three other tissues associated with a digestive system that is of interest to the tissue engineering community are

oesophagus, pancreas, and intestine. Though classical tissue engineering methods were used to engineer oesophagus [253], pancreas [253], and intestine [254], bioprinting of these tissues have not been attempted yet.

5.9.2. Challenges and future outlook

The need for the artificial liver is on the rise. Bioprinting is a potential technology to fabricate functional liver tissue and even whole functional liver. However, the main obstacle is the limited availability of primary hepatic cells due to the difficulty in obtaining liver biopsies from each patient [252]. In addition to the scarce availability of primary hepatocytes, they lose their function gradually when they are cultured ex vivo [247, 249]. Hence, use of stem cells would be the alternate method. Some studies [251, 252] have used pluripotent stem cells for bioprinting and then differentiating them into hepatocytes or HLCs. However, the post-printing viability reported in these studies is <65%. Further studies on optimizing the protocol and procedures to increase the cell viability and long-term post-printing functionality are needed, along with fundamental molecular pathways involved in the differentiation process. Bioprinting of oesophagus, pancreas, and intestine could be explored in the future.

5.10. Urinary system

The urinary system consists of the kidneys, urinary bladder, urethra, and the urinary tract. The main functions of this system are excretion of bodily wastes, and regulation of blood pH, electrolytes, and metabolites. In addition to these, the kidneys perform endocrinologic, metabolic, immunologic and hemodynamic functions. Bioengineering of artificial kidneys is of immense interest to both researchers and clinicians, considering the huge demand.

5.10.1. The kidneys

The number of patients with chronic renal failure is on the rise. About 9.4% of the adults in the US suffer from chronic kidney disease, with 400,000 end-stage renal diseases (ESRD) patients depending on dialysis [255]. There are only two treatment options for ESRD patients namely, dialysis, and kidney transplantation. Dialysis helps in fulfilling the filtration function of the kidneys but it doesn't help in other metabolic and endocrinologic functions, thereby impacting on the patient's health. Kidney transplantation, on the other hand, suffers from a shortage of donor organs. Moreover, the need for lifelong immunosuppressive drugs also significantly influences patient's quality of life, with 20% of patients facing acute rejection within 5 years, and 40% of patients facing death or loss of function within 10 years [256]. Multifunctionality and complex architecture of the kidneys hinder the fabrication of biomimetic artificial kidneys.

The works on bioengineering artificial kidneys started as early as 1980, with cells (proximal renal tubular cells) seeded on porous polymeric scaffolds placed in series with a hemofiltration circuit [255, 257]. Though the functionality of the construct in terms of urine filtration, improved metabolism, and improved cardiovascular stability was tested positive, the nature of the clinical trials didn't lead to a conclusive evidence of significant impact on survival. There has not been much progress since on engineered functional kidneys. With the advent of bioprinting, fabrication of functional kidneys seems a futuristic reality, though far on the horizon. Only a few studies were reported on the use of bioprinting for kidney fabrication. Homan et al. [258] bioprinted 3D human renal proximal tubules (PTs) with proximal tubule epithelial cells (PTECs) (2×10^7 cells/ml) suspended in a gelatin/fibrin hydrogel (7.5% w/v, and 10 mg/ml respectively), as shown in Fig. 10. The bioprinted PT had an open lumen architecture, with enhanced epithelial morphology and functions compared to the 2D controls. Self-assembly of tissue spheroids to fabricate a kidney mini-tissue is another approach explored for bioengineering of kidney. One such study [259] reported the formation of a kidney mini-tissue by re-aggregation and self-assembly of a simple suspension of isolated renogenic stem cells. Though the self-assembled mini-tissue had morphological similarities of the native tissue, with a branched urinary collecting duct system, excretory nephrons connected to the collecting duct tree and with Bowman's capsules, proximal tubules, loops of Henle and distal tubules, and successfully transplanted in vivo, aggregation and function on the macro-scale has not yet been demonstrated [256]. Bioprinting could be used to accomplish this task of building a human-scale renal tissue using self-assembly of tissue or cell spheroids. Kasyanov et al. [260] used 3D printing to fabricate the structure of kidney arterial vascular tree using silicon droplets as physical analogues of tissue spheroids. Though no cells were printed in this study, it demonstrates the capability of bioprinting to print such human-scale constructs using tissue spheroids.

Apart from the kidneys, other tissues and organs of the urinary system that are engineered are the urinary bladder, urethra, and the urinary tract. Bladder dysfunction, caused by a variety of congenital and acquired conditions, affects 400 million people worldwide [261]. Current treatment methods include reconstructive procedures with native non-urologic tissues such as skin or gastrointestinal segments, which results in significant complications due to the incompatibility of the grafted tissue to the long-term exposure of urine [261]. Hence, there is a need for artificial bioengineered bladders. Although traditional tissue engineering strategies such as cells seeded on porous polymeric scaffolds had been explored (reviewed in detail elsewhere [261, 262]), fabrication of functional bladder remains elusive. Bioprinting of bladder is yet to be explored. Xu et al. [124] used microvalve bioprinting to print a bladder tissue construct from primary SMCs (isolated from rat bladder tissue) ($0.1–1 \times 10^6$ cells/ml) suspended in a collagen hydrogel (0.2% w/v). Though post-printing viability was >90%, the printed tissue was morphologically dissimilar from that of a native rat bladder as showed by the histological studies. Similarly, Zhang et al. [263] bioprinted urethra with PCL/PLCL blend for fabrication of scaffolds, and extrusion of urothelial cells (UCs) (isolated from New Zealand white rabbits), and bladder SMCs (isolated from rabbit bladder) suspended in a gelatin/fibrin/hyaluronic acid hydrogel (35, 30, and 3 mg/ml respectively). Post-printing cell viability was over 80% after 7 days and the printed construct had morphological and mechanical properties similar to that of the native tissue. Bioprinting has not yet been explored for fabrication of urinary tract, although bioengineering of urinary tract itself is not new [264].

5.10.2. Challenges and future outlook

Bioprinted functional kidneys would be of immense help to the patients with ESRD. However, there are many challenges that are to be overcome before functional kidneys are bioprinted. The first challenge is the architectural complexity of kidney and limited availability of primary cells [255]. Hence, use of iPSCs to get differentiated nephron progenitor cells (NPCs) and other renal cells has to be explored [263]. Secondly, the formation of nephrons equivalent to that of the native kidney (one million nephrons approximately) is a challenge. Strategies for improving the efficiency of nephron formation has to be focused. The third challenge lies in the formulation of a bioink that will resemble the complex renal structure and functionality [265]. Bioprinting of tissue spheroids, enabling the formation of kidney tissue by self-assembly is a potential approach. Bioprinting of other tissues of urinary system such as the urethra, bladder, and urinary tract could be considered as these structures less complex compared to kidneys.

5.11. Circulatory/cardiovascular system

The circulatory system or cardiovascular system consists of heart and blood vessels which include arteries, veins, and capillaries. Cardiovascular disease accounts for nearly 20 million deaths worldwide annually, making it the leading cause of mortality [131]. >80,000 heart-valve replacements are performed annually in the US alone,

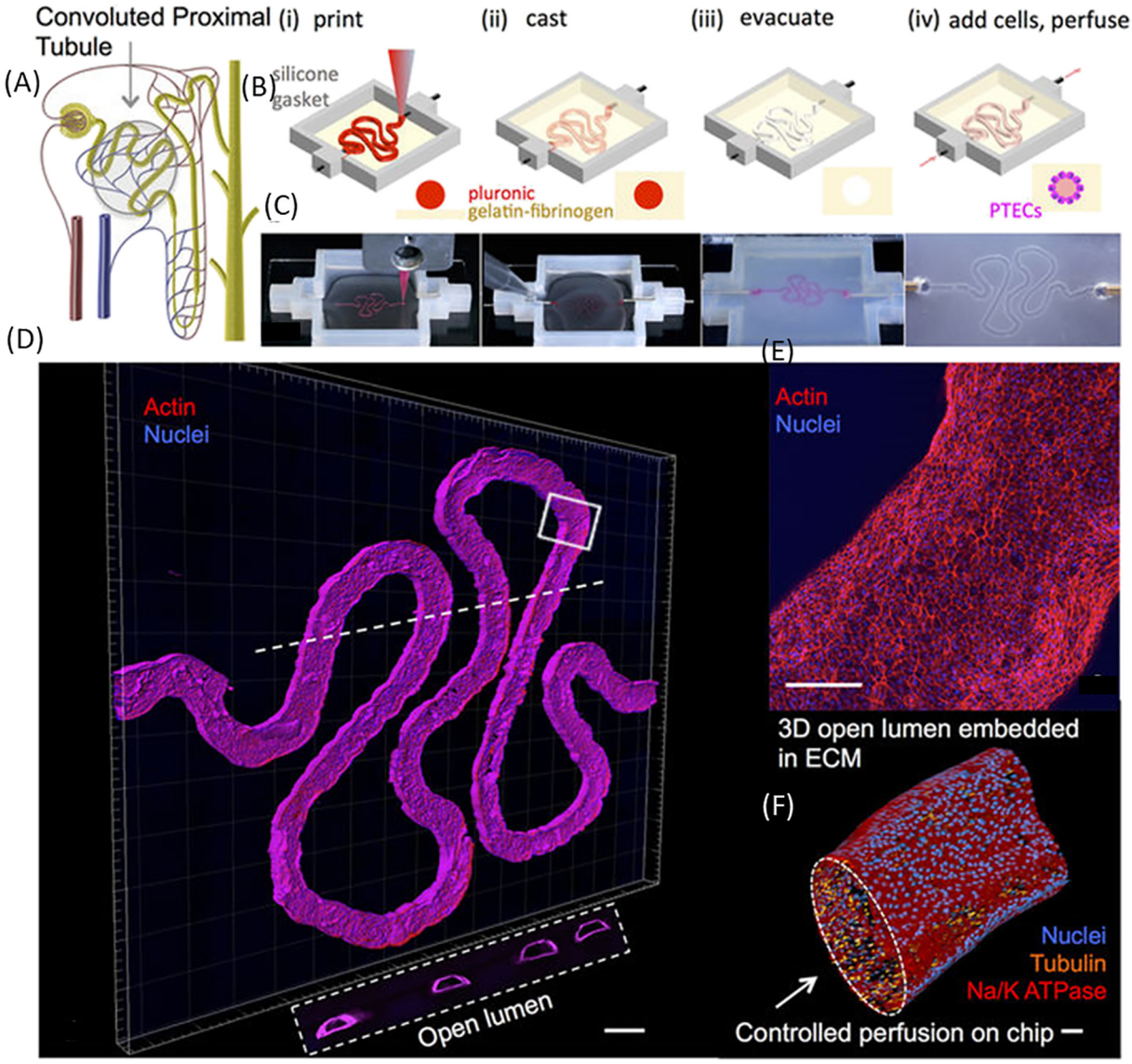

Fig. 10. Bioprinting in Urinary System (a–c) 3D convoluted renal proximal tubule on the chip. (d–f) 3D rendering of the printed convoluted proximal tubule acquired by confocal microscopy, where actin is stained in red and nuclei are blue; the white dotted line denotes the location of the cross-sectional view shown below in which PTEC cells circumscribe the open lumens in 3D. Scale bar = 50 μm.
Reprinted with permission from [258].

with the replacement of other cardiovascular tissues such as arteries, and myocardium in addition [266]. For the valve replacement surgeries, currently, mechanical and biological prosthetic valves are employed. While mechanical valves have high durability, the thrombogenicity of such valves is a major concern. Hence, the patients have to take blood-thinning medication for the rest of their lifetime. On the other hand, biological prosthetic valves suffer from many other disadvantages. Allografts and xenografts could lead to immune rejection, degeneration over time, and thrombosis while autografts (usually pulmonary autografts) are associated with complicated surgical procedures with possible requirement of a re-operation in 10–20 years [267]. Tissue engineered heart valves are potential alternatives that could possibly overcome the disadvantages of both mechanical and biological prosthetic valves. Various tissue engineering methods such as the use of decellularized xenogenic tissues, and cells seeded on polymeric scaffolds, were used to fabricate heart valves and been reviewed elsewhere [268]. However, the native anatomy of the cardiac valve could not be recapitulated and the heterogenic cell population could not be replicated by these methods [269].

Bioprinting is being increasingly used for the engineering of biomimetic heart valves. The advantages of bioprinting over other tissue engineering methods include accurate replication of the complex biomimetic architecture (e.g. the tri-leaflet valves), ability to fabricate mechanically heterogenic structure, and spatial control of valve cells (such as valve interstitial cells (VIC) and SMCs) [131]. Duan et al. [270] bioprinted an aortic valve conduit from porcine aortic VICs and human aortic root SMCs (isolated from the aortic root of a 12-year old young patient) (2×10^6 cells/ml) suspended in a gelatin/alginate hydrogel (0.06, and 0.05 g/ml respectively). Post-printing cell viability after 7 days was over 80%. This study only evaluated the post-printing cell viability of valve cells. In another study [271], human aortic valve interstitial cells (HAVICs) (isolated from the aortic valve leaflets of the donor heart from a 12-year-old patient) (5×10^6 cells/ml) suspended in a methacrylated hyaluronic acid (Me-HA)/methacrylated gelatin (Me-Gel) hydrogel (4% w/v of Me-HA, and 6%, 10%, 12% w/v of Me-Gel) was used to bioprint a tri-leaflet valve (Fig. 11). Maintaining a post-printing cell viability of over 90% after 7 days, histology and immunohistochemistry demonstrated significant gene expressions of αSMA, vimentin, periostin, and collagen 1A1 showing that the cells proliferated

normally post-printing and secreted their own ECM. However, the study is a short-term study (7 days) and the printed construct did not fulfil the mechanical performance of native valve tissue.

Other cardiac tissues save heart valves such as myocardium has also been bioprinted. Gaebel et al. [272] patterned HUVECs (4×10^6 cells/ml) and hMSCs (2×10^6 cells/ml) using laser-based bioprinting (LIFT method) on a polyester urethane urea (PEUU) cardiac patch. PEUU patch with randomly seeded cells without bioprinting was used as the control. In vivo studies on infarcted zone of rat hearts (after left anterior descending (LAD)-ligation) demonstrated that the bioprinted patch with spatial cell arrangement had more blood vessel formation, enhanced capillary density, and resulted in significant improvement in the functionality of the infarcted hearts in rats, 8 weeks after transplantation, compared to the control. In another study [273], human fetal cardiomyocyte progenitor cells (hCMPCs) (30×10^6 cells/ml) suspended in alginate hydrogel (7.5% w/v) were printed using extrusion bioprinting into a tissue construct with cardiogenic potential. Post-printing cell viability after 7 days was 89% and the cells maintained their cardiac lineage with upregulated gene expression of the early cardiac transcription factors Nkx2.5, Gata-4 and Mef-2c and the sarcomeric protein TroponinT. In a similar study [274], cardiac tissue constructs printed from hCMPCs (30×10^6 cells/ml) suspended in gelatin/hyaluronic acid matrix (commercial hydrogel: HyStem matrix, Sigma) were implanted into 10–12 weeks aged infarcted female NOD-SCID mice (after left anterior descending (LAD)-ligation) for in vivo studies. A 4-week follow-up study showed significant reduction in adverse remodeling, enhanced cardiac performance, and a temporal increase in cardiac and vascular differentiation of hCMPCs, as evaluated by MRI and histology.

Although primary cardiac cells could be isolated and proliferated ex vivo, the demand far exceeds the supply [275].The use of iPSCs is an alternate and highly potential option. Kerscher et al. [276] used human iPSCs (26×10^6 cells/ml) suspended in GelMA hydrogel (15% w/v) to bioprint cardiac tissues that differentiated post-printing. Cells continued to differentiate and spontaneous contractions were initiated on day 8 of

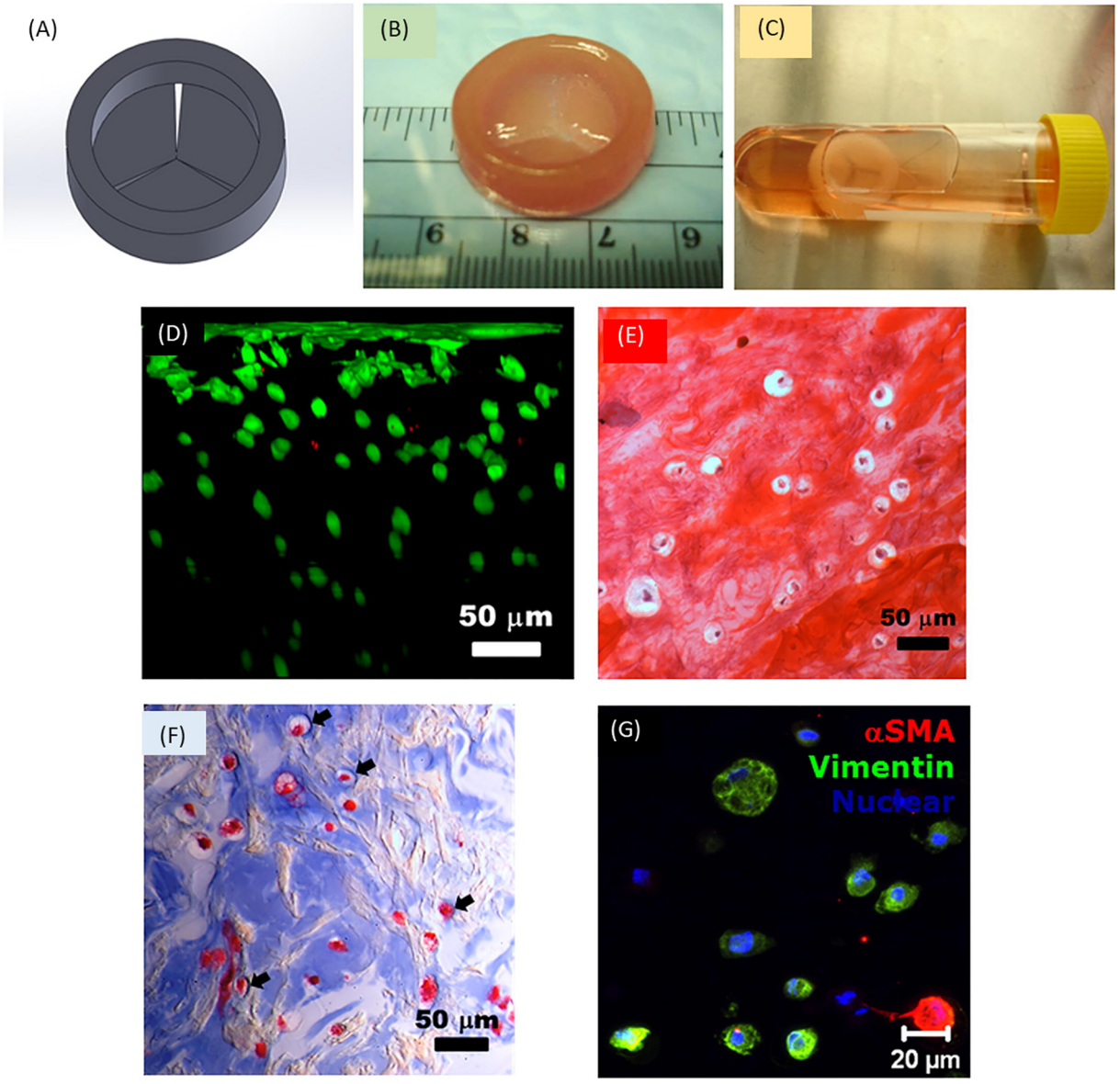

Fig. 11. Bioprinting in Circulatory System (A–G) Bioprinting of heart valve conduit with encapsulation of HAVIC within the leaflets: (A) heart valve model designed by Solidworks®; (B) as-printed valve conduit; (C) the bioprinted valve conduit kept intact after 7-day static culture in culture tube; (D) Live/Dead image; (E, F) histological staining of bioprinted leaflets after 7-day culture. (G) representative image of immunohistochemical staining for αSMA (green) and vimentin (red), and Draq 5 counterstaining for cell nuclei (blue).
Reprinted with permission from [271].

differentiation with synchronicity, frequency, and velocity of contraction increasing over time up to day 40, with cardiac gene expressions upregulated. In another study by Ong et al. [277], mixed cell spheroids of human induced pluripotent stem cell-derived cardiomyocytes (hiPSC-CMs), fibroblasts (FB) and endothelial cells (EC) of different ratios (CM:FB:EC = 70:15:15, 70:0:30, 45:40:15) were bioprinted into cardiac patches. While patches of all cell ratios beat spontaneously after bioprinting, exhibiting ventricular-like action potential waveforms and electrical conduction, patches with a low percentage of FBs exhibited higher conduction velocities and longer action potential duration. Immunohistochemistry and immunofluorescence images also demonstrated the presence of CD31+ protein representing blood vessel formation, and Cx43 representing the main cardiac gap junction protein. The bioprinted patches were implanted on to the heart of nude rats (NIH RNU sp./sp. rats, NTac:NIH-Foxn1rnu, 12 weeks, female, 165–195 g, Taconic). The implanted patches engrafted well on to the myocardium and were vascularized. However, neither long-term follow up studies were made nor the hearts functionally analyzed in this study. Both these studies failed to attain the conduction velocities and rate of beating similar to the native human heart and possessed weak mechanical properties.

5.11.1. Challenges and future outlook

Bioprinting functional cardiac patches could help in the treatment of patients with myocardial infarction, and bioprinted blood vessels in the valve-replacement surgeries. Focussed efforts on bringing bioprinted valves (from patient's own cells) to the clinical practice are necessary to replace the mechanical and bioprosthetic valves currently in the market. Avenues to use iPSCs also should be explored further, given the limited availability of primary cells. Formulating an ideal 'cardiac bioink' with appropriate stiffness and cell microenvironment is still a challenge [131], and development of in situ crosslinkable bioinks with spatially and temporally controllable crosslink rate and degree is an interesting future direction. Though the macrostructure of the whole heart could be printed and partially functional cardiac tissues could be bioprinted, bioprinting (organ printing) of a fully functional heart is still very far from reality.

5.12. Summary

In summary, bioprinting has been explored widely for fabrication of several different tissues pertaining to different organ systems (summarized in Table 4). While some tissue types such as bone, and skin had garnered ample attention in the bioprinting space, there are many areas yet to be explored such as lymphatic tissues and endocrine glands. In addition to the unique challenges pertaining to the application of bioprinting in each organ system as summarized in the respective sections, there are several common challenges concerning bioprinting. Limited availability of primary cells, bioprinting in clinically relevant sizes, bioinks with appropriate rheological properties, vascularization and innervation are the key challenges. Utilization of stem cells to get the desired cell lineage using directed differentiation is a possible solution to overcome the challenge of limited availability of primary cells. Bioprinting tissues in clinically relevant sizes are another challenge. Extrusion bioprinting is the only method available now which is capable of producing human-scale tissues. However, maintaining cell viability throughout the entire thickness and ensuring homogenous perfusion of nutrients and growth factors throughout the 3D structure is a humongous task. Bioprinting a developmental precursor or self-assembly of several small tissue constructs into the whole organ are some of the alternate approaches. Bioink development with appropriate rheological properties suitable for printing and biologically mimicking the ECM of respective tissues is still a challenge. Use of decellularized ECM and development of bioactive polymer blends for tissue-specific bioinks is a possible solution. Finally, vascularization and innervation of the bioprinted constructs is both a challenge and an interesting future direction. Incorporation of relevant growth factors and cells to promote vasculature and nerve growth, the combinatory approach of bioprinting and microfluidics are some of the future areas of research to get a vascularized and innervated bioprinted tissue. Potential future directions and focus areas in each of the organ systems are summarized in Table 3.

6. Implications of 3D bioprinting in drug discovery, development, and delivery systems

The rise of bioprinting could revolutionize the whole pharmaceutical paradigm which includes drug discovery, development and delivery systems. There are two major stages in bringing a new drug to the market namely, drug discovery (pre-clinical stage) and drug development (clinical stage) [278]. Drug discovery involves multiple types and multiple cycles of tests of large number of molecular compounds to narrow down to a few drugs with beneficial effects against the target clinical conditions, while drug development deals with further development of the selected drug with regard to its absorption, metabolization, excretion, optimal dosage requirements, toxicity, and its interaction with other drugs and treatment methods [11]. Drug delivery, which refers to the optimal transport of the drug in the body to achieve the desired therapeutic effect, also needs to be considered during the drug development stage. Bioprinting could play a role in all these three stages. In order to reduce the inherently high cost and long lead times involved with the drug development process, pharmaceutical industries are moving from the traditional drug development paradigm (Fig. 12(A)) to an alternative drug development paradigm called "quick-win, fast-fail" (Fig. 12(B)) [279]. The important stages in the traditional drug development cycle are drug discovery and pre-clinical phase, clinical phase (Phases I, II, and III), FDA review and approval, followed by Phase IV clinical trials and marketing. Of these different phases, the most expensive phase is the clinical phase, that contributes to almost 60% of the total cost and majority of the cycle time [11]. The "quick-win, fast-fail" strategy aims to reduce the time and cost involved in this phase of the drug discovery cycle, by focussing on reaching the proof-of-concept (POC) efficiently, as shown in Fig. 12(B).

To make the "quick-win, fast-fail" strategy work, the high rate of attrition has to be overcome by minimizing the technical uncertainties in the early stages of development. Non-clinical toxicology was the highest cause of attrition, attributing to 40% of all the failures, based on the conclusions arrived from the analysis of 10-year data obtained from four principal pharmaceutical companies [280]. About 94% of the drugs that passed the pre-clinical trials fail in the clinical phase [281]. The main reason for such a high attrition rate is the non-availability of biomimetic 3D in vitro models for drug toxicity testing. Most of the drug toxicity tests and assays are still performed on traditional 2D monolayer culture systems that do not mimic the native 3D tissue microenvironment [282]. Hence, there is a huge discrepancy between the pre-clinical in vitro results and the clinical in vivo results. 3D bioprinting has the potential to fabricate biomimetic tissues and many such tissues have already been printed as discussed in the previous section. These bioprinted tissues could be used as the in vitro drug testing models to evaluate the drug toxicity, thereby producing results similar to the future in vivo testing and hence reducing the high attrition rate, and the associated research expenses. Chang et al. [246] used a bioprinting-microfluidics combinatorial approach to fabricate a 3D liver tissue that could be used as an in vitro drug metabolism model to assess the drug pharmacokinetic profiles. In another study [283], a high-throughput miniature drug-screening platform was developed using inkjet bioprinting, where Escherichia coli-laden alginate hydrogel was bioprinted to array a chip on coverslips. On printing droplets of a mixture of three antibiotics (penicillin/streptomycin, antimycotic, and kanamycin sulfate) over the same spot of cells, the cell viability, functionality and antibacterial effects of antibiotics were evaluated against the micro-pipetted samples (control). The experimental and control

Table 3
Potential future directions and focus areas of bioprinting in different organ systems.

Organ system	Future directions and focus areas
Skeletal system	✓ Bioprinting bone in clinically relevant sizes (scalability) ✓ Alternate approaches such as bioprinting with microcarriers [158], and bioprinting a developmental precursor [160] to achieve clinically relevant sizes ✓ Bioreactor systems to maintain cell viability and nutrient perfusion throughout the 3D human-size bioprinted tissue ✓ Bioprinting tissues with zonal architecture, with zone--specific compositional and mechanical heterogeneity ✓ Seamless integration of different tissue types/interfacial tissue engineering (e.g. cartilage and subchondral bone) ✓ Differentiation protocols for stem cell differentiation to chondrocyte lineage (due to the scarcity of primary cells)
Muscular system	✓ Bioprinting muscle tissue is still not explored widely and preliminary studies in this area are required ✓ Bioprinting of muscles with different shapes (deltoid, rhomboid, latissimus, teres (round), trapezius), and direction of muscle fibers (rectus (straight); transverse (across); oblique (diagonally); orbicularis (circular)) could be explored ✓ Bioprinting of integrated multi-phasic structures such as MTU or muscle-bone or muscle-tendon-bone structure ✓ Bioprinting of vascularized and innervated skeletal muscle tissue
Nervous system	✓ Given the complexity of the tissue, only a few studies are reported to date ✓ Bioprinting a biomimetic neural/brain tissue with its intricate layered microarchitecture ✓ Neural stem cell differentiation studies using different hydrogel types and incorporation of growth factors that induce differentiation in vivo by localized growth factor delivery should be explored
Lymphatic system	✓ Bioprinting of lymphatic vessels and lymph nodes is an unexplored area with huge research and clinical potential ✓ Incorporation of cells and growth factors related to the lymphatic system in the bioprinting of other vascularized tissues ✓ Bioprinting of lymph nodes for development of artificial immune systems based therapeutic devices
Endocrine system	✓ Differentiation protocols for stem cell differentiation to endocrinal cells (due to the scarcity of primary cells) ✓ Development of suitable bioinks that can comfortably host the highly sensitive endocrinal cells ✓ Bioprinting insulin-producing β cell constructs for treatment of diabetes ✓ Bioprinting a fully functional endocrine gland with all the different types of cells and cytoarchitecture
Reproductive system	✓ Bioprinting has not yet been explored for addressing the problems of male and female infertility ✓ Bioprinted reproductive system tissues such as phallic tissue, uterus, ovary, and cervicovaginal tissue ✓ Differentiation protocols for stem cell differentiation (due to the scarcity of primary cells from reproductive tissues) ✓ Bioprinting of uterus
Integumentary system	✓ Bioprinting of a fully-functional skin with all the cell types and skin appendages ✓ In situ skin bioprinting systems for wound management of burn wounds ✓ Testing protocols for evaluating the functionality of bioprinted skin tissue ✓ Steps for regulatory approval and commercialization ✓ Bioprinted skin for drug and cosmetic testing in industries
Respiratory system	✓ Differentiation protocols for stem cell differentiation to lung-specific cell lineage (due to the scarcity of primary cells) ✓ Bioprinting of cell-laden hydrogels on the decellularized ECM to fabricate the lungs ✓ Bioprinting of trachea/airway and the alveolar space ✓ A combination of bioprinting and microfluidics might advance the research of bioprinting lungs to the next level
Digestive system	✓ Differentiation protocols for stem cell differentiation to hepatic cell lineage (due to the scarcity of primary cells) ✓ Protocols and mechanisms to maintain the functionality of primary hepatic cells ex vivo for an extended period ✓ Improve the post-printing cell viability and long-term functionality of the bioprinted liver tissue ✓ Bioprinting of oesophagus, pancreas, and intestine
Urinary system	✓ Bioprinting of kidneys, given its architectural complexity ✓ Use of iPSCs to get differentiated nephron progenitor cells (NPCs) and other renal cells (due to the scarcity of primary cells) ✓ Strategies for improving the efficiency of nephron formation ✓ Development of bioink that will resemble the complex renal structure and functionality ✓ Bioprinting of tissue spheroids, enabling the formation of kidney tissue by self-assembly is a potential approach ✓ Bioprinting of urethra, bladder, and urinary tract
Circulatory system	✓ Focussed efforts on bringing bioprinted valves (from patient's own cells) to the clinical practice ✓ Formulating an ideal 'cardiac bioink' with appropriate stiffness and cell microenvironment ✓ Development of in situ crosslinkable bioinks with spatially and temporally controllable crosslink rate and degree ✓ Bioprinting functional cardiac patches for treatment of myocardial infarction

groups showed similar results, thus proving the suitability of the bioprinted model to be used for high-throughput screening. By using this process, spots of diameter 150–240 μm can be printed at a rate of 213 assays per second, thus demonstrating a theoretical capability of running >18 million targets per day. Bioprinted tissue models are even available commercially (exVive3D™ liver tissue models) that could be used to screen drugs [284].

The possible use of bioprinting in drug discovery and development process is shown in Fig. 12(C). Bioprinting could be used in almost all the stages of drug discovery and development. Nonetheless, use of bioprinting in all the stages should be justifiable in terms of cost-benefit analysis and commercial viability [11]. Bioprinting has the potential to be used predominantly in the pre-clinical phase of the drug development cycle, including target selection, efficacy screening, toxicity analysis, high-throughput screening, and phenotypic screening.

Bioprinting is a potential tool that could be used in the field of personalized medicine. Personalized or precision medicine is a niche field, where therapeutic interventions are designed based on an individual's need or clinical condition. Personalized medicine is more relevant to cancer as cancer is a disease of the genome [285]. Different tumors having the same DNA might exhibit different gene expression pattern and profile. This heterogeneity (both intra-tumor and inter-tumor) complicates the treatment procedure since a common treatment method or drug designed based on the population level might not work. Hence, personalized treatment taking into account the individual's disease history, and gene makeup becomes necessary. In vitro tumor models serve as a platform to study the cancer metabolism and metastasis. However, traditional 2D and 3D cancer models suffer from numerous limitations including non-biomimicry, lack of vascularization, and inability to represent the highly complex tumor microenvironment (TME) [4]. 3D Bioprinting is capable of fabricating biomimetic, vascularized, and highly complex TME, overcoming the challenges of the traditional tumor models. The bioprinted TME, with relevant physical and chemical cues, proper cancer cell/matrix composition, with heterogeneous cell populations (cancer epithelial cells, stromal cells, immune cells, tumor-associated fibroblasts, and microvascular cells) and properties corresponding to the type and stage of cancer could be used as in vitro tumor models to study the cancer mechanism and metastasis for accurate personalized anti-cancer drug screening [4]. This is a very recent field of research and there are only a few studies reporting bioprinting of cancer models for anti-cancer drug screening [286–288]. Bioprinted metastasis-on-a-chip platforms [289, 290] are further developments in the field that could eventually lead to effective precision medicine treatments.

Table 4
Bioprinting of tissues pertaining to different organ systems.

Tissue type	Bioprinting method	Bioink	Cells	Cell concentration (cells/ml)	Post-printing cell viability	Reference
Bone	Extrusion-based bioprinting	Alginate (2% w/v)	BMSCs (obtained from iliac bone marrow aspirates of two-year-old Dutch milk goats)	1×10^6	>90% after 2 weeks	[152]
	Extrusion-based bioprinting	Alginate/gelatin (5% w/v each)	SaOS-2 (human osteogenic sarcoma cells)	5×10^5	>90% after 6 days	[153]
	Inkjet bioprinting	PEG-GelMA (10% w/v of PEG and 1.5% w/v of GelMA, supplemented with 0.05% w/v of Irgacure 2959)	hMSCs (harvested from a 22 year old male)	6×10^6	>90% after 21 days	[154]
	Microvalve bioprinting	Agarose/collagen (3 different concentrations - 0.5/0.21, 1/0.1, 2/0.05 g/ml)	hMSCs (isolated from femoral heads bone marrow of patients receiving hip-joint arthroplasty)	1.6×10^6	98% after 21 days	[155]
	Stereolithography bioprinting	GelMA (10% w/v)	hMSCs HUVECs	hMSCs - 2×10^5 HUVECs – 1×10^6	Viable up to 4 weeks (% not mentioned)	[157]
	Extrusion-based bioprinting	GelMA-gellan gum (10% w/v GelMA supplemented with 5.4% w/v D-mannose and 0.1% w/v of Irgacure 2959, and 1% w/v gellan gum)	BMSCs (isolated from the long bones of 2–4 weeks old Lewis rats)	8×10^6	>90% after 3 days	[158]
	Laser-based bioprinting	nano hydroxyapatite–collagen (1.2% w/v in 2 mg/ml type I rat collagen)	BMSCs (multipotent mouse bone marrow stromal precursor D1 cell line (ATCC))	120×10^6	Viable up to 42 days (% not mentioned)	[159]
	Extrusion-based bioprinting	Gamma-irradiated alginate incorporating Arg-Gly-Asp (RGD) specific adhesion peptides (RGD-γ alginate hydrogel) (2.45% w/v)	BMSCs (isolated from the femoral shaft of 4-month-old pigs)	20×10^6	Viable up to 12 weeks (% not mentioned)	[160]
Cartilage	Microvalve bioprinting	Nanocellulose/Alginate (2.5% w/v each)	hNCs (human nasoseptal chondrocytes)	15×10^6	>85% after 7 days	[163]
	Extrusion-based bioprinting	Collagen (10–20 mg/ml)	Meniscal fibrochondrocytes (isolated from 1 to 3 day old bovine joints)	10×10^6	>90% after 10 days	[164]
	Extrusion-based bioprinting	Nanocellulose/Alginate (60/40, dry wt% ratio)	iPSCs (human-derived induced pluripotent stem cells)	20×10^6	Viable up to 6 weeks (% not mentioned)	[166]
	Extrusion-based bioprinting	Alginate (3.5% w/v), Agarose (2% w/v), PEGMA (BioINK™, a commercial product), and GelMA (10% w/v with 0.05% Irgacure)	BMSCs (obtained from the femur of a 4 month old porcine donor)	20×10^6	>80% after 4 weeks	[167]
	Extrusion-based bioprinting	Gellan (3% w/v)/alginate (2% w/v)/BioCartilage (cartilage extracellular matrix particles) (40% w/w)	Bovine chondrocytes (harvested from full thickness articular cartilage of the lateral and medial femoral condyles of four 6 month old calves)	6×10^6	>95% after 7 days	[168]
	Extrusion-based bioprinting	Gelatin-methacryloyl/hyaluronic acid methacryloyl (GelMa/HAMa) (10% GelMA, and 2% HAMa)	ADSCs (Adipose Derived Stromal cells isolated from sheep infrapatellar fat pad)	5×10^6	>90% after 7 days	[169]
	Inkjet bioprinting	PEGDA (10% w/v, supplemented with 0.05% of Irgacure).	human chondrocytes	5×10^6	Viable up to 6 weeks (% not mentioned)	[170]
Muscle	Inkjet bioprinting	Cell culture media	MDSCs (primary muscle-derived stem cells isolated from adult mice)	Not reported	Not reported	[178]
	Inkjet bioprinting	Phosphate-buffered saline (PBS)	Mouse C2C12 myoblasts	8×10^6	Viable up to 14 days (% not mentioned)	[179]
	Extrusion-based bioprinting	Gelatin/fibrinogen/hyaluronic acid/glycerol hydrogel (35, 20, 3 mg/ml, and 10% *v*/v respectively)	Mouse C2C12 myoblasts	3×10^6	>90% after 1 day	[180]
	Extrusion-based bioprinting	Gelatin/fibrinogen/hyaluronic acid hydrogel (35, 25, and 3 mg/ml respectively)	Mouse C2C12 myoblasts NIH/3T3 fibroblasts	40×10^6	>80% after 7 days	[176]
Neural tissue	Extrusion-based bioprinting	Polyurethane (PU) nanoparticle bioink (25–30% w/v)	MNSCs (Murine Neural Stem Cells isolated from adult mouse brain)	4×10^6	>90% after 3 days	[182]
	Extrusion-based bioprinting	fibrin-factor XIII-hyaluronic acid hydrogel (50 mg/ml, 1 U/ml, and 4 mg/ml respectively) was printed into a thrombin/PVA solution (50 U/ml, and 1.4% w/v respectively)	Schwann cells (isolated in primary culture from the sciatic nerve of Sprague-Dawley rats)	2×10^5	>95% after 7 days	[183]
	Extrusion-based bioprinting	MNSCs in collagen (0.87–1.74 mg/ml) VEGF in fibrin (62.8 mg/ml)	MNSCs (C17.2 line)	1×10^6	>90% after 3 days	[188]
	Stereolithography	GelMA/graphene nanoplatelets	MNSCs	2×10^6	Viable up to	[186]

(continued on next page)

Table 4 (*continued*)

Tissue type	Bioprinting method	Bioink	Cells	Cell concentration (cells/ml)	Post-printing cell viability	Reference
	bioprinting	(10–20% w/v, and 1 mg/ml respectively, supplemented with 0.5% w/v Irgacure)			14 days (% not mentioned)	
	Extrusion-based bioprinting	RGD peptide modified gellan gum (0.5% w/v)	Primary cortical neurons (harvested from E18 embryos of BALB/cArcAusb mice)	1×10^6	>70% after 5 days	[189]
Lymphatic tissue	Inkjet bioprinting	Collagen peptide modified –alginate (concentration not mentioned)	Data not available	Data not available	Data not available	[196]
	Extrusion-based bioprinting	Alginate (concentration not mentioned)	Data not available	Data not available	Data not available	[196]
Endocrinal tissue (Thyroid)	Extrusion-based bioprinting	Collagen (3.12 mg/ml)	Thyroid spheroids (explanted from e14.5 mouse embryos) and Allantoic spheroids (explanted from e8.5 mouse embryos)	Data not available	Viable up to 5 weeks (% not mentioned)	[199]
Endocrinal tissue (Pancreatic)	Extrusion-based bioprinting	Alginate/gelatin (4%/5% w/v)	INS1E β-cell line (derived from rat insulinoma)	10×10^6	>95% after 21 days	[200]
	Extrusion-based bioprinting	Fibrinogen (10 mg/ml)	β cells differentiated from hPSCs (Harvard University Embryonic Stem cell 8 line (HUES8))	5×10^6	Viable up to 12 weeks (% not mentioned)	[201]
Skin	Laser-based bioprinting	A 1:1 mixture of ethylenediaminetetraacetic acid (EDTA) human blood plasma and alginate hydrogel (4 wt%)	NIH3T3 fibroblasts and HaCaT keratinocytes	$1–2 \times 10^6$	>98% after 1 day	[85]
	Laser-based bioprinting	Collagen (3 mg/ml)	NIH3T3 Swiss albino fibroblasts and HaCaT human immortalized keratinocytes	1.5×10^6	Viable up to 10 days (% not mentioned)	[224]
	Microvalve bioprinting	Collagen (2.05 mg/ml)	Primary adult human dermal fibroblasts and primary adult human epidermal keratinocytes	1×10^6	>80% after 1 day	[226]
	Microvalve bioprinting	Collagen (3 mg/ml)	Fibroblasts (HFF-1 from ATCC) and HaCaT keratinocytes	2×10^6 (fibroblasts) 5×10^6 (keratinocytes)	>95% after 1 day	[227]
	Microvalve bioprinting	PEG-based photo-polymerizable bioink (concentration not mentioned)	Primary human dermal fibroblasts and primary human epidermal keratinocytes	5×10^6 (fibroblasts) 1×10^7 (keratinocytes)	>90% after 7 weeks	[228]
	Microvalve bioprinting	Collagen (6 mg/ml)	Human dermal fibroblasts, human epidermal melanocytes, and human epidermal keratinocytes	1×10^6 (fibroblasts) 7×10^6 (melanocytes) 2×10^7 (keratinocytes)	Viable up to 10 days (% not mentioned)	[231]
	Extrusion-based bioprinting	Cell culture media	Primary human dermal fibroblasts and primary human epidermal keratinocytes	1.75×10^4 (fibroblasts) 0.6×10^6 (keratinocytes)	Viable up to 9 days (% not mentioned)	[229]
	Extrusion-based bioprinting	Gelatin/alginate/fibrinogen hydrogel (10%, 0.5%, and 2% w/v respectively)	Primary human dermal fibroblasts and primary human epidermal keratinocytes	1×10^6	Viable up to 26 days (% not mentioned)	[230]
	Extrusion-based bioprinting	Gelatin/alginate hydrogel (20%, and 4% w/v respectively)	Epithelial progenitors and dermal homogenates (isolated from wild-type C57/B16 mice aged 3–4 weeks)	Data not available	Viable up to 14 days (% not mentioned)	[130]
Lung tissue	Microvalve bioprinting	Cell culture media	A549 cells (alveolar epithelial type II cells; AT-II) and EA. hy926 cells (an endothelial hybrid human cell line derived by fusing human umbilical vein endothelial cells (HUV-EC) with A549 cells)	4.5×10^6	Viable up to 72 h (% not mentioned)	[240]
Liver tissue	Microvalve bioprinting	Alginate (3% w/v)	HepG2 cells	$1–4 \times 10^6$	Viable up to 48 h (% not mentioned)	[246]
	Extrusion-based bioprinting	NovoGel^R 2.0 hydrogel (concentration not mentioned)	Primary human hepatocytes, hepatic stellates, HUVEC cells, and non-parenchymal cells	150×10^6	Viable up to 28 days (% not mentioned)	[247]
	Inkjet bioprinting	Galactosylated alginate (12 mg/ml)	Primary mouse hepatocytes (isolated from the liver tissue of male 6- to 8-week-old ICR 12 mice)	Data not available	>85% after 2 days	[248]
	Extrusion-based bioprinting	Alginate (3% w/v)	Primary mouse hepatocytes (isolated from the livers of 6–8 weeks old mice)	4×10^7	Viable up to 14 days (% not mentioned)	[249]
	Extrusion-based	Cell culture media	Primary mouse hepatocytes	1×10^4	Viable up to	[250]

Table 4 (*continued*)

Tissue type	Bioprinting method	Bioink	Cells	Cell concentration (cells/ml)	Post-printing cell viability	Reference
	bioprinting				60 days (% not mentioned)	
	Microvalve bioprinting	Alginate (1.5% w/v)	hiPSCs (human induced pluripotent stem cell lines,RCi-22 and RCi-50); hESCs (human Embryonic stem cell lines,RC-6 and RC-10)	1×10^7	>55% after 1 days	[251]
	Stereolithography bioprinting	hiPSC-HPCs in GelMA hydrogel (5% w/v, supplemented with 0.3% w/v LAP as photoinitiator); HUVECs and ADSCs in GelMA/GMHA hydrogel (2.5% and 1% w/v respectively, supplemented with 0.45% w/v LAP as photoinitiator)	hiPSC-HPCs (hiPSC-derived hepatic progenitor cells), HUVECs, and ADSCs	2×10^5	>65% after 7 days	[252]
Renal tissue (Kidney)	Extrusion-based bioprinting	Gelatin/fibrin hydrogel (7.5% w/v, and 10 mg/ml respectively)	PTECs (proximal tubule epithelial cells, human immortalized)	2×10^7	Viable up to 65 days (% not mentioned)	[258]
Urinary bladder	Microvalve bioprinting	Collagen (0.2% w/v)	Primary SMCs (isolated from rat bladder tissue)	$0.1–1 \times 10^6$	>90% after 5 days	[124]
Urethra	Extrusion-based bioprinting	Gelatin/fibrin/hyaluronic acid (35, 30, and 3 mg/ml respectively)	UCs (urothelial cells isolated from New Zealand white rabbits) and bladder SMCs (isolated from rabbit bladder)	10×10^6	>80% after 7 days	[263]
Cardiac tissue	Extrusion-based bioprinting	Gelatin/alginate (0.06, and 0.05 g/ml respectively)	Porcine aortic VICs and human aortic root SMCs (isolated from the aortic root of a 12-year old young patient)	2×10^6	>80% after 7 days	[270]
	Extrusion-based bioprinting	Methacrylated hyaluronic acid (Me-HA)/methacrylated gelatin (Me-Gel) (4% w/v of Me-HA, and 6%, 10%, 12% w/v of Me-Gel)	HAVICs (human aortic valve interstitial cells isolated from the aortic valve leaflets of the donor heart from a 12-year-old patient)	5×10^6	>90% after 7 days	[271]
	Laser-based bioprinting	Cell culture media	HUVECs and hMSCs	4×10^6 (HUVECs) and 2×10^6 (hMSCs)	Viable up to 8 days (% not mentioned)	[272]
	Extrusion-based bioprinting	Alginate (7.5% w/v)	hCMPCs (human fetal cardiomyocyte progenitor cells)	30×10^6	>85% after 7 days	[273]
	Extrusion-based bioprinting	Gelatin/hyaluronic acid matrix (commercial hydrogel: HyStem matrix, Sigma)	hCMPCs (human fetal cardiomyocyte progenitor cells)	30×10^6	Viable up to 4 weeks (% not mentioned)	[274]
	Extrusion-based bioprinting	GelMA (15% w/v)	human iPSCs	26×10^6	Viable up to 40 days (% not mentioned)	[276]
	Inkjet bioprinting	Cell culture media	hiPSC-CMs (human induced pluripotent stem cell-derived cardiomyocytes), fibroblasts and endothelial cells	Data not available	>90% after 7 days	[277]

In addition to its potential applications in drug discovery and development, bioprinting can also be used in drug delivery systems. 3D printing of drug solutions on to implants [291, 292], drug-eluting devices such as a stent or catheter [293], 3D printed tablets with customized drug release profiles [294, 295], and transdermal delivery systems [296, 297] are some of the applications of general 3D printing in drug delivery systems. Drugs can also be combined with the bioprinting process. For example, a bioprinted tissue for implantation into a tumor resected site might be loaded with appropriate anti-cancer drugs with a required release profile. Yi et al. [298] used 3D printing to fabricate a biodegradable local drug delivery patch composed of a blend of PLGA, PCL, and 5-fluorouracil that was later implanted to the bottom of subcutaneously grafted pancreatic cancers in athymic mice. With the ability to manipulate the geometry of the patch and hence the release kinetics, drug release over four weeks with the suppressed growth of the pancreatic cancer xenografts in mice was achieved.

Thus, 3D bioprinting could have huge implications in the drug discovery, development, and delivery systems. If used wisely, bioprinting could considerably reduce the drug discovery time and cost, by reducing the high attrition rate in the pre-clinical phase to the clinical phase. Bioprinted tissues and in vitro tumor models fabricated from the patient's own cells could be used to design personalized medicine. Bioprinting, combined with anti-cancer drugs, could be used as local drug delivery devices [299] for targeted and controlled drug release, thus overcoming the limitations of conventional chemotherapy.

7. Conclusions and future perspectives

3D bioprinting is an emerging technology in the field of tissue engineering and regenerative medicine. In this review, we deliberated the current status and contemporary issues of bioprinting for regenerative medicine, pertaining to eleven organ systems of human body including skeletal, muscular, nervous, lymphatic, endocrine, reproductive, integumentary, respiratory, digestive, urinary, and circulatory systems. There has been a commendable and substantial progress in the bioprinting arena in the recent past. Although successful bioprinting of various tissue types had been reported, taking the technology from the bench to the bedside still requires focussed efforts on many fronts. The following recommendations are put forward to make the field of bioprinting more translational in nature:

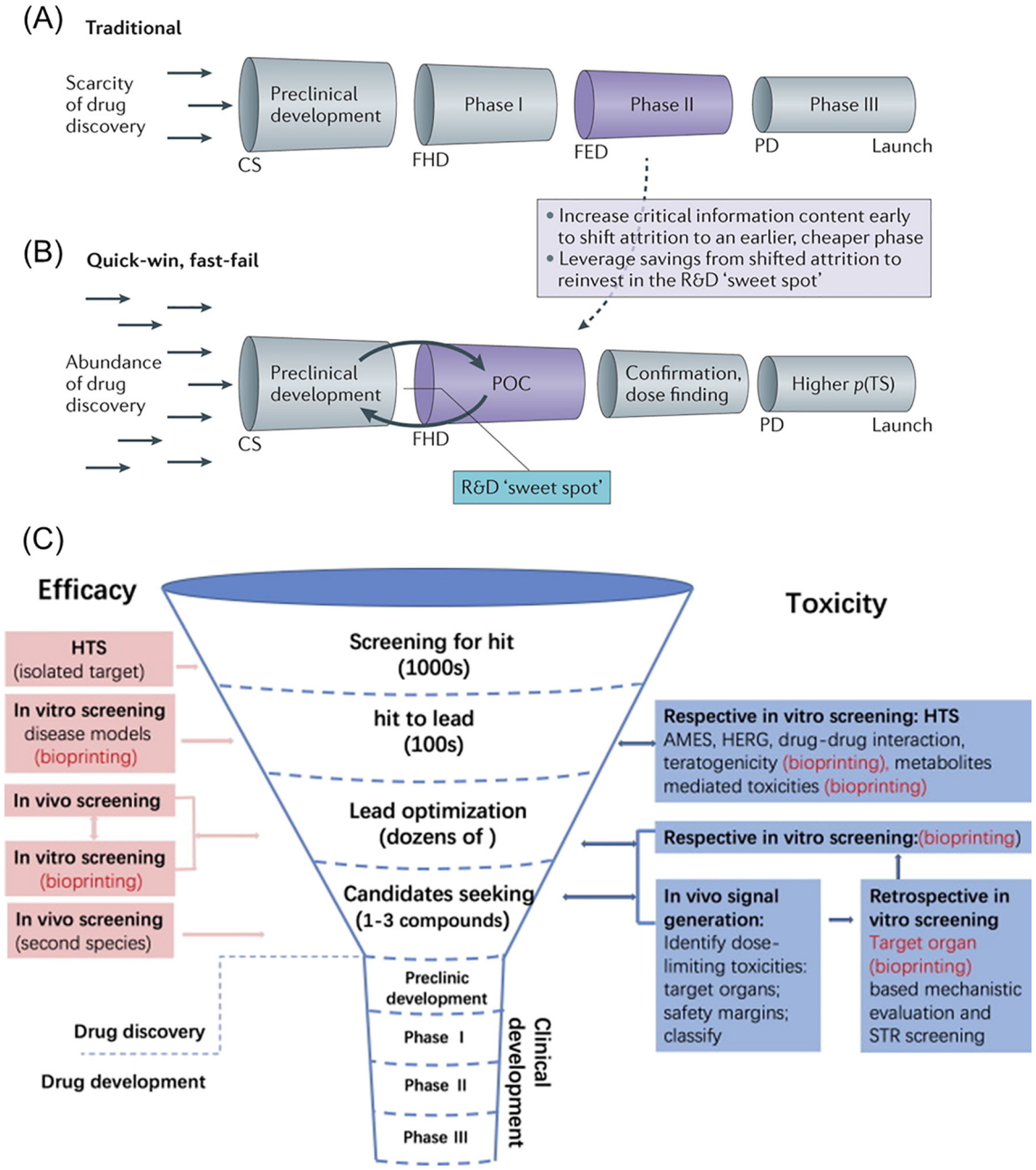

Fig. 12. (A) The traditional drug development model, and (B) The "quick-win, fast-fail" drug development model, with a greater focus on reaching proof-of-concept (POC) efficiently, faster and with lower cost — technical uncertainty is intentionally decreased before the expensive later development stages (Phase II and Phase III). The reduced number of new molecular entities entering Phase II and Phase III advance with a higher probability of technical success (p(TS)). Any savings gained from this paradigm can be reinvested to further enhance research and development (R&D) productivity. CS, candidate selection; FED, first efficacy dose; FHD, first human dose; PD, product decision. Reprinted with permission from [279]. (C) Schemes of applications of bioprinting on drug discovery and development process. Reprinted with permission from [11].

- Computational simulation and mathematical models for study of tissue growth or tissue fusion post-printing might help in designing and optimizing the bioprinting process. Such studies are lacking at present and are a potential area to focus in the future.
- Many of the published studies on bioprinting employ immortalized, cancer-derived cells lines which possess high resistance to stresses caused during the bioprinting process. Hence, use of primary cells, where possible, is highly recommended.
- Long-term studies on evaluation of post-printing cell viability, cell phenotype changes, and functionality are needed as many studies reported are short-term studies (1 day to 2 weeks)
- Bioprinting of human-scale tissues is still a challenge and focussing on the scalability of bioprinting technology is necessary. Of all the bioprinting methods, only extrusion-based bioprinting has the potential to fabricate volumetric human-scale tissues but lacks speed and resolution. Strategies to improve the speed and resolution of extrusion-based bioprinting method might help in realizing the goal of printing tissues of clinically relevant sizes.
- Bioprinting a developmental precursor [160] that would serve as a template for in vivo organogenesis is a potential alternate approach to achieve human-scale tissue bioprinting
- Maintenance of cell viability and nutrient perfusion throughout the 3D tissue structure is a big challenge, even if bioprinting of human-scale tissues are achieved. Hence, suitable post-processing strategies

such as perfusion bioreactors have to be developed in parallel.

- ➢ Development of hybrid systems, integrating different bioprinting modalities is essential to bioprint tissues and organs with a highly complex cytoarchitecture. Such a system should be capable of printing multiple materials, heterogeneous cell populations, and other associated growth factors and nutrients.
- ➢ Since most of the bioprinting methods are nozzle-based processes, strategies to avoid nozzle clogging or easy de-clogging of nozzles during the process is a potential focus area, especially during extended period of printing human-scale tissues and with high cell concentration.
- ➢ Development of bioinks with properties mimicking the native tissue ECM for different tissues is a prime area of focus within bioprinting. Currently, only a limited number of hydrogels are used; new bioinks with tuneable mechanical and rheological properties have to be developed.
- ➢ A deeper understanding of cell-matrix (bioink) interaction, in terms of mechanobiology and molecular pathways are needed to substantiate the claim of safe transplantation of bioprinted tissues into humans.
- ➢ 4D bioprinting is a future area of research, where smart hydrogels (responsive to external stimuli such as temperature, pH, light, electric or magnetic field) are utilized. Bioprinted constructs made of smart hydrogels could change their shape and/or function when an external stimuli is applied. Where direct replication of the native tissue is not possible, 4D bioprinting is useful, in the sense that 3D bioprinted construct in a particular shape when subjected to physiological conditions such as pH or temperature, could reshape or change their function to biomimic the native tissue.
- ➢ Finally, the ethical, social and regulatory issues concerning bioprinting technology and bioprinted tissues and organs [3, 10] have to be adequately addressed for successful market translation of this technology.

References

[1] S. Vijayavenkataraman, W.F. Lu, J.Y.H. Fuh, 3D bioprinting of skin: a state-of-the-art review on modelling, materials, and processes, Biofabrication 8 (2016).
[2] Y.J. Seol, H.W. Kang, S.J. Lee, A. Atala, J.J. Yoo, Bioprinting technology and its applications, Eur. J. Cardiothorac. Surg. 46 (2014) 342–348.
[3] S. Vijayavenkataraman, A perspective on bioprinting ethics, Artif. Organs 40 (2016) 1033–1038.
[4] Y.S. Zhang, M. Duchamp, R. Oklu, L.W. Ellisen, R. Langer, A. Khademhosseini, Bioprinting the cancer microenvironment, ACS Biomater. Sci. Eng. 2 (2016) 1710–1721.
[5] H. Cui, M. Nowicki, J.P. Fisher, L.G. Zhang, 3D bioprinting for organ regeneration, Adv. Healthc. Mater. (2017) 6.
[6] I.T. Ozbolat, M. Hospodiuk, Current advances and future perspectives in extrusion-based bioprinting, Biomaterials 76 (2016) 321–343.
[7] C.Y. Liaw, M. Guvendiren, Current and emerging applications of 3D printing in medicine, Biofabrication 9 (2017).
[8] S. Jie, Y. Haoyong, T.L. Chaw, C.C. Chiang, S. Vijayavenkataraman, An interactive upper limb rehab device for elderly stroke patients, Procedia CIRP 60 (2017) 488–493.
[9] C. Wu, B. Wang, C. Zhang, R.A. Wysk, Y.W. Chen, Bioprinting: an assessment based on manufacturing readiness levels, Crit. Rev. Biotechnol. 37 (2017) 333–354.
[10] S. Vijayavenkataraman, W.F. Lu, J.Y.H. Fuh, 3D bioprinting – an Ethical, Legal and Social Aspects (ELSA) framework, Bioprinting 1-2 (2016) 11–21.
[11] W. Peng, P. Datta, B. Ayan, V. Ozbolat, D. Sosnoski, I.T. Ozbolat, 3D bioprinting for drug discovery and development in pharmaceutics, Acta Biomater. 4 (2017), 63.
[12] S. Vijayavenkataraman, J.Y. Fuh, W.F. Lu, 3D printing and 3D bioprinting in pediatrics, Bioengineering 4 (2017) 63.
[13] M. Rodríguez-Salvador, R.M. Rio-Belver, G. Garechana-Anacabe, Scientometric and patentometric analyses to determine the knowledge landscape in innovative technologies: the case of 3D bioprinting, PLoS One 12 (2017).
[14] MarketsandMarkets™ INC, 3D Bioprinting Market by Technology (Microextrusion, Inkjet, Laser, Magnetic), Material (Cells, Hydrogels, Extracellular Matrices, Biomaterials), Application (Clinical (Bone, Cartilage, Skin) & Research (Regenerative Medicine)) - Global Forecasts to 2021, 2017.
[15] L. Feldkamp, L. Davis, J. Kress, Practical cone-beam algorithm, J. Opt. Soc. Am. A 1 (1984) 612–619.
[16] C.K. Chua, W.Y. Yeong, Bioprinting: Principles and Applications, World Scientific Publishing Co Inc, 2014.
[17] J.J. Ballyns, L.J. Bonassar, Image-guided tissue engineering, J. Cell. Mol. Med. 13 (2009) 1428–1436.
[18] R. Landers, U. Hübner, R. Schmelzeisen, R. Mülhaupt, Rapid prototyping of scaffolds derived from thermoreversible hydrogels and tailored for applications in tissue engineering, Biomaterials 23 (2002) 4437–4447.
[19] B. Van Rietbergen, R. Müller, D. Ulrich, P. Rüegsegger, R. Huiskes, Tissue stresses and strain in trabeculae of a canine proximal femur can be quantified from computer reconstructions, J. Biomech. 32 (1999) 165–173.
[20] A. Kriete, A. Breithecker, W. Rau, 3D imaging of lung tissue by confocal microscopy and micro-CTSpie Bios Conf Proc 2001, pp. 469–476.
[21] H.S. Tuan, D.W. Hutmacher, Application of micro CT and computation modeling in bone tissue engineering, Comput. Aided Des. 37 (2005) 1151–1161.
[22] S.Y. Nam, L.M. Ricles, L.J. Suggs, S.Y. Emelianov, Imaging strategies for tissue engineering applications, Tissue Eng. B Rev. 21 (2014) 88–102.
[23] J.M. Theysohn, S. Maderwald, O. Kraff, C. Moenninghoff, M.E. Ladd, S.C. Ladd, Subjective acceptance of 7 Tesla MRI for human imaging, MAGMA 21 (2008) 63.
[24] E. Terreno, D.D. Castelli, A. Viale, S. Aime, Challenges for molecular magnetic resonance imaging, Chem. Rev. 110 (2010) 3019–3042.
[25] M. Elliott, A. Thrush, Measurement of resolution in intravascular ultrasound images, Physiol. Meas. 17 (1996) 259.
[26] P.N. Wells, H.-D. Liang, Medical ultrasound: imaging of soft tissue strain and elasticity, J. R. Soc. Interface 8 (2011) 1521–1549.
[27] L.W. Dobrucki, A.J. Sinusas, PET and SPECT in cardiovascular molecular imaging, Nat. Rev. Cardiol. 7 (2010) 38–47.
[28] J. Kim, Y. Piao, T. Hyeon, Multifunctional nanostructured materials for multimodal imaging, and simultaneous imaging and therapy, Chem. Soc. Rev. 38 (2009) 372–390.
[29] R. Karch, F. Neumann, M. Neumann, W. Schreiner, Staged growth of optimized arterial model trees, Ann. Biomed. Eng. 28 (2000) 495–511.
[30] M. McCormick, X. Liu, J. Jomier, C. Marion, L. Ibanez, ITK: enabling reproducible research and open science, Front. Neuroinform. 8 (2014).
[31] W. Sun, B. Starly, A. Darling, C. Gomez, Computer-aided tissue engineering: application to biomimetic modelling and design of tissue scaffolds, Biotechnol. Appl. Biochem. 39 (2004) 49–58.
[32] I.T. Ozbolat, A. Khoda, M. Marchany, J.A. Gardella, B. Koc, Hybrid tissue scaffolds for controlled release applications: a study on design and fabrication of hybrid and heterogeneous tissue scaffolds for controlled release applications is presented in this paper, Virtual Phys. Prototyping, 7, 2012, pp. 37–47.
[33] J. Freund, K. Sloan, Accelerated volume rendering using homogeneous region encoding, Proceedings of the 8th conference on Visualization'97IEEE Computer Society Press 1997, p. 191 , (ff).
[34] P. Sabella, A rendering algorithm for visualizing 3D scalar fields, ACM SIGGRAPH Computer Graphics, 22, 1988, pp. 51–58.
[35] S.M. Morvan, G.M. Fadel, Heterogeneous solids: possible representation schemes, Proceedings of the Solid Freeform Fabrication Symposium, Austin, TX 1999, pp. 187–197.
[36] A.A. Requicha, Representations of rigid solid objects, Computer Aided Design Modelling, Systems Engineering, CAD-Systems, Springer 1980, pp. 1–78.
[37] C.-M. Cheah, C.-K. Chua, K.-F. Leong, C.-H. Cheong, M.-W. Naing, Automatic algorithm for generating complex polyhedral scaffold structures for tissue engineering, Tissue Eng. 10 (2004) 595–610.
[38] S.J. Hollister, R.A. Levy, T.M. Chu, J.W. Halloran, S.E. Feinberg, An image-based approach for designing and manufacturing craniofacial scaffolds, Int. J. Oral Maxillofac. Surg. 29 (2000) 67–71.
[39] M. Smith, C. Flanagan, J. Kemppainen, J. Sack, H. Chung, S. Das, S. Hollister, S. Feinberg, Computed tomography-based tissue-engineered scaffolds in craniomaxillofacial surgery, Int. J. Med. Rob. Comput. Assisted Surg. 3 (2007) 207–216.
[40] D. Yoo, Heterogeneous minimal surface porous scaffold design using the distance field and radial basis functions, Med. Eng. Phys. 34 (2012) 625–639.
[41] S.C. Kapfer, S.T. Hyde, K. Mecke, C.H. Arns, G.E. Schröder-Turk, Minimal surface scaffold designs for tissue engineering, Biomaterials 32 (2011) 6875–6882.
[42] S. Giannitelli, D. Accoto, M. Trombetta, A. Rainer, Current trends in the design of scaffolds for computer-aided tissue engineering, Acta Biomater. 10 (2014) 580–594.
[43] J.W. Jung, H.-G. Yi, T.-Y. Kang, W.-J. Yong, S. Jin, W.-S. Yun, D.-W. Cho, Evaluation of the effective diffusivity of a freeform fabricated scaffold using computational simulation, J. Biomech. Eng. 135 (2013) 084501.
[44] C.X. Lam, M.M. Savalani, S.-H. Teoh, D.W. Hutmacher, Dynamics of in vitro polymer degradation of polycaprolactone-based scaffolds: accelerated versus simulated physiological conditions, Biomed. Mater. 3 (2008) 034108.
[45] E. Saito, Y. Liu, F. Migneco, S.J. Hollister, Strut size and surface area effects on long-term in vivo degradation in computer designed poly (l-lactic acid) three-dimensional porous scaffolds, Acta Biomater. 8 (2012) 2568–2577.
[46] A.L. Olivares, È. Marsal, J.A. Planell, D. Lacroix, Finite element study of scaffold architecture design and culture conditions for tissue engineering, Biomaterials 30 (2009) 6142–6149.
[47] H. Singh, S.-H. Teoh, H.T. Low, D. Hutmacher, Flow modelling within a scaffold under the influence of uni-axial and bi-axial bioreactor rotation, J. Biotechnol. 119 (2005) 181–196.
[48] D.W. Hutmacher, H. Singh, Computational fluid dynamics for improved bioreactor design and 3D culture, Trends Biotechnol. 26 (2008) 166–172.
[49] S. Truscello, G. Kerckhofs, S. Van Bael, G. Pyka, J. Schrooten, H. Van Oosterwyck, Prediction of permeability of regular scaffolds for skeletal tissue engineering: a combined computational and experimental study, Acta Biomater. 8 (2012) 1648–1658.
[50] B. Porter, R. Zauel, H. Stockman, R. Guldberg, D. Fyhrie, 3-D computational modeling of media flow through scaffolds in a perfusion bioreactor, J. Biomech. 38 (2005) 543–549.

[51] Y. Yao, W.D. Chen, W.Y. Jin, The influence of pore structure on internal flow field shear stress within scaffold, Advanced Materials Research, Trans Tech Publ 2011, pp. 771–775.
[52] K. Garikipati, E. Arruda, K. Grosh, H. Narayanan, S. Calve, A continuum treatment of growth in biological tissue: the coupling of mass transport and mechanics, J. Mech. Phys. Solids 52 (2004) 1595–1625.
[53] A. Menzel, Modelling of anisotropic growth in biological tissues, Biomech. Model. Mechanobiol. 3 (2005) 147–171.
[54] S.M. Klisch, A. Hoger, Volumetric growth of thermoelastic materials and mixtures, Math. Mech. Solids 8 (2003) 377–402.
[55] J.M. Pérez-Pomares, R.A. Foty, Tissue fusion and cell sorting in embryonic development and disease: biomedical implications, BioEssays 28 (2006) 809–821.
[56] F. Graner, J.A. Glazier, Simulation of biological cell sorting using a two-dimensional extended Potts model, Phys. Rev. Lett. 69 (1992) 2013.
[57] J.A. Glazier, F. Graner, Simulation of the differential adhesion driven rearrangement of biological cells, Phys. Rev. E 47 (1993) 2128.
[58] E. Palsson, H.G. Othmer, A model for individual and collective cell movement in *Dictyostelium discoideum*, Proc. Natl. Acad. Sci. 97 (2000) 10448–10453.
[59] A.F. Marée, P. Hogeweg, How amoeboids self-organize into a fruiting body: multicellular coordination in *Dictyostelium discoideum*, Proc. Natl. Acad. Sci. 98 (2001) 3879–3883.
[60] J. Murray, D. Manoussaki, S. Lubkin, R. Vernon, A mechanical theory of in vitro vascular network formation, Vascular Morphogenesis: In Vivo, In Vitro, In Mente, Springer 1996, pp. 173–188.
[61] J.L. Semple, N. Woolridge, C.J. Lumsden, In vitro, in vivo, in silico: computational systems in tissue engineering and regenerative medicine, Tissue Eng. 11 (2005) 341–356.
[62] R.Z. Lin, H.Y. Chang, Recent advances in three-dimensional multicellular spheroid culture for biomedical research, Biotechnol. J. 3 (2008) 1172–1184.
[63] J.C. Mombach, D. Robert, F. Graner, G. Gillet, G.L. Thomas, M. Idiart, J.-P. Rieu, Rounding of aggregates of biological cells: experiments and simulations, Physica A 352 (2005) 525–534.
[64] P. Marmottant, A. Mgharbel, J. Käfer, B. Audren, J.-P. Rieu, J.-C. Vial, B. Van Der Sanden, A.F. Marée, F. Graner, H. Delanoë-Ayari, The role of fluctuations and stress on the effective viscosity of cell aggregates, Proc. Natl. Acad. Sci. 106 (2009) 17271–17275.
[65] A.B. Bortz, M.H. Kalos, J.L. Lebowitz, A new algorithm for Monte Carlo simulation of Ising spin systems, J. Comput. Phys. 17 (1975) 10–18.
[66] E. Flenner, L. Janosi, B. Barz, A. Neagu, G. Forgacs, I. Kosztin, Kinetic Monte Carlo and cellular particle dynamics simulations of multicellular systems, Phys. Rev. E 85 (2012) 031907.
[67] Y. Sun, Q. Wang, Modeling and simulations of multicellular aggregate self-assembly in biofabrication using kinetic Monte Carlo methods, Soft Matter 9 (2013) 2172–2186.
[68] X. Yang, V. Mironov, Q. Wang, Modeling fusion of cellular aggregates in biofabrication using phase field theories, J. Theor. Biol. 303 (2012) 110–118.
[69] K. Jakab, C. Norotte, F. Marga, K. Murphy, G. Vunjak-Novakovic, G. Forgacs, Tissue engineering by self-assembly and bio-printing of living cells, Biofabrication 2 (2010) 022001.
[70] A.N. Mehesz, J. Brown, Z. Hajdu, W. Beaver, J. Da Silva, R. Visconti, R. Markwald, V. Mironov, Scalable robotic biofabrication of tissue spheroids, Biofabrication 3 (2011) 025002.
[71] D. Chrisey, A. Pique, J. Fitz-Gerald, R. Auyeung, R. McGill, H. Wu, M. Duignan, New approach to laser direct writing active and passive mesoscopic circuit elements, Appl. Surf. Sci. 154 (2000) 593–600.
[72] N.R. Schiele, D.T. Corr, Y. Huang, N.A. Raof, Y. Xie, D.B. Chrisey, Laser-based direct-write techniques for cell printing, Biofabrication 2 (2010) 032001.
[73] M. Duocastella, M. Colina, J. Fernández-Pradas, P. Serra, J. Morenza, Study of the laser-induced forward transfer of liquids for laser bioprinting, Appl. Surf. Sci. 253 (2007) 7855–7859.
[74] M. Gruene, A. Deiwick, L. Koch, S. Schlie, C. Unger, N. Hofmann, I. Bernemann, B. Glasmacher, B. Chichkov, Laser printing of stem cells for biofabrication of scaffold-free autologous grafts, Tissue Eng. Part C Methods 17 (2010) 79–87.
[75] L. Koch, A. Deiwick, S. Schlie, S. Michael, M. Gruene, V. Coger, D. Zychlinski, A. Schambach, K. Reimers, P.M. Vogt, B. Chichkov, Skin tissue generation by laser cell printing, Biotechnol. Bioeng. 109 (2012) 1855–1863.
[76] B. Hopp, T. Smausz, N. Barna, C. Vass, Z. Antal, L. Kredics, D. Chrisey, Time-resolved study of absorbing film assisted laser induced forward transfer of *Trichoderma longibrachiatum conidia*, J. Phys. D. Appl. Phys. 38 (2005) 833.
[77] B. Hopp, T. Smausz, N. Kresz, N. Barna, Z. Bor, L. Kolozsvári, D.B. Chrisey, A. Szabó, A. Nógrádi, Survival and proliferative ability of various living cell types after laser-induced forward transfer, Tissue Eng. 11 (2005) 1817–1823.
[78] J.A. Barron, D.B. Krizman, B.R. Ringeisen, Laser printing of single cells: statistical analysis, cell viability, and stress, Ann. Biomed. Eng. 33 (2005) 121–130.
[79] C.M. Othon, X. Wu, J.J. Anders, B.R. Ringeisen, Single-cell printing to form three-dimensional lines of olfactory ensheathing cells, Biomed. Mater. 3 (2008) 034101.
[80] T. Patz, A. Doraiswamy, R. Narayan, W. He, Y. Zhong, R. Bellamkonda, R. Modi, D. Chrisey, Three-dimensional direct writing of B35 neuronal cells, J Biomed Mater Res B Appl Biomater 78 (2006) 124–130.
[81] F. Guillemot, A. Souquet, S. Catros, B. Guillotin, Laser-assisted cell printing: principle, physical parameters versus cell fate and perspectives in tissue engineering, Nanomedicine 5 (2010) 507–515.
[82] Y. Nahmias, D.J. Odde, Micropatterning of living cells by laser-guided direct writing: application to fabrication of hepatic-endothelial sinusoid-like structures, Nat. Protoc. 1 (2006) 2288.
[83] Y. Nahmias, R.E. Schwartz, C.M. Verfaillie, D.J. Odde, Laser-guided direct writing for three-dimensional tissue engineering, Biotechnol. Bioeng. 92 (2005) 129–136.
[84] R.D. Pedde, B. Mirani, A. Navaei, T. Styan, S. Wong, M. Mehrali, A. Thakur, N.K. Mohtaram, A. Bayati, A. Dolatshahi-Pirouz, M. Nikkhah, S.M. Willerth, M. Akbari, Emerging biofabrication strategies for engineering complex tissue constructs, Adv. Mater. 29 (2017).
[85] L. Koch, S. Kuhn, H. Sorg, M. Gruene, S. Schlie, R. Gaebel, B. Polchow, K. Reimers, S. Stoelting, N. Ma, Laser printing of skin cells and human stem cells, Tissue Eng. Part C Methods 16 (2009) 847–854.
[86] P. Wu, B. Ringeisen, J. Callahan, M. Brooks, D. Bubb, H. Wu, A. Piqué, B. Spargo, R. McGill, D. Chrisey, The deposition, structure, pattern deposition, and activity of biomaterial thin-films by matrix-assisted pulsed-laser evaporation (MAPLE) and MAPLE direct write, Thin Solid Films 398 (2001) 607–614.
[87] P. Wu, B. Ringeisen, Development of human umbilical vein endothelial cell (HUVEC) and human umbilical vein smooth muscle cell (HUVSMC) branch/stem structures on hydrogel layers via biological laser printing (BioLP), Biofabrication 2 (2010) 014111.
[88] Y.K. Nahmias, B.Z. Gao, D.J. Odde, Dimensionless parameters for the design of optical traps and laser guidance systems, Appl. Opt. 43 (2004) 3999–4006.
[89] V. Dinca, E. Kasotakis, J. Catherine, A. Mourka, A. Ranella, A. Ovsianikov, B.N. Chichkov, M. Farsari, A. Mitraki, C. Fotakis, Directed three-dimensional patterning of self-assembled peptide fibrils, Nano Lett. 8 (2008) 538–543.
[90] M. Colina, P. Serra, J.M. Fernández-Pradas, L. Sevilla, J.L. Morenza, DNA deposition through laser induced forward transfer, Biosens. Bioelectron. 20 (2005) 1638–1642.
[91] V. Lee, G. Singh, J.P. Trasatti, C. Bjornsson, X. Xu, T.N. Tran, S.S. Yoo, G. Dai, P. Karande, Design and fabrication of human skin by three-dimensional bioprinting, Tissue Eng. Part C Methods 20 (2014) 473–484.
[92] T. Smausz, B. Hopp, G. Kecskemeti, Z. Bor, Study on metal microparticle content of the material transferred with absorbing film assisted laser induced forward transfer when using silver absorbing layer, Appl. Surf. Sci. 252 (2006) 4738–4742.
[93] H.E. Burks, T.B. Phamduy, M.S. Azimi, J. Saksena, M.E. Burow, B.M. Collins-Burow, D.B. Chrisey, W.L. Murfee, Laser direct-write onto live tissues: a novel model for studying cancer cell migration, J. Cell. Physiol. 231 (2016) 2333–2338.
[94] Lord Rayleigh, On the instability of jets, Proc. Lond. Math. Soc. 10 (1878) 4–13.
[95] H. Gudapati, M. Dey, I. Ozbolat, A comprehensive review on droplet-based bioprinting: past, present and future, Biomaterials 102 (2016) 20–42.
[96] T. Xu, W. Zhao, J.M. Zhu, M.Z. Albanna, J.J. Yoo, A. Atala, Complex heterogeneous tissue constructs containing multiple cell types prepared by inkjet printing technology, Biomaterials 34 (2013) 130–139.
[97] X. Cui, T. Boland, Human microvasculature fabrication using thermal inkjet printing technology, Biomaterials 30 (2009) 6221–6227.
[98] M. Matsusaki, K. Sakaue, K. Kadowaki, M. Akashi, Three-dimensional human tissue chips fabricated by rapid and automatic inkjet cell printing, Adv. Healthc. Mater. 2 (2013) 534–539.
[99] K. Arai, S. Iwanaga, H. Toda, C. Genci, Y. Nishiyama, M. Nakamura, Three-dimensional inkjet biofabrication based on designed images, Biofabrication 3 (2011) 034113.
[100] Y. Nishiyama, M. Nakamura, C. Henmi, K. Yamaguchi, S. Mochizuki, H. Nakagawa, K. Takiura, Development of a three-dimensional bioprinter: construction of cell supporting structures using hydrogel and state-of-the-art inkjet technology, J. Biomech. Eng. 131 (2009).
[101] S.V. Murphy, A. Atala, 3D bioprinting of tissues and organs, Nat. Biotechnol. 32 (2014) 773–785.
[102] H. Saijo, K. Igawa, Y. Kanno, Y. Mori, K. Kondo, K. Shimizu, S. Suzuki, D. Chikazu, M. Iino, M. Anzai, Maxillofacial reconstruction using custom-made artificial bones fabricated by inkjet printing technology, J. Artif. Organs 12 (2009) 200–205.
[103] J.A. Inzana, D. Olvera, S.M. Fuller, J.P. Kelly, O.A. Graeve, E.M. Schwarz, S.L. Kates, H.A. Awad, 3D printing of composite calcium phosphate and collagen scaffolds for bone regeneration, Biomaterials 35 (2014) 4026–4034.
[104] X. Cui, K. Breitenkamp, M.G. Finn, M. Lotz, D.D. D'Lima, Direct human cartilage repair using three-dimensional bioprinting technology, Tissue Eng. Part A 18 (2012) 1304–1312.
[105] T. Xu, K.W. Binder, M.Z. Albanna, D. Dice, W. Zhao, J.J. Yoo, A. Atala, Hybrid printing of mechanically and biologically improved constructs for cartilage tissue engineering applications, Biofabrication 5 (2013).
[106] K.W. Binder, W. Zhao, T. Aboushwareb, D. Dice, A. Atala, J.J. Yoo, In situ bioprinting of the skin for burns, J. Am. Coll. Surg. 211 (2010) S76.
[107] T. Xu, C. Baicu, M. Aho, M. Zile, T. Boland, Fabrication and characterization of bio-engineered cardiac pseudo tissues, Biofabrication 1 (2009) 035001.
[108] C. Tse, R. Whiteley, T. Yu, J. Stringer, S. MacNeil, J.W. Haycock, P.J. Smith, Inkjet printing Schwann cells and neuronal analogue NG108-15 cells, Biofabrication 8 (2016) 015017.
[109] M.S. Onses, E. Sutanto, P.M. Ferreira, A.G. Alleyne, J.A. Rogers, Mechanisms, capabilities, and applications of high-resolution electrohydrodynamic jet printing, Small 11 (2015) 4237–4266.
[110] H. Liu, S. Vijayavenkataraman, D. Wang, L. Jing, J. Sun, K. He, Influence of electrohydrodynamic jetting parameters on the morphology of PCL scaffolds, Int. J. Bioprinting 3 (2017).
[111] H. Wang, S. Vijayavenkataraman, Y. Wu, Z. Shu, J. Sun, J.F.Y. Hsi, Investigation of process parameters of electrohydro-dynamic jetting for 3D printed PCL fibrous scaffolds with complex geometries, Int. J. Bioprinting 2 (2016).
[112] J. Sun, S. Vijayavenkataraman, H. Liu, An overview of scaffold design and fabrication technology for engineered knee meniscus, Materials 10 (2017) 29.

[113] A. Jaworek, A. Krupa, Classification of the modes of EHD spraying, J. Aerosol Sci. 30 (1999) 873–893.
[114] S.N. Jayasinghe, A.N. Qureshi, P.A. Eagles, Electrohydrodynamic jet processing: an advanced electric-field-driven jetting phenomenon for processing living cells, Small 2 (2006) 216–219.
[115] P.A. Eagles, A.N. Qureshi, S.N. Jayasinghe, Electrohydrodynamic jetting of mouse neuronal cells, Biochem. J. 394 (2006) 375–378.
[116] A. Kwok, S. Arumuganathar, S. Irvine, J.R. McEwan, S.N. Jayasinghe, A hybrid bio-jetting approach for directly engineering living cells, Biomed. Mater. 3 (2008) 025008.
[117] L. Gasperini, D. Maniglio, A. Motta, C. Migliaresi, An electrohydrodynamic bioprinter for alginate hydrogels containing living cells, Tissue Eng. Part C Methods 21 (2014) 123–132.
[118] K. Shigeta, Y. He, E. Sutanto, S. Kang, A.-P. Le, R.G. Nuzzo, A.G. Alleyne, P.M. Ferreira, Y. Lu, J.A. Rogers, Functional protein microarrays by electrohydrodynamic jet printing, Anal. Chem. 84 (2012) 10012–10018.
[119] J.-U. Park, J.H. Lee, U. Paik, Y. Lu, J.A. Rogers, Nanoscale patterns of oligonucleotides formed by electrohydrodynamic jet printing with applications in biosensing and nanomaterials assembly, Nano Lett. 8 (2008) 4210–4216.
[120] V.L. Workman, L.B. Tezera, P.T. Elkington, S.N. Jayasinghe, Controlled generation of microspheres incorporating extracellular matrix fibrils for three-dimensional cell culture, Adv. Funct. Mater. 24 (2014) 2648–2657.
[121] U. Demirci, G. Montesano, Single cell epitaxy by acoustic picolitre droplets, Lab Chip 7 (2007) 1139–1145.
[122] W.L. Ng, J.M. Lee, W.Y. Yeong, M. Win Naing, Microvalve-based bioprinting-process, bio-inks and applications, Biomater. Sci. 5 (2017) 632–647.
[123] S. Moon, S.K. Hasan, Y.S. Song, F. Xu, H.O. Keles, F. Manzur, S. Mikkilineni, J.W. Hong, J. Nagatomi, E. Haeggstrom, A. Khademhosseini, U. Demirci, Layer by layer three-dimensional tissue epitaxy by cell-laden hydrogel droplets, Tissue Eng. Part. C Methods 16 (2010) 157–166.
[124] F. Xu, S. Moon, A. Emre, E. Turali, Y. Song, S. Hacking, J. Nagatomi, U. Demirci, A droplet-based building block approach for bladder smooth muscle cell (SMC) proliferation, Biofabrication 2 (2010) 014105.
[125] L. Horvath, Y. Umehara, C. Jud, F. Blank, A. Petri-Fink, B. Rothen-Rutishauser, Engineering an in vitro air-blood barrier by 3D bioprinting, Sci. Rep. 5 (2015).
[126] N. Xu, X. Ye, D. Wei, J. Zhong, Y. Chen, G. Xu, D. He, 3D artificial bones for bone repair prepared by computed tomography-guided fused deposition modeling for bone repair, ACS Appl. Mater. Interfaces 6 (2014) 14952–14963.
[127] B. Byambaa, N. Annabi, K. Yue, G. Trujillo-de Santiago, M.M. Alvarez, W. Jia, M. Kazemzadeh-Narbat, S.R. Shin, A. Tamayol, A. Khademhosseini, Bioprinted osteogenic and vasculogenic patterns for engineering 3D bone tissue, Adv. Healthc. Mater. 6 (2017).
[128] V.H. Mouser, R. Levato, L.J. Bonassar, D.D. D'Lima, D.A. Grande, T.J. Klein, D.B. Saris, M. Zenobi-Wong, D. Gawlitta, J. Malda, Three-dimensional bioprinting and its potential in the field of articular cartilage regeneration, Cartilage 1947603516665445 (2016).
[129] J. Kim, I. Ko, Y. Seol, A. Atala, J. Yoo, S. Lee, 3D Bioprinting of Functional Skeletal Muscle Tissue for Volumetric Muscle Tissue Loss, Tissue Engineering Part A, Mary Ann Liebert, Inc, 140 Huguenot Street, 3rd FL, New Rochelle, NY 10801 USA, 2016 S5.
[130] S. Huang, B. Yao, J. Xie, X. Fu, 3D bioprinted extracellular matrix mimics facilitate directed differentiation of epithelial progenitors for sweat gland regeneration, Acta Biomater. 32 (2016) 170–177.
[131] B. Duan, State-of-the-art review of 3D bioprinting for cardiovascular tissue engineering, Ann. Biomed. Eng. 45 (2017) 195–209.
[132] F.Y. Hsieh, S.H. Hsu, 3D bioprinting: a new insight into the therapeutic strategy of neural tissue regeneration, Organogenesis 11 (2015) 153–158.
[133] T. Billiet, E. Gevaert, T. De Schryver, M. Cornelissen, P. Dubruel, The 3D printing of gelatin methacrylamide cell-laden tissue-engineered constructs with high cell viability, Biomaterials 35 (2014) 49–62.
[134] J. Malda, J. Visser, F.P. Melchels, T. Jüngst, W.E. Hennink, W.J.A. Dhert, J. Groll, D.W. Hutmacher, 25th anniversary article: engineering hydrogels for biofabrication, Adv. Mater. 25 (2013) 5011–5028.
[135] B. Duan, L.A. Hockaday, K.H. Kang, J.T. Butcher, 3D bioprinting of heterogeneous aortic valve conduits with alginate/gelatin hydrogels, J. Biomed. Mater. Res. Part A 101 (A) (2013) 1255–1264.
[136] R. Chang, J. Nam, W. Sun, Effects of dispensing pressure and nozzle diameter on cell survival from solid freeform fabrication–based direct cell writing, Tissue Eng. A 14 (2008) 41–48.
[137] C.W. Hull, Apparatus for production of three-dimensional objects by stereolithography, Google Patents, 1986.
[138] P. Soman, P.H. Chung, A.P. Zhang, S. Chen, Digital microfabrication of user-defined 3D microstructures in cell-laden hydrogels, Biotechnol. Bioeng. 110 (2013) 3038–3047.
[139] K. Arcaute, B.K. Mann, R.B. Wicker, Stereolithography of three-dimensional bioactive poly (ethylene glycol) constructs with encapsulated cells, Ann. Biomed. Eng. 34 (2006) 1429–1441.
[140] J.L. Curley, S.R. Jennings, M.J. Moore, Fabrication of micropatterned hydrogels for neural culture systems using dynamic mask projection photolithography, J. Vis. Exp. 48 (2011), e2636.
[141] K.-S. Lee, R.H. Kim, D.-Y. Yang, S.H. Park, Advances in 3D nano/microfabrication using two-photon initiated polymerization, Prog. Polym. Sci. 33 (2008) 631–681.
[142] F.P. Melchels, J. Feijen, D.W. Grijpma, A review on stereolithography and its applications in biomedical engineering, Biomaterials 31 (2010) 6121–6130.
[143] B. Dhariwala, E. Hunt, T. Boland, Rapid prototyping of tissue-engineering constructs, using photopolymerizable hydrogels and stereolithography, Tissue Eng. 10 (2004) 1316–1322.
[144] Z. Wang, R. Abdulla, B. Parker, R. Samanipour, S. Ghosh, K. Kim, A simple and high-resolution stereolithography-based 3D bioprinting system using visible light crosslinkable bioinks, Biofabrication 7 (2015).
[145] B.S. Kim, J.-S. Lee, G. Gao, D.-W. Cho, Direct 3D cell-printing of human skin with functional transwell system, Biofabrication 9 (2017) 025034.
[146] C.R. Black, V. Goriainov, D. Gibbs, J. Kanczler, R.S. Tare, R.O. Oreffo, Bone Tissue Engineering, Current Molecular Biology Reports, 1, 2015 132–140.
[147] A.R. Amini, C.T. Laurencin, S.P. Nukavarapu, Bone tissue engineering: recent advances and challenges, Crit. Rev. Biomed. Eng. 40 (2012).
[148] V. Mouriño, A.R. Boccaccini, Bone tissue engineering therapeutics: controlled drug delivery in three-dimensional scaffolds, J. R. Soc. Interface rsif20090379 (2009).
[149] H. Seitz, W. Rieder, S. Irsen, B. Leukers, C. Tille, Three-dimensional printing of porous ceramic scaffolds for bone tissue engineering, J Biomed Mater Res B Appl Biomater 74 (2005) 782–788.
[150] G. Gao, X. Cui, Three-dimensional bioprinting in tissue engineering and regenerative medicine, Biotechnol. Lett. 38 (2016) 203–211.
[151] D.W. Hutmacher, Scaffolds in tissue engineering bone and cartilage, Biomaterials 21 (2000) 2529–2543.
[152] N.E. Fedorovich, J.R. De Wijn, A.J. Verbout, J. Alblas, W.J. Dhert, Three-dimensional fiber deposition of cell-laden, viable, patterned constructs for bone tissue printing, Tissue Eng. A 14 (2008) 127–133.
[153] M. Neufurth, X. Wang, H.C. Schröder, Q. Feng, B. Diehl-Seifert, T. Ziebart, R. Steffen, S. Wang, W.E. Müller, Engineering a morphogenetically active hydrogel for bioprinting of bioartificial tissue derived from human osteoblast-like SaOS-2 cells, Biomaterials 35 (2014) 8810–8819.
[154] G. Gao, A.F. Schilling, K. Hubbell, T. Yonezawa, D. Truong, Y. Hong, G. Dai, X. Cui, Improved properties of bone and cartilage tissue from 3D inkjet-bioprinted human mesenchymal stem cells by simultaneous deposition and photocrosslinking in PEG-GelMA, Biotechnol. Lett. 37 (2015) 2349–2355.
[155] D.F. Duarte Campos, A. Blaeser, K. Buellesbach, K.S. Sen, W. Xun, W. Tillmann, H. Fischer, Bioprinting organotypic hydrogels with improved mesenchymal stem cell remodeling and mineralization properties for bone tissue engineering, Adv. Healthc. Mater. 5 (2016) 1336–1345.
[156] S. Vijayavenkataraman, Z. Shuo, J.Y. Fuh, W.F. Lu, Design of three-dimensional scaffolds with tunable matrix stiffness for directing stem cell lineage specification: an in silico study, Bioengineering 4 (2017) 66.
[157] H. Cui, W. Zhu, M. Nowicki, X. Zhou, A. Khademhosseini, L.G. Zhang, Hierarchical fabrication of engineered vascularized bone biphasic constructs via dual 3D bioprinting: integrating regional bioactive factors into architectural design, Adv. Healthc. Mater. 5 (2016) 2174–2181.
[158] R. Levato, J. Visser, J.A. Planell, E. Engel, J. Malda, M.A. Mateos-Timoneda, Biofabrication of tissue constructs by 3D bioprinting of cell-laden microcarriers, Biofabrication 6 (2014).
[159] V. Keriquel, H. Oliveira, M. Rémy, S. Ziane, S. Delmond, B. Rousseau, S. Rey, S. Catros, J. Amédée, F. Guillemot, J.C. Fricain, In situ printing of mesenchymal stromal cells, by laser-assisted bioprinting, for in vivo bone regeneration applications, Sci. Rep. 7 (2017).
[160] A.C. Daly, G.M. Cunniffe, B.N. Sathy, O. Jeon, E. Alsberg, D.J. Kelly, 3D bioprinting of developmentally inspired templates for whole bone organ engineering, Adv. Healthc. Mater. 5 (2016) 2353–2362.
[161] A.C. Daly, F.E. Freeman, T. Gonzalez-Fernandez, S.E. Critchley, J. Nulty, D.J. Kelly, 3D bioprinting for cartilage and osteochondral tissue engineering, Adv. Healthc. Mater. 6 (2017), 1700298.
[162] Y. Zhang, J.M. Jordan, Epidemiology of osteoarthritis, Clin. Geriatr. Med. 26 (2010) 355–369.
[163] K. Markstedt, A. Mantas, I. Tournier, H. Martínez Ávila, D. Hägg, P. Gatenholm, 3D bioprinting human chondrocytes with nanocellulose-alginate bioink for cartilage tissue engineering applications, Biomacromolecules 16 (2015) 1489–1496.
[164] S. Rhee, J.L. Puetzer, B.N. Mason, C.A. Reinhart-King, L.J. Bonassar, 3D bioprinting of spatially heterogeneous collagen constructs for cartilage tissue engineering, ACS Biomater. Sci. Eng. 2 (2016) 1800–1805.
[165] C. Di Bella, A. Fosang, D.M. Donati, G.G. Wallace, P.F. Choong, 3D bioprinting of cartilage for orthopedic surgeons: reading between the lines, Front. Surg. 2 (2015).
[166] D. Nguyen, D.A. Hägg, A. Forsman, J. Ekholm, P. Nimkingratana, C. Brantsing, T. Kalogeropoulos, S. Zaunz, S. Concaro, M. Brittberg, Cartilage tissue engineering by the 3D bioprinting of iPS cells in a nanocellulose/alginate bioink, Sci. Rep. 7 (2017) 658.
[167] A.C. Daly, S.E. Critchley, E.M. Rencsok, D.J. Kelly, A comparison of different bioinks for 3D bioprinting of fibrocartilage and hyaline cartilage, Biofabrication 8 (2016).
[168] M. Kesti, C. Eberhardt, G. Pagliccia, D. Kenkel, D. Grande, A. Boss, M. Zenobi-Wong, Bioprinting complex cartilaginous structures with clinically compliant biomaterials, Adv. Funct. Mater. 25 (2015) 7406–7417.
[169] S. Duchi, C. Onofrillo, C.D. O'Connell, R. Blanchard, C. Augustine, A.F. Quigley, R.M.I. Kapsa, P. Pivonka, G. Wallace, C. Di Bella, P.F.M. Choong, Handheld co-axial bioprinting: application to in situ surgical cartilage repair, Sci. Rep. 7 (2017).
[170] X. Cui, G. Gao, T. Yonezawa, G. Dai, Human cartilage tissue fabrication using three-dimensional inkjet printing technology, J. Vis. Exp. 88 (2014), e51294.
[171] D.P. Forrestal, T.J. Klein, M.A. Woodruff, Challenges in engineering large customized bone constructs, Biotechnol. Bioeng. 114 (2017) 1129–1139.
[172] B. Sharma, C.G. Williams, T.K. Kim, D. Sun, A. Malik, M. Khan, K. Leong, J.H. Elisseeff, Designing zonal organization into tissue-engineered cartilage, Tissue Eng. 13 (2007) 405–414.
[173] T.J. Klein, S.C. Rizzi, J.C. Reichert, N. Georgi, J. Malda, W. Schuurman, R.W. Crawford, D.W. Hutmacher, Strategies for zonal cartilage repair using hydrogels, Macromol. Biosci. 9 (2009) 1049–1058.

[174] J. Yang, Y.S. Zhang, K. Yue, A. Khademhosseini, Cell-laden hydrogels for osteochondral and cartilage tissue engineering, Acta Biomater. 57 (2017) 1–25.
[175] J. San Choi, S.J. Lee, G.J. Christ, A. Atala, J.J. Yoo, The influence of electrospun aligned poly (ε-caprolactone)/collagen nanofiber meshes on the formation of self-aligned skeletal muscle myotubes, Biomaterials 29 (2008) 2899–2906.
[176] T.K. Merceron, M. Burt, Y.-J. Seol, H.-W. Kang, S.J. Lee, J.J. Yoo, A. Atala, A 3D bioprinted complex structure for engineering the muscle–tendon unit, Biofabrication 7 (2015) 035003.
[177] S. Levenberg, J. Rouwkema, M. Macdonald, E.S. Garfein, D.S. Kohane, D.C. Darland, R. Marini, C.A. Van Blitterswijk, R.C. Mulligan, P.A. D'Amore, Engineering vascularized skeletal muscle tissue, Nat. Biotechnol. 23 (2005) 879.
[178] J.A. Phillippi, E. Miller, L. Weiss, J. Huard, A. Waggoner, P. Campbell, Microenvironments engineered by inkjet bioprinting spatially direct adult stem cells toward muscle-and bone-like subpopulations, Stem Cells 26 (2008) 127–134.
[179] X. Cui, G. Gao, Y. Qiu, Accelerated myotube formation using bioprinting technology for biosensor applications, Biotechnol. Lett. 35 (2013) 315–321.
[180] H.-W. Kang, S.J. Lee, I.K. Ko, C. Kengla, J.J. Yoo, A. Atala, A 3D bioprinting system to produce human-scale tissue constructs with structural integrity, Nat. Biotechnol. 34 (2016) 312–319.
[181] N.C.I., U. S. National Institutes of Health, SEER Training Modules, Anatomy and Physiology, 2018.
[182] F.-Y. Hsieh, H.-H. Lin, S.-h. Hsu, 3D bioprinting of neural stem cell-laden thermoresponsive biodegradable polyurethane hydrogel and potential in central nervous system repair, Biomaterials 71 (2015) 48–57.
[183] S. England, A. Rajaram, D.J. Schreyer, X. Chen, Bioprinted fibrin-factor XIII-hyaluronate hydrogel scaffolds with encapsulated Schwann cells and their in vitro characterization for use in nerve regeneration, Bioprinting 5 (2017) 1–9.
[184] S. Goenka, V. Sant, S. Sant, Graphene-based nanomaterials for drug delivery and tissue engineering, J. Control. Release 173 (2014) 75–88.
[185] S.K. Lee, H. Kim, B.S. Shim, Graphene: an emerging material for biological tissue engineering, Carbon Lett. 14 (2013) 63–75.
[186] W. Zhu, B.T. Harris, L.G. Zhang, Gelatin methacrylamide hydrogel with graphene nanoplatelets for neural cell-laden 3D bioprintingEngineering in Medicine and Biology Society (EMBC), 2016 IEEE 38th Annual International Conference of the, IEEE 2016, pp. 4185–4188.
[187] K.-H. Liao, Y.-S. Lin, C.W. Macosko, C.L. Haynes, Cytotoxicity of graphene oxide and graphene in human erythrocytes and skin fibroblasts, ACS Appl. Mater. Interfaces 3 (2011) 2607–2615.
[188] Y.-B. Lee, S. Polio, W. Lee, G. Dai, L. Menon, R.S. Carroll, S.-S. Yoo, Bio-printing of collagen and VEGF-releasing fibrin gel scaffolds for neural stem cell culture, Exp. Neurol. 223 (2010) 645–652.
[189] R. Lozano, L. Stevens, B.C. Thompson, K.J. Gilmore, R. Gorkin, E.M. Stewart, M. in het Panhuis, M. Romero-Ortega, G.G. Wallace, 3D printing of layered brain-like structures using peptide modified gellan gum substrates, Biomaterials 67 (2015) 264–273.
[190] M. Schaupper, M. Jeltsch, S. Rohringer, H. Redl, W. Holnthoner, Lymphatic vessels in regenerative medicine and tissue engineering, Tissue Eng. B Rev. 22 (2016) 395–407.
[191] T. ting Dai, Z. hua Jiang, S. li Li, G. dong Zhou, J.D. Kretlow, W. gang Cao, W. Liu, Y. lin Cao, Reconstruction of lymph vessel by lymphatic endothelial cells combined with polyglycolic acid scaffolds: a pilot study, J. Biotechnol. 150 (2010) 182–189.
[192] L. Gibot, T. Galbraith, B. Kloos, S. Das, D.A. Lacroix, F.A. Auger, M. Skobe, Cell-based approach for 3D reconstruction of lymphatic capillaries in vitro reveals distinct functions of HGF and VEGF-C in lymphangiogenesis, Biomaterials 78 (2016) 129–139.
[193] C.L.E. Helm, A. Zisch, M.A. Swartz, Engineered blood and lymphatic capillaries in 3-D VEGF-fibrin-collagen matrices with interstitial flow, Biotechnol. Bioeng. 96 (2007) 167–176.
[194] S. Suematsu, T. Watanabe, Generation of a synthetic lymphoid tissue-like organoid in mice, Nat. Biotechnol. 22 (2004) 1539.
[195] T. Cupedo, A. Stroock, M. Coles, Application of tissue engineering to the immune system: development of artificial lymph nodes, Front. Immunol. 3 (2012).
[196] M. Nakamura, K. Arai, T. Mimura, J. Tagawa, H. Yoshida, K. Kato, T. Nakaji-Hirabayashi, Y. Kobayashi, T. Watanabe, Engineering of Artificial Lymph Node, Synthetic Immunology, Springer, 2016 181–200.
[197] J.J. Iliff, M. Wang, Y. Liao, B.A. Plogg, W. Peng, G.A. Gundersen, H. Benveniste, G.E. Vates, R. Deane, S.A. Goldman, A paravascular pathway facilitates CSF flow through the brain parenchyma and the clearance of interstitial solutes, including amyloid β, Sci. Transl. Med. 4 (2012) 147ra111.
[198] E. Crivellato, A. Vacca, D. Ribatti, Setting the stage: an anatomist's view of the immune system, Trends Immunol. 25 (2004) 210–217.
[199] E.A. Bulanova, E.V. Koudan, J. Degosserie, C. Heymans, F.D. Pereira, V.A. Parfenov, Y. Sun, Q. Wang, S.A. Akhmedova, I.K. Sviridova, Bioprinting of functional vascularized mouse thyroid gland construct, Biofabrication 9 (2017) 034105.
[200] G. Marchioli, L. van Gurp, P. Van Krieken, D. Stamatialis, M. Engelse, C. Van Blitterswijk, M. Karperien, E. de Koning, J. Alblas, L. Moroni, Fabrication of three-dimensional bioplotted hydrogel scaffolds for islets of Langerhans transplantation, Biofabrication 7 (2015) 025009.
[201] J. Song, J.R. Millman, Economic 3D-printing approach for transplantation of human stem cell-derived β-like cells, Biofabrication 9 (2016) 015002.
[202] H. Campo, I. Cervelló, C. Simón, Bioengineering the uterus: an overview of recent advances and future perspectives in reproductive medicine, Ann. Biomed. Eng. 45 (2017) 1710–1717.
[203] A. Atala, Tissue engineering and regenerative medicine: concepts for clinical application, Rejuvenation Res. 7 (2004) 15–31.
[204] C.-Y. Kuo, H. Baker, M.H. Fries, J.J. Yoo, P.C. Kim, J.P. Fisher, Bioengineering strategies to treat female infertility, Tissue Eng. B Rev. 23 (2017) 294–306.
[205] U. Bentin-Ley, B. Pedersen, S. Lindenberg, J.F. Larsen, L. Hamberger, T. Horn, Isolation and culture of human endometrial cells in a three-dimensional culture system, J. Reprod. Fertil. 101 (1994) 327–332.
[206] S.C. Schutte, R.N. Taylor, A tissue-engineered human endometrial stroma that responds to cues for secretory differentiation, decidualization, and menstruation, Fertil. Steril. 97 (2012) 997–1003.
[207] H. Wang, F. Pilla, S. Anderson, S. Martínez-Escribano, I. Herrer, J.M. Moreno-Moya, S. Musti, S. Bocca, S. Oehninger, J.A. Horcajadas, A novel model of human implantation: 3D endometrium-like culture system to study attachment of human trophoblast (Jar) cell spheroids, Mol. Hum. Reprod. 18 (2011) 33–43.
[208] M. House, C.C. Sanchez, W.L. Rice, S. Socrate, D.L. Kaplan, Cervical tissue engineering using silk scaffolds and human cervical cells, Tissue Eng. A 16 (2010) 2101–2112.
[209] S. MacKintosh, L. Serino, P. Iddon, R. Brown, R. Conlan, C. Wright, T. Maffeis, M. Raxworthy, I. Sheldon, A three-dimensional model of primary bovine endometrium using an electrospun scaffold, Biofabrication 7 (2015) 025010.
[210] J.W. Taveau, M. Tartaglia, D. Buchannan, B. Smith, G. Koenig, K. Thomfohrde, B. Stouch, S. Jeck, C.H. Greene, Regeneration of uterine horn using porcine small intestinal submucosa grafts in rabbits, J. Investig. Surg. 17 (2004) 81–92.
[211] X.a. Li, H. Sun, N. Lin, X. Hou, J. Wang, B. Zhou, P. Xu, Z. Xiao, B. Chen, J. Dai, Regeneration of uterine horns in rats by collagen scaffolds loaded with collagen-binding human basic fibroblast growth factor, Biomaterials 32 (2011) 8172–8181.
[212] N. Lin, X.a. Li, T. Song, J. Wang, K. Meng, J. Yang, X. Hou, J. Dai, Y. Hu, The effect of collagen-binding vascular endothelial growth factor on the remodeling of scarred rat uterus following full-thickness injury, Biomaterials 33 (2012) 1801–1807.
[213] M.M. Laronda, A.E. Jakus, K.A. Whelan, J.A. Wertheim, R.N. Shah, T.K. Woodruff, Initiation of puberty in mice following decellularized ovary transplant, Biomaterials 50 (2015) 20–29.
[214] S.A. Pangas, H. Saudye, L.D. Shea, T.K. Woodruff, Novel approach for the three-dimensional culture of granulosa cell–oocyte complexes, Tissue Eng. 9 (2003) 1013–1021.
[215] M. Xu, P.K. Kreeger, L.D. Shea, T.K. Woodruff, Tissue-engineered follicles produce live, fertile offspring, Tissue Eng. 12 (2006) 2739–2746.
[216] S.P. Krotz, J.C. Robins, T.-M. Ferruccio, R. Moore, M.M. Steinhoff, J.R. Morgan, S. Carson, In vitro maturation of oocytes via the pre-fabricated self-assembled artificial human ovary, J. Assist. Reprod. Genet. 27 (2010) 743–750.
[217] R. Mhaskar, Amniotic membrane for cervical reconstruction, Int. J. Gynecol. Obstet. 90 (2005) 123–127.
[218] J.-X. Ding, X.-J. Chen, X.-y. Zhang, Y. Zhang, K.-Q. Hua, Acellular porcine small intestinal submucosa graft for cervicovaginal reconstruction in eight patients with malformation of the uterine cervix, Hum. Reprod. 29 (2014) 677–682.
[219] A.M. Raya-Rivera, D. Esquiliano, R. Fierro-Pastrana, E. López-Bayghen, P. Valencia, R. Ordorica-Flores, S. Soker, J.J. Yoo, A. Atala, Tissue-engineered autologous vaginal organs in patients: a pilot cohort study, Lancet 384 (2014) 329–336.
[220] R.T. Kershen, J.J. Yoo, R.B. Moreland, R.J. Krane, A. Atala, Reconstitution of human corpus cavernosum smooth muscle in vitro and in vivo, Tissue Eng. 8 (2002) 515–524.
[221] T.G. Kwon, J.J. Yoo, A. Atala, Autologous penile corpora cavernosa replacement using tissue engineering techniques, J. Urol. 168 (2002) 1754–1758.
[222] M. Vermeulen, J. Poels, F. de Michele, A. des Rieux, C. Wyns, Restoring fertility with cryopreserved prepubertal testicular tissue: perspectives with hydrogel encapsulation, nanotechnology, and bioengineered scaffolds, Ann. Biomed. Eng. (2017) 1–12.
[223] T.M. Research, Tissue Engineered Skin Substitutes Market (by Type—Acellular, Cellular Allogeneic, Cellular Autologous, and Others; by Application—Burn Injury, Diabetic/Vascular Ulcer, and Others)—Global Industry Analysis, Size, Share, Growth, Trends, and Forecast 2015–2023, 2015.
[224] L. Koch, A. Deiwick, S. Schlie, S. Michael, M. Gruene, V. Coger, D. Zychlinski, A. Schambach, K. Reimers, P.M. Vogt, Skin tissue generation by laser cell printing, Biotechnol. Bioeng. 109 (2012) 1855–1863.
[225] S. Michael, H. Sorg, C.-T. Peck, L. Koch, A. Deiwick, B. Chichkov, P.M. Vogt, K. Reimers, Tissue engineered skin substitutes created by laser-assisted bioprinting form skin-like structures in the dorsal skin fold chamber in mice, PLoS One 8 (2013) e57741.
[226] W. Lee, J.C. Debasitis, V.K. Lee, J.-H. Lee, K. Fischer, K. Edminster, J.-K. Park, S.-S. Yoo, Multi-layered culture of human skin fibroblasts and keratinocytes through three-dimensional freeform fabrication, Biomaterials 30 (2009) 1587–1595.
[227] V. Lee, G. Singh, J.P. Trasatti, C. Bjornsson, X. Xu, T.N. Tran, S.-S. Yoo, G. Dai, P. Karande, Design and fabrication of human skin by three-dimensional bioprinting, Tissue Eng. Part C Methods 20 (2013) 473–484.
[228] M. Rimann, E. Bono, H. Annaheim, M. Bleisch, U. Graf-Hausner, Standardized 3D bioprinting of soft tissue models with human primary cells, J. Lab. Autom. 21 (2016) 496–509.
[229] N. Cubo, M. Garcia, J.F. del Cañizo, D. Velasco, J.L. Jorcano, 3D bioprinting of functional human skin: production and in vivo analysis, Biofabrication 9 (2016) 015006.
[230] L.J. Pourchet, A. Thepot, M. Albouy, E.J. Courtial, A. Boher, L.J. Blum, C.A. Marquette, Human skin 3D bioprinting using scaffold-free approach, Adv. Healthc. Mater. 6 (2017).
[231] D. Min, W. Lee, I.H. Bae, T.R. Lee, P. Croce, S.S. Yoo, Bioprinting of biomimetic skin containing melanocytes, Exp. Dermatol. 27 (2017) 453–459.
[232] S. Vijayavenkataraman, 3D bioprinted skin: the first 'to-be' successful printed organ? Future Medicine, 2017.
[233] T.H. Petersen, E.A. Calle, L. Zhao, E.J. Lee, L. Gui, M.B. Raredon, K. Gavrilov, T. Yi, Z.W. Zhuang, C. Breuer, Tissue-engineered lungs for in vivo implantation, Science 329 (2010) 538–541.
[234] J.B. Orens, E.R. Garrity Jr., General overview of lung transplantation and review of organ allocation, Proc. Am. Thorac. Soc. 6 (2009) 13–19.

[235] Y. Shan, Y. Wang, J. Li, H. Shi, Y. Fan, J. Yang, W. Ren, X. Yu, Biomechanical properties and cellular biocompatibility of 3D printed tracheal graft, Bioprocess Biosyst. Eng. (2017) 1–11.
[236] P. Macchiarini, P. Jungebluth, T. Go, M.A. Asnaghi, L.E. Rees, T.A. Cogan, A. Dodson, J. Martorell, S. Bellini, P.P. Parnigotto, Clinical transplantation of a tissue-engineered airway, Lancet 372 (2008) 2023–2030.
[237] M. Weidenbecher, H.M. Tucker, D.A. Gilpin, J.E. Dennis, Tissue-engineered trachea for airway reconstruction, Laryngoscope 119 (2009) 2118–2123.
[238] N. Hamilton, A.J. Bullock, S. MacNeil, S.M. Janes, M. Birchall, Tissue engineering airway mucosa: a systematic review, Laryngoscope 124 (2014) 961–968.
[239] J.E. Nichols, J. Cortiella, Engineering of a complex organ: progress toward development of a tissue-engineered lung, Proc. Am. Thorac. Soc. 5 (2008) 723–730.
[240] L. Horváth, Y. Umehara, C. Jud, F. Blank, A. Petri-Fink, B. Rothen-Rutishauser, Engineering an in vitro air-blood barrier by 3D bioprinting, Sci. Rep. 5 (2015) 7974.
[241] A. Wilson, L. Ikonomou, Development and Bioengineering of Lung Regeneration, Organ Regeneration Based on Developmental Biology, Springer, 2017 237–257.
[242] L.A. van Grunsven, 3D in vitro models of liver fibrosis, Adv. Drug Deliv. Rev. 121 (2017) 133–146.
[243] A. Collin de l'Hortet, K. Takeishi, J. Guzman-Lepe, K. Handa, K. Matsubara, K. Fukumitsu, K. Dorko, S. Presnell, H. Yagi, A. Soto-Gutierrez, Liver-regenerative transplantation: regrow and reset, Am. J. Transplant. 16 (2016) 1688–1696.
[244] L.G. Griffith, A. Wells, D.B. Stolz, Engineering liver, Hepatology 60 (2014) 1426–1434.
[245] S. Eguchi, S.C. Chen, J. Rozga, A.A. Demetriou, Tissue engineering: liver, Yearbook of Cell and Tissue Transplantation 1996–1997, Springer Netherlands 1996, pp. 247–252.
[246] R. Chang, K. Emami, H. Wu, W. Sun, Biofabrication of a three-dimensional liver micro-organ as an in vitro drug metabolism model, Biofabrication 2 (2010) 045004.
[247] D.G. Nguyen, J. Funk, J.B. Robbins, C. Crogan-Grundy, S.C. Presnell, T. Singer, A.B. Roth, Bioprinted 3D primary liver tissues allow assessment of organ-level response to clinical drug induced toxicity in vitro, PLoS One 11 (2016) e0158674.
[248] K. Arai, T. Yoshida, M. Okabe, M. Goto, T.A. Mir, C. Soko, Y. Tsukamoto, T. Akaike, T. Nikaido, K. Zhou, Fabrication of 3D-culture platform with sandwich architecture for preserving liver-specific functions of hepatocytes using 3D bioprinter, J. Biomed. Mater. Res. A 105 (2017) 1583–1592.
[249] Y. Kim, K. Kang, J. Jeong, S.S. Paik, J.S. Kim, S.A. Park, W.D. Kim, J. Park, D. Choi, Three-dimensional (3D) printing of mouse primary hepatocytes to generate 3D hepatic structure, Ann. Surg. Treat. Res. 92 (2017) 67–72.
[250] H. Kizawa, E. Nagao, M. Shimamura, G. Zhang, H. Torii, Scaffold-free 3D bio-printed human liver tissue stably maintains metabolic functions useful for drug discovery, Biochem. Biophys. Rep. 10 (2017) 186–191.
[251] A. Faulkner-Jones, C. Fyfe, D.-J. Cornelissen, J. Gardner, J. King, A. Courtney, W. Shu, Bioprinting of human pluripotent stem cells and their directed differentiation into hepatocyte-like cells for the generation of mini-livers in 3D, Biofabrication 7 (2015) 044102.
[252] X. Ma, X. Qu, W. Zhu, Y.-S. Li, S. Yuan, H. Zhang, J. Liu, P. Wang, C.S.E. Lai, F. Zanella, Deterministically patterned biomimetic human iPSC-derived hepatic model via rapid 3D bioprinting, Proc. Natl. Acad. Sci. 113 (2016) 2206–2211.
[253] G. Totonelli, P. Maghsoudlou, J.M. Fishman, G. Orlando, T. Ansari, P. Sibbons, M.A. Birchall, A. Pierro, S. Eaton, P. De Coppi, Esophageal tissue engineering: a new approach for esophageal replacement, World J Gastroenterol: WJG 18 (2012) 6900.
[254] R. Choi, J. Vacanti, Preliminary studies of tissue-engineered intestine using isolated epithelial organoid units on tubular synthetic biodegradable scaffolds, Transplant. Proc, Elsevier 1997, pp. 848–851.
[255] M.L.L. Madariaga, H.C. Ott, Bioengineering kidneys for transplantation, Semin. Nephrol, Elsevier 2014, pp. 384–393.
[256] A. Peloso, R. Katari, S.V. Murphy, J.P. Zambon, A. DeFrancesco, A.C. Farney, J. Rogers, R.J. Stratta, T.M. Manzia, G. Orlando, Prospect for kidney bioengineering: shortcomings of the status quo, Expert. Opin. Biol. Ther. 15 (2015) 547–558.
[257] P. Aebischer, T. Ip, G. Panol, P. Galletti, The bioartificial kidney: progress towards an ultrafiltration device with renal epithelial cells processing, Life Support Syst. 5 (1986) 159–168.
[258] K.A. Homan, D.B. Kolesky, M.A. Skylar-Scott, J. Herrmann, H. Obuobi, A. Moisan, J.A. Lewis, Bioprinting of 3D convoluted renal proximal tubules on perfusable chips, Sci. Rep. 6 (2016).
[259] M. Unbekandt, J.A. Davies, Dissociation of embryonic kidneys followed by reaggregation allows the formation of renal tissues, Kidney Int. 77 (2010) 407–416.
[260] V. Kasyanov, K. Brakke, T. Vilbrandt, R. Moreno-Rodriguez, A. Nagy-Mehesz, R. Visconti, R. Markwald, I. Ozolanta, R. Rezende, A. Lixandrão Filho, Toward organ printing: design characteristics, virtual modelling and physical prototyping vascular segments of kidney arterial tree: this paper highlights the main issues regarding design characteristics, virtual modeling and physical prototyping of vascular kidney arterial segments, Virtual Phys. Prototyping, 6, 2011, pp. 197–213.
[261] S. Korossis, F. Bolland, E. Ingham, J. Fisher, J. Kearney, J. Southgate, Tissue engineering of the urinary bladder: considering structure-function relationships and the role of mechanotransduction, Tissue Eng. 12 (2006) 635–644.
[262] A. Atala, Tissue engineering of human bladder, Br. Med. Bull. 97 (2011) 81–104.
[263] K. Zhang, Q. Fu, J. Yoo, X. Chen, P. Chandra, X. Mo, L. Song, A. Atala, W. Zhao, 3D bioprinting of urethra with PCL/PLCL blend and dual autologous cells in fibrin hydrogel: an in vitro evaluation of biomimetic mechanical property and cell growth environment, Acta Biomater. 50 (2017) 154–164.
[264] M.M. Elsawy, A. de Mel, Biofabrication and biomaterials for urinary tract reconstruction, Res. Reports Urology, 9, 2017, pp. 79–92.
[265] G. Reint, A. Rak-Raszewska, S.J. Vainio, Kidney development and perspectives for organ engineering, Cell Tissue Res. (2017) 1–13.
[266] M.S. Lundberg, Cardiovascular tissue engineering research support at the National Heart, Lung, and Blood Institute, Circ. Res. 112 (2013) 1097–1103.
[267] C. Harris, B. Croce, C. Cao, Tissue and mechanical heart valves, Annals of Cardiothoracic Surgery, 4, 2015, p. 399.
[268] E. Filova, F. Straka, T. Mirejovsky, J. Masin, L. Bacakova, Tissue-engineered heart valves, Physiol. Res. 58 (2009) S141.
[269] D.Y. Cheung, B. Duan, J.T. Butcher, Current progress in tissue engineering of heart valves: multiscale problems, multiscale solutions, Expert. Opin. Biol. Ther. 15 (2015) 1155–1172.
[270] B. Duan, L.A. Hockaday, K.H. Kang, J.T. Butcher, 3D bioprinting of heterogeneous aortic valve conduits with alginate/gelatin hydrogels, J. Biomed. Mater. Res. A 101 (2013) 1255–1264.
[271] B. Duan, E. Kapetanovic, L.A. Hockaday, J.T. Butcher, Three-dimensional printed trileaflet valve conduits using biological hydrogels and human valve interstitial cells, Acta Biomater. 10 (2014) 1836–1846.
[272] R. Gaebel, N. Ma, J. Liu, J. Guan, L. Koch, C. Klopsch, M. Gruene, A. Toelk, W. Wang, P. Mark, Patterning human stem cells and endothelial cells with laser printing for cardiac regeneration, Biomaterials 32 (2011) 9218–9230.
[273] R. Gaetani, P.A. Doevendans, C.H. Metz, J. Alblas, E. Messina, A. Giacomello, J.P. Sluijter, Cardiac tissue engineering using tissue printing technology and human cardiac progenitor cells, Biomaterials 33 (2012) 1782–1790.
[274] R. Gaetani, D.A. Feyen, V. Verhage, R. Slaats, E. Messina, K.L. Christman, A. Giacomello, P.A. Doevendans, J.P. Sluijter, Epicardial application of cardiac progenitor cells in a 3D-printed gelatin/hyaluronic acid patch preserves cardiac function after myocardial infarction, Biomaterials 61 (2015) 339–348.
[275] M. Noseda, M. Abreu-Paiva, M.D. Schneider, The quest for the adult cardiac stem cell, Circ. J. 79 (2015) 1422–1430.
[276] P. Kerscher, J.A. Kaczmarek, S.E. Head, M.E. Ellis, W.J. Seeto, J. Kim, S. Bhattacharya, V. Suppiramaniam, E.A. Lipke, Direct production of human cardiac tissues by pluripotent stem cell encapsulation in gelatin methacryloyl, ACS Biomater. Sci. Eng. 3 (2016) 1499–1509.
[277] C.S. Ong, T. Fukunishi, H. Zhang, C.Y. Huang, A. Nashed, A. Blazeski, D. DiSilvestre, L. Vricella, J. Conte, L. Tung, Biomaterial-free three-dimensional bioprinting of cardiac tissue using human induced pluripotent stem cell derived cardiomyocytes, Sci. Rep. 7 (2017).
[278] A. Amir-Aslani, V. Mangematin, The future of drug discovery and development: shifting emphasis towards personalized medicine, Technol. Forecast. Soc. Chang. 77 (2010) 203–217.
[279] P.K. Owens, E. Raddad, J.W. Miller, J.R. Stille, K.G. Olovich, N.V. Smith, R.S. Jones, J.C. Scherer, A decade of innovation in pharmaceutical R&D: the Chorus model, Nat. Rev. Drug Discov. 14 (2014) nrd4497.
[280] M.J. Waring, J. Arrowsmith, A.R. Leach, P.D. Leeson, S. Mandrell, R.M. Owen, G. Pairaudeau, W.D. Pennie, S.D. Pickett, J. Wang, An analysis of the attrition of drug candidates from four major pharmaceutical companies, Nat. Rev. Drug Discov. 14 (2015) 475–486.
[281] S. Knowlton, S. Tasoglu, A bioprinted liver-on-a-chip for drug screening applications, Trends Biotechnol. 34 (2016) 681–682.
[282] K. Wrzesinski, S.J. Fey, From 2D to 3D-a new dimension for modelling the effect of natural products on human tissue, Curr. Pharm. Des. 21 (2015) 5605–5616.
[283] J.I. Rodríguez-Dévora, B. Zhang, D. Reyna, Z.-d. Shi, T. Xu, High throughput miniature drug-screening platform using bioprinting technology, Biofabrication 4 (2012) 035001.
[284] I.T. Ozbolat, W. Peng, V. Ozbolat, Application areas of 3D bioprinting, Drug Discov. Today 21 (2016) 1257–1271.
[285] M. Verma, Personalized medicine and cancer, J. Pers. Med. 2 (2012) 1–14.
[286] Y. Zhao, R. Yao, L. Ouyang, H. Ding, T. Zhang, K. Zhang, S. Cheng, W. Sun, Three-dimensional printing of Hela cells for cervical tumor model in vitro, Biofabrication 6 (2014) 035001.
[287] F. Xu, J. Celli, I. Rizvi, S. Moon, T. Hasan, U. Demirci, A three-dimensional in vitro ovarian cancer coculture model using a high-throughput cell patterning platform, Biotechnol. J. 6 (2011) 204–212.
[288] J.M. Grolman, D. Zhang, A.M. Smith, J.S. Moore, K.A. Kilian, Rapid 3D extrusion of synthetic tumor microenvironments, Adv. Mater. 27 (2015) 5512–5517.
[289] T.Q. Huang, X. Qu, J. Liu, S. Chen, 3D printing of biomimetic microstructures for cancer cell migration, Biomed. Microdevices 16 (2014) 127–132.
[290] W. Zhu, B. Holmes, R.I. Glazer, L.G. Zhang, 3D printed nanocomposite matrix for the study of breast cancer bone metastasis, Nanomed. Nanotechnol. Biol. Med. 12 (2016) 69–79.
[291] Y. Gu, X. Chen, J.-H. Lee, D.A. Monteiro, H. Wang, W.Y. Lee, Inkjet printed antibiotic- and calcium-eluting bioresorbable nanocomposite micropatterns for orthopedic implants, Acta Biomater. 8 (2012) 424–431.
[292] P.J. Tarcha, D. Verlee, H.W. Hui, J. Setesak, B. Antohe, D. Radulescu, D. Wallace, The application of ink-jet technology for the coating and loading of drug-eluting stents, Ann. Biomed. Eng. 35 (2007) 1791–1799.
[293] N. Sandler, I. Salmela, A. Fallarero, A. Rosling, M. Khajeheian, R. Kolakovic, N. Genina, J. Nyman, P. Vuorela, Towards fabrication of 3D printed medical devices to prevent biofilm formation, Int. J. Pharm. 459 (2014) 62–64.
[294] D.-G. Yu, C. Branford-White, Z.-H. Ma, L.-M. Zhu, X.-Y. Li, X.-L. Yang, Novel drug delivery devices for providing linear release profiles fabricated by 3DP, Int. J. Pharm. 370 (2009) 160–166.
[295] A. Goyanes, J. Wang, A. Buanz, R.n. Martínez-Pacheco, R. Telford, S. Gaisford, A.W. Basit, 3D printing of medicines: engineering novel oral devices with unique design and drug release characteristics, Mol. Pharm. 12 (2015) 4077–4084.

[296] R.D. Boehm, P.R. Miller, R. Singh, A. Shah, S. Stafslien, J. Daniels, R.J. Narayan, Indirect rapid prototyping of antibacterial acid anhydride copolymer microneedles, Biofabrication 4 (2012) 011002.
[297] R.D. Boehm, P.R. Miller, W.A. Schell, J.R. Perfect, R.J. Narayan, Inkjet printing of amphotericin B onto biodegradable microneedles using piezoelectric inkjet printing, JOM 65 (2013) 525–533.
[298] H.-G. Yi, Y.-J. Choi, K.S. Kang, J.M. Hong, R.G. Pati, M.N. Park, I.K. Shim, C.M. Lee, S.C. Kim, D.-W. Cho, A 3D-printed local drug delivery patch for pancreatic cancer growth suppression, J. Control. Release 238 (2016) 231–241.
[299] A.A. Konta, M. García-Piña, D.R. Serrano, Personalised 3D printed medicines: which techniques and polymers are more successful? Bioengineering 4 (2017) 79.